University of Pennsylvania
ScholarlyCommons

Publicly Accessible Penn Dissertations

1-1-2013

Notch Signaling and Bone Fracture Healing

Michael I. Dishowitz
University of Pennsylvania, michael.dishowitz@gmail.com

Follow this and additional works at: http://repository.upenn.edu/edissertations

 Part of the Biology Commons, and the Biomedical Commons

Recommended Citation
Dishowitz, Michael I., "Notch Signaling and Bone Fracture Healing" (2013). *Publicly Accessible Penn Dissertations*. 630.
http://repository.upenn.edu/edissertations/630

This paper is posted at ScholarlyCommons. http://repository.upenn.edu/edissertations/630
For more information, please contact libraryrepository@pobox.upenn.edu.

Notch Signaling and Bone Fracture Healing

Abstract
Bone fractures can exhibit delayed or non-union healing. Current treatments have well- documented limitations. Although morphological aspects of fracture healing are well- characterized, molecular mechanisms that regulate the complex progression of healing are poorly understood. Therefore, a need persists for the identification of novel pathways that regulate fracture healing, and for development of therapeutics targeting these pathways to enhance regeneration. Notch signaling regulates bone development, and many aspects of bone development are recapitulated during repair. Notch signaling is also required for repair of other tissues, and enhancing Notch signaling promotes regeneration. Therefore, the objective of this thesis was to determine the role of Notch signaling during bone fracture healing, and to create a translatable therapy targeting the pathway to enhance bone tissue formation. We hypothesized that (i) Notch signaling components are active during bone repair; (ii) inhibition of Notch signaling alters healing; (iii) expression of the Jagged1 ligand in mesenchymal cells regulates bone formation; and (iv) therapeutic delivery of Jagged1 will activate the Notch signaling pathway and promote osteogenesis.

We first characterized activation of Notch signaling during tibial fracture and calvarial defect healing, and demonstrated that Notch signaling components are active during both methods of repair with Jagged1 the most highly upregulated ligand. Then we determined the importance of Notch signaling by using a temporally controlled inducible model (Mx1- Cre;dnMAMLf/-) to impair canonical signaling in all cells during tibial fracture and calvarial defect healing, and demonstrated that Notch inhibition alters the temporal progression of events required for healing, including inflammation, cartilage formation, callus vascularization and bone remodeling. Next we deleted Jagged1 in mesenchymal progenitors (Prx1-Cre;Jagged1f/f) or committed osteoblasts (Col2.3-Cre;Jagged1f/f), and determined that Jagged1 promotes bone formation during development. Finally, we developed a biomaterial construct comprised of Jagged1 and a poly(β-amino ester) scaffold, and demonstrated that it activates Notch signaling and enhances osteoblast differentiation.

This thesis identified Notch signaling as an important regulator of fracture healing, developed a translatable therapeutic targeting the pathway to improve bone tissue formation. The study design outlined can also serve as a model for the discovery of novel pathways that regulate, and therefore could enhance, bone fracture healing.

Degree Type
Dissertation

Degree Name
Doctor of Philosophy (PhD)

Graduate Group
Bioengineering

First Advisor
Kurt Hankenson

This dissertation is available at ScholarlyCommons: http://repository.upenn.edu/edissertations/630

Keywords
bone, fracture, Jagged1, Notch signaling, orthopaedics

Subject Categories
Biology | Biomedical

This dissertation is available at ScholarlyCommons: http://repository.upenn.edu/edissertations/630

NOTCH SIGNALING AND BONE FRACTURE HEALING

Michael I. Dishowitz

A DISSERTATION in Bioengineering

Presented to the Faculties of the University of Pennsylvania in Partial Fulfillment of the

Requirements for the Degree of Doctor of Philosophy

2013

_____

Supervisor of Dissertation

Dr. Kurt D. Hankenson, Dean W. Richardson Chair in Equine Disease Research, Associate Professor of Equine Musculoskeletal Research

_____

Graduate Group Chairperson

Dr. Daniel A. Hammer, Alfred G. and Meta A. Ennis Professor of Bioengineering and Chemical and Biomolecular Engineering

Dissertation Committee

Dr. Jason A. Burdick (Chair), Associate Professor of Bioengineering

Dr. Kathleen M. Loomes, Associate Professor of Pediatrics at the Children's Hospital of Philadelphia

Dr. Robert L. Mauck, Associate Professor of Orthopaedic Surgery and Bioengineering

Dr. Louis J. Soslowsky, Fairhill Professor of Orthopaedic Surgery and Professor of Bioengineering

ACKNOWLEDGEMENTS

I would like to thank my thesis committee for guiding me along the way through graduate school. To Dr. Jason Burdick, thank you for advising me through the final phase of my thesis. The skills I have learned collaborating with you and your lab have prepared me for the next stages of my career. To Dr. Kathy Loomes, it is because of you that I understand the potential impact my research could have on those with clinical Notch disorders. To Dr. Rob Mauck, I have always respected the way you approach your work and the thought process you go about every day life. It is always a pleasure speaking with you. I would like to especially thank Dr. Lou Soslowsky. You taught me the skills I needed to eventually become a successful scientist. I will forever be grateful for the amount of time you spent training me. And most importantly to my advisor Dr. Kurt Hankenson, you challenged me to achieve things I didn't realize I could, and you allowed me the freedom I needed to develop into a confident independent scientist. Thank you for exposing me to so many opportunities atypical to other graduate students.

I would like to thank those I have worked with along the way, including current and former members of the Hankenson lab Dr. Shawn Terkhorn, Jason Combs, Dr. Fengchang Zhu, Lorraine Mutyaba, Derek Dopkin, Sandy Bostic, Joel Takacs, Mike Karp, Andrew Barr, and Drs. Emily Miedel and Nicole Belkin; our very close collaborators Drs. Jaimo Ahn, Susan Volk and Samir Mehta; members of the Burdick lab, including Drs. Darren Brey, Harini Sundararaghavan, Ross Marklein, Sudhir Khetan, and Brendan Purcell; Dr. Tina Bales from the Loomes lab; and Bob Caron from the PCMD histology core.. I would like to especially thank all of my friends who have been so important to me both before and during graduate school, and will continue to afterwards.

Finally, I would like to thank my Mom, Dad and brother Ben for being an incredibly loving and supportive family. I couldn't have asked for a better family to be a part of. It is to you that I owe my success. I would also like to thank my in-laws, Joe, Alicia, Ryan, Nathan, Patrick, Eileen, Tom and Mary. And most importantly, I would like to thank my wife Jamie. I love you and couldn't imagine going through life with anyone else. And of course I can't forget Roscoe. Thank you for just being around.

ABSTRACT

NOTCH SIGNALING AND BONE FRACTURE HEALING

Michael I. Dishowitz

Kurt D. Hankenson, D.V.M., Ph.D.

Bone fractures can exhibit delayed or non-union healing. Current treatments have well-documented limitations. Although morphological aspects of fracture healing are well-characterized, molecular mechanisms that regulate the complex progression of healing are poorly understood. Therefore, a need persists for the identification of novel pathways that regulate fracture healing, and for development of therapeutics targeting these pathways to enhance regeneration. Notch signaling regulates bone development, and many aspects of bone development are recapitulated during repair. Notch signaling is also required for repair of other tissues, and enhancing Notch signaling promotes regeneration. Therefore, the objective of this thesis was to determine the role of Notch signaling during bone fracture healing, and to create a translatable therapy targeting the pathway to enhance bone tissue formation. We hypothesized that (i) Notch signaling components are active during bone repair; (ii) inhibition of Notch signaling alters healing; (iii) expression of the Jagged1 ligand in mesenchymal cells regulates bone formation; and (iv) therapeutic delivery of Jagged1 will activate the Notch signaling pathway and promote osteogenesis.

We first characterized activation of Notch signaling during tibial fracture and calvarial defect healing, and demonstrated that Notch signaling components are active during both methods of repair with Jagged1 the most highly upregulated ligand. Then we determined the importance of Notch signaling by using a temporally controlled inducible model (Mx1-Cre;dnMAML$^{f/-}$) to impair canonical signaling in all cells during tibial fracture and calvarial defect healing, and demonstrated that Notch inhibition alters the temporal progression of events required for healing, including inflammation, cartilage formation, callus vascularization and bone remodeling. Next we deleted Jagged1 in mesenchymal progenitors (Prx1-Cre;Jagged1$^{f/f}$) or

committed osteoblasts (Col2.3-Cre;Jagged1$^{f/f}$), and determined that Jagged1 promotes bone formation during development. Finally, we developed a biomaterial construct comprised of Jagged1 and a poly(β-amino ester) scaffold, and demonstrated that it activates Notch signaling and enhances osteoblast differentiation.

This thesis identified Notch signaling as an important regulator of fracture healing, developed a translatable therapeutic targeting the pathway to improve bone tissue formation. The study design outlined can also serve as a model for the discovery of novel pathways that regulate, and therefore could enhance, bone fracture healing.

TABLE OF CONTENTS

LIST OF TABLES

LIST OF FIGURES

CHAPTER 1

Introduction to Bone Fracture Healing and the Notch Signaling Pathway

1.1 Clinical Significance of Bone Fractures

It is estimated that approximately 7.9 million fractures occur in the United States each year, and although the majority of fractures heal with standard care, approximately 10-13% have reported to exhibit delayed healing or develop into non-unions [1, 2]. Direct treatment costs are approximately $3,400-$5,300 per fracture. However, the total financial burden to society is approximately $12,500-17,300 per fracture when including associated costs such as lost productivity [3]. Direct and societal costs are of course much higher for fractures that experience delayed healing due to increased medical visits and continued loss of productivity. Furthermore, fractures in an elderly population have increased costs upwards of $81,300 per injury, of which nursing facility expenses account for nearly half, as well as result in an increased mortality rate [4].

To treat severe injuries, therapeutic approaches have focused on delivery of osteoinductive (biological cues to stimulate osteoblast activity) and osteoconductive (scaffold or other cue to support bone formation) signals. Autologous bone grafts often harvested from the patient's iliac crest are considered the gold standard of care, but can result in significant donor site morbidity and post-surgical pain, and yield only a limited amount of graft material [5]. Demineralized bone matrix, a common allograft therapeutic, is more readily available but has limited osteoinductive potential and can induce immunogenic reactions [5]. More recently, growth factor-based therapies have been developed to promote bone formation. Use of bone morphogenetic proteins (BMPs) has become one of the more common treatments [6, 7]. However, recent reports suggest that BMPs lack the clinical efficiency and safety that has been widely demonstrated in pre-clinical animal models [8, 9]. Furthermore, gene-based therapeutics that deliver osteoinductive genetic information to cells have demonstrated suboptimal efficiency

[10] or induced significant immunogenic responses [11]. Therefore, a clinical need persists for the development of new methods to enhance bone fracture healing.

1.2 Bone Fracture Healing

Bone fracture healing occurs through a series of carefully regulated spatiotemporal events that recapitulate many aspects of embryological bone development (Figure 1.1) [12-14]. Endochondral bones such as the tibia and femur heal primarily through endochondral ossification. Following injury, inflammation and hematoma formation mediate an influx of undifferentiated mesenchymal cells to the site of injury that rapidly proliferate to produce the initial fibrovascular callus. These cells then condense and undergo chondrogenic differentiation to produce an avascular cartilaginous callus. Terminal chondrocyte hypertrophy and cartilage matrix mineralization are then followed by apoptosis and resorption, which allows for vascular invasion of the callus. During this cartilage-to-bone transition, the vascular network mediates an influx of osteoprogenitor cells that undergo differentiation and produce immature bone on top of the resorbing cartilage matrix. Concomitantly, periosteal-derived osteoblasts form a mineralized bony shell surrounding the callus. Over time, the callus matures and is remodeled through osteoblast-mediated bone formation and osteoclast-mediated bone resorption, ultimately restoring the structure and function of the original bone. Alternatively, intramembranous bones such as the calvarium as well as other bones that are rigidly fixed during repair heal through intramembranous ossification, which involves direct bone formation without a cartilage precursor [15, 16].

Although physiological mechanisms of fracture healing are well-characterized, molecular signals that control the complex temporal progression of events required for healing are poorly understood, with most investigations limited to understanding the role(s) of the BMP [17] and Wnt [18, 19] signaling pathways. Elucidating the significance of novel signaling pathways that regulate fracture healing will allow for the identification of novel therapeutic targets to improve bone repair.

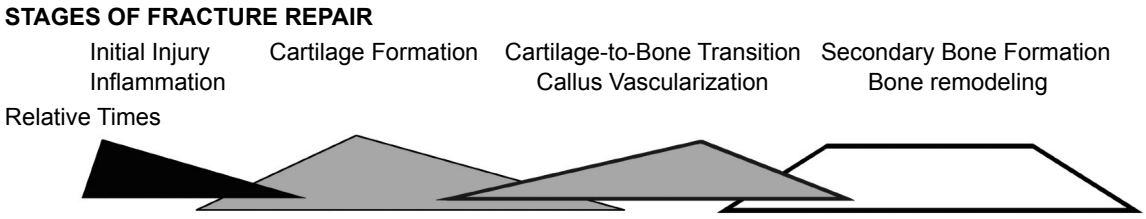

Figure 1.1. Schematic of the temporal progression of endochondral fracture repair. Figure adapted from Gerstenfeld et al. [20]

1.3 Notch Signaling Pathway

The Notch signaling pathway is a developmentally conserved cell-to-cell signaling pathway that regulates cell proliferation, differentiation, fate determination and apoptosis [21]. Activation of the pathway occurs when a Notch ligand (Jagged 1,2 and Delta-like 1,4) expressed on the surface of a signaling cell interacts with a Notch receptor (Notch 1-4) expressed on the surface of a receiving cell. The Notch intracellular domain (NICD) is released via a two-stage proteolytic event mediated first by the ADAM family metalloproteinase tumor necrosis factor α conversion enzyme (ADAM/TACE), and then by the γ-secretase complex comprised of Presenilins 1 and 2. Once released, NICD translocates to the nucleus where it binds to Recombination Signal Binding Protein For Immunoglobulin Kappa J Region (RBPjκ), converting it from a transcriptional repressor into an activator. Mastermind-like protein (MAML) then binds to create the NICD-RBPjκ-MAML complex and serves as a scaffold to recruit other co-activators necessary to initiate transcription of canonical Notch target gene families Hes and Hey (Figure 1.2) [22-24].

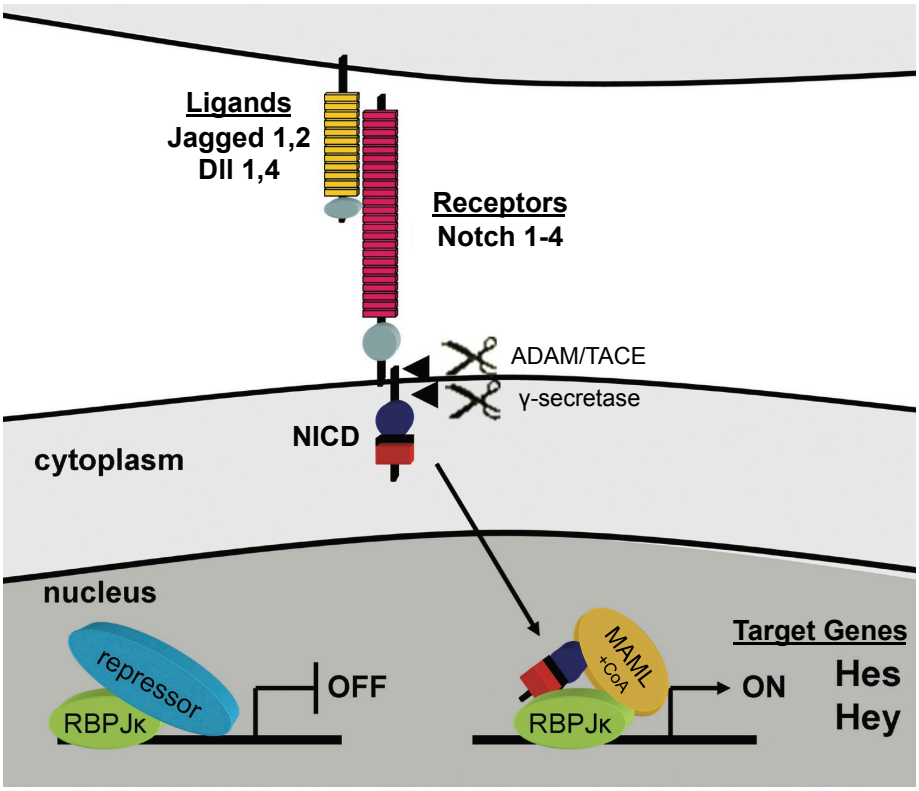

Figure 1.2. Schematic of the Notch signaling pathway. Figure adapted from Fischer et al. [25]

1.4 Notch Signaling and Bone Formation

The Notch signaling pathway regulates mesenchymal cell lineage behavior and embryological bone formation [26-33]. Deletion of Notch components in undifferentiated mesenchymal progenitor cells stimulates osteoblast differentiation and early bone formation, which is ultimately lost during aging due to depletion of the progenitor pool [26]. Constitutive activation of Notch in committed but not completely mature osteoblasts promotes proliferation while inhibiting differentiation, resulting in osteosclerotic immature bone formation that does not properly mature [27]. These results demonstrate that activation of Notch signaling maintains osteoprogenitor cells in an undifferentiated state. Deletion of Notch components in the same committed osteoblast population or in mature osteoblasts does not alter early bone formation, but instead results in osteopenia during aging due to increased osteoclast activity [26-28],

demonstrating that activation of Notch signaling in mature osteoblasts promotes net bone gain by secondarily inhibiting osteoclast activity.

Transient activation of Notch signaling in progenitor cells is required to initiate chondrogenesis [34]. However, constitutive expression of Notch components prevents differentiation from occurring [29, 30, 34], whereas sustained inhibition in undifferentiated mesenchymal progenitor cells or committed chondrogenic cells results in the pathological overproduction of chondrocytes [29, 30]. Reactivation of Notch is then required for proper terminal hypertrophic chondrocyte maturation [31]. These results demonstrate that while transient activation is required to initiate chondrogenesis, constitutive activation of Notch signaling inhibits differentiation, but must be reactivated to complete terminal differentiation.

Since many aspects of bone development are recapitulated during repair, these results collectively suggest that Notch signaling also regulates bone fracture healing.

1.5 Notch and Vasculogenesis

Bone formation during development and fracture repair is dependent upon proper vascularization, which mediates an influx of osteogenic cells to sites of new bone formation. Various gain-of-function and loss-of-function models have demonstrated that Notch signaling is a critical regulator of vascular development. With regards to ligand activity, homozygous Jagged1 deletion [35] as well as Dll4 haploinsufficiency [36, 37] results in embryonic lethality due to vascular defects. With regards to receptor activity, conditional Notch4 gain-of-function in VEGFR-expressing cells results in embryonic lethality due to a restricted and disorganized vascular network [38]. Interestingly, homozygous Notch4 deleted mice develop normally, but homozygous Notch1 deleted mice as well as double homozygous Notch1 and Notch4 deleted mice show vascular remodeling defects that result in embryonic lethality [39]. Furthermore, Notch1 deletion in Tie2-expressing endothelium-specific cells also produce vascular abnormalities that result in embryonic lethality [40]. The fact that gain-of-function and loss-of-function of Notch components both result in embryonic lethality suggests that the proper spatiotemporal expression of Notch components is required for proper vascular developmental patterning and remodeling.

Notch signaling has also been shown to regulate postnatal angiogenesis and vasculogenesis. Use of various tissue-specific and inducible Jagged1 gain- and loss-of-function mouse models have demonstrated that Jagged1 promotes angiogenesis and vessel sprouting by antagonizing Dll4-Notch interactions, which are inhibitory [41]. Jagded1 expression also promotes endothelial cell proliferation, differentiation and migration, whereas Dll1 has no effect [42].

1.6 The Notch Ligand Jagged1 (Jag1)

Clinically, loss-of-function mutations to Jagged1 are primarily responsible for Alagille Syndrome (ALGS) [43, 44]. ALGS incorporates a wide range of developmental defects, including chronic liver cholestasis, bile duct paucity, cardiovascular disease, kidney and pancreatic disease, craniofacial development alterations and other musculoskeletal defects [45]. ALGS patients present with decreased bone mass [46] and increased risk of fracture [47], which is often assumed to be secondary to chronic liver cholestasis, where the resulting malabsorption of fat soluble vitamins and minerals is believed to be primarily responsible for impaired skeletal development. However, liver transplantations, which are common treatments for ALGS patients, have not been able to recover normal bone growth [46, 48]. A recent study demonstrated a direct role for Jagged1 in craniofacial development [49] and a SNP at the Jagged1 locus is associated with bone mass. Furthermore, Jagged1 is the mostly highly expressed Notch ligand in mesenchymal cells during skeletal development [30], (as stated above) enhances vasculogenesis by promoting endothelial cell proliferation, differentiation and migration [41, 42], and its expression in mesenchymal lineage cells promotes hematopoietic stem cell expansion [50, 51] and inhibits osteoclast differentiation [52]. These results suggest that Jagged1 activity in mesenchymal lineage cells directly regulates bone formation.

1.7 Notch and Regeneration

Notch signaling is upregulated following injury to many tissues including skin [53], retina [54], brain [55, 56], heart [57], intestine [58], kidney [59, 60] and pancreas [61]. Activation of Notch signaling is required for successful wound healing [53] and regeneration of muscle [62].

Manipulations to Notch signaling can also enhance tissue regeneration. Specifically, transient upregulation of Notch signaling via adenoviral transfection of NICD significantly improved myocardial function in infarcted hearts [57]. These results identify Notch as a potential therapeutic target for other injuries as well where the pathway is endogenously active.

Interestingly, *in vivo* delivery of soluble Notch ligands Jagged1 or Dll4 through an osmotic pump did not improve healing following ischemic-induced brain injuries [55, 63]. However, previous studies have demonstrated a requirement for Notch ligands to be immobilized to a substrate in order to active NICD cleavage and downstream Notch signaling, such that free-floating soluble ligands are also able to bind to receptors but instead effectively inhibit the pathway [64-69]. It has been hypothesized that the naturally-occurring immobilized state of a membrane-bound Notch ligand is required to apply a pulling force on the extracellular domain of the Notch receptor, which precedes cleavage of the intracellular domain (NICD) [70]. These results demonstrate the requirement for ligand immobilization to activate the Notch signaling pathway for therapeutic applications.

1.8 Use of Poly(β-amino ester)s for Therapeutic Applications

A combinatorial library of degradable, photocrosslinkable, acrylate-terminated poly(β-amino ester)s (PBAE) comprised of amines and diacrylates was developed for the rapid screening and design of biomaterials for a variety of therapeutic applications (Figure 1.3) [71]. Polymerization occurs through step-growth with resulting linear macromers containing ester and tertiary amines in their backbones. Following addition of a photoinitiator and exposure to UV light, crosslinking occurs between the functionalized acrylate groups. After photocrosslinking, PBAE networks degrade via hydrolysis to their backbone esters into small molecule bis(β-amino acid)s, diol products, and poly(acrylic acid) kinetic chains. PBAEs are clinically advantageous polymers to use as therapeutics because they are simple to synthesize with no byproducts formed, thus eliminating the need for multiple purification steps, and are inexpensive and commercially available. Mechanical properties and degradation rates of PBAEs can be controlled by altering the diacrylate-to-amine molar ratio [72], further expanding their applicability.

PBAEs have successfully been used for a variety of therapeutic applications. PBAEs have been used as gene-delivery vehicles for cardiovascular therapeutics [73] and as nonviral DNA vectors for cancer therapeutics [74]. PBAE nanoparticles have also shown to be effective drug delivery vehicles for targeting cancerous cells [75]. Importantly, one PBAE in particular, diethylene glycol diacrylate combined with isobutylamine, has demonstrated osteoconductive properties when used as a scaffold carrier for BMP delivery [76].

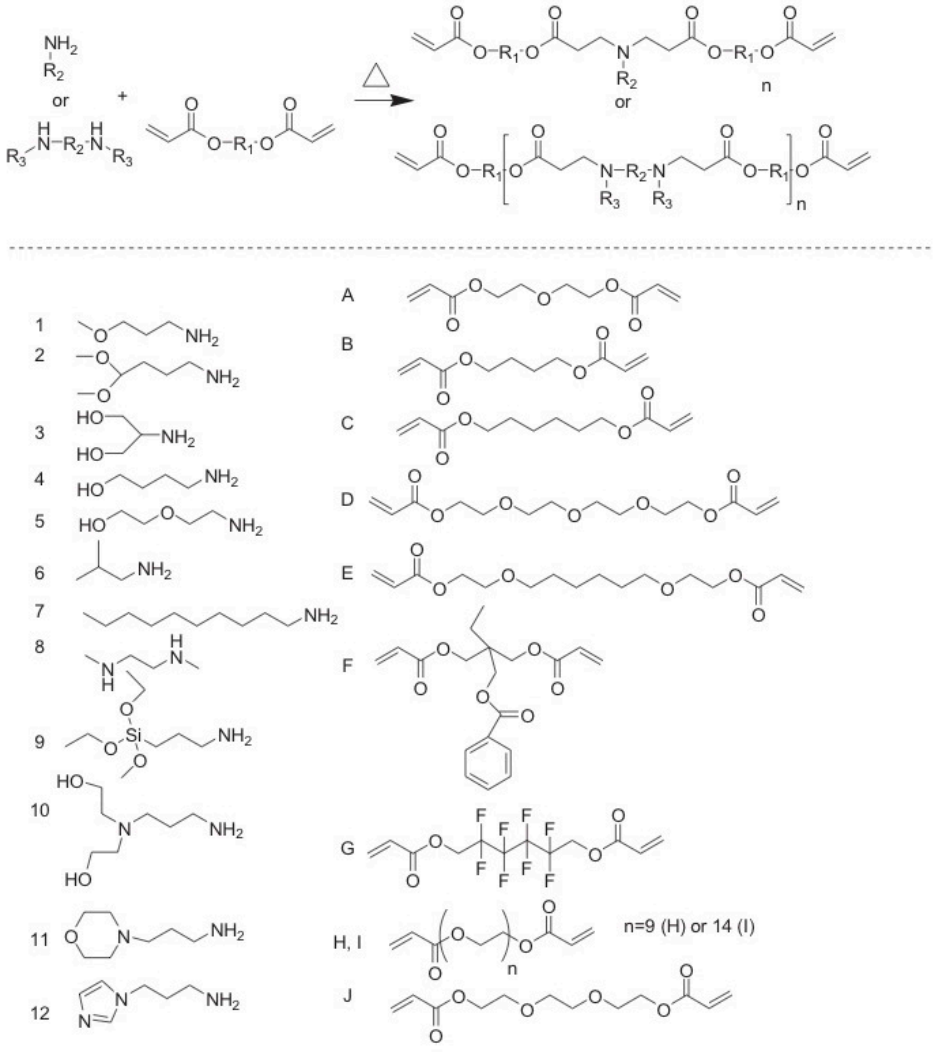

Figure 1.3. General poly(β-amino ester) polymerization schematic and chemical structures. Synthesis of amines and diacrylates (top). Monomers depicting the 12 amines and 10 diacrylates (bottom). Figure from Anderson et al. [71]

1.9 Conclusions

This chapter provides an overview of the Notch signaling pathway and bone fracture healing. The Notch signaling pathway has been shown to regulate embryological bone development. Since many aspects of development are recapitulated during repair, Notch signaling may also regulate bone fracture healing. Furthermore, activation of the pathway has been shown to promote regeneration of other tissues, identifying it as a potential therapeutic to also enhance regeneration of bone. The work described in this thesis will report on the comprehensive assessment of Notch signaling during fracture. The significance of Notch signaling will be determined by blocking canonical Notch signaling during fracture healing. The role of Jagged1 specifically during bone development and remodeling will also be assessed by deleting the gene in the osteoblast lineage, and finally, we will develop a biomaterial by delivering the Jagged1 ligand to promote bone healing.

1.10 References

1. Praemer, A., et al., *Musculoskeletal Conditions in the United States*1999: American Academy of Orthopaedic Surgeons.
2. Audige, L., et al., *Path analysis of factors for delayed healing and nonunion in 416 operatively treated tibial shaft fractures.* Clin Orthop Relat Res, 2005. **438**: p. 221-32.
3. Busse, J.W., et al., *An economic analysis of management strategies for closed and open grade I tibial shaft fractures.* Acta Orthop, 2005. **76**(5): p. 705-12.
4. Braithwaite, R.S., N.F. Col, and J.B. Wong, *Estimating hip fracture morbidity, mortality and costs.* J Am Geriatr Soc, 2003. **51**(3): p. 364-70.
5. Dimitriou, R., et al., *Bone regeneration: current concepts and future directions.* BMC Med, 2011. **9**: p. 66.
6. Friedlaender, G.E., et al., *Osteogenic protein-1 (bone morphogenetic protein-7) in the treatment of tibial nonunions.* J Bone Joint Surg Am, 2001. **83-A Suppl 1**(Pt 2): p. S151-8.
7. Govender, S., et al., *Recombinant human bone morphogenetic protein-2 for treatment of open tibial fractures: a prospective, controlled, randomized study of four hundred and fifty patients.* J Bone Joint Surg Am, 2002. **84-A**(12): p. 2123-34.
8. Einhorn, T.A., *Clinical applications of recombinant human BMPs: early experience and future development.* J Bone Joint Surg Am, 2003. **85-A Suppl 3**: p. 82-8.
9. Carragee, E.J., et al., *Future directions for The spine journal: managing and reporting conflict of interest issues.* Spine J, 2011. **11**(8): p. 695-7.
10. Partridge, K.A. and R.O. Oreffo, *Gene delivery in bone tissue engineering: progress and prospects using viral and nonviral strategies.* Tissue Eng, 2004. **10**(1-2): p. 295-307.
11. Hannallah, D., et al., *Retroviral delivery of Noggin inhibits the formation of heterotopic ossification induced by BMP-4, demineralized bone matrix, and trauma in an animal model.* J Bone Joint Surg Am, 2004. **86-A**(1): p. 80-91.

12. Vortkamp, A., et al., *Recapitulation of signals regulating embryonic bone formation during postnatal growth and in fracture repair.* Mech Dev, 1998. **71**(1-2): p. 65-76.

13. Ferguson, C., et al., *Does adult fracture repair recapitulate embryonic skeletal formation?* Mech Dev, 1999. **87**(1-2): p. 57-66.

14. Gerstenfeld, L.C., et al., *Fracture healing as a post-natal developmental process: molecular, spatial, and temporal aspects of its regulation.* J Cell Biochem, 2003. **88**(5): p. 873-84.

15. Einhorn, T.A., *The cell and molecular biology of fracture healing.* Clin Orthop Relat Res, 1998(355 Suppl): p. S7-21.

16. McKibbin, B., *The biology of fracture healing in long bones.* J Bone Joint Surg Br, 1978. **60-B**(2): p. 150-62.

17. Tsuji, K., et al., *BMP2 activity, although dispensable for bone formation, is required for the initiation of fracture healing.* Nat Genet, 2006. **38**(12): p. 1424-9.

18. Minear, S., et al., *Wnt proteins promote bone regeneration.* Sci Transl Med, 2010. **2**(29): p. 29ra30.

19. Komatsu, D.E., et al., *Modulation of Wnt signaling influences fracture repair.* J Orthop Res, 2010. **28**(7): p. 928-36.

20. Gerstenfeld, L.C. and T.A. Einhorn, *Developmental aspects of fracture healing and the use of pharmacological agents to alter healing.* J Musculoskelet Neuronal Interact, 2003. **3**(4): p. 297-303; discussion 320-1.

21. Artavanis-Tsakonas, S., M.D. Rand, and R.J. Lake, *Notch signaling: cell fate control and signal integration in development.* Science, 1999. **284**(5415): p. 770-6.

22. Iso, T., L. Kedes, and Y. Hamamori, *HES and HERP families: multiple effectors of the Notch signaling pathway.* J Cell Physiol, 2003. **194**(3): p. 237-55.

23. Zanotti, S. and E. Canalis, *Notch and the skeleton.* Mol Cell Biol, 2010. **30**(4): p. 886-96.

24. Engin, F. and B. Lee, *NOTCHing the bone: insights into multi-functionality.* Bone, 2010. **46**(2): p. 274-80.

25. Fischer, A. and M. Gessler, *Delta-Notch--and then? Protein interactions and proposed modes of repression by Hes and Hey bHLH factors.* Nucleic Acids Res, 2007. **35**(14): p. 4583-96.

26. Hilton, M.J., et al., *Notch signaling maintains bone marrow mesenchymal progenitors by suppressing osteoblast differentiation.* Nat Med, 2008. **14**(3): p. 306-14.

27. Engin, F., et al., *Dimorphic effects of Notch signaling in bone homeostasis.* Nat Med, 2008. **14**(3): p. 299-305.

28. Zanotti, S., et al., *Notch inhibits osteoblast differentiation and causes osteopenia.* Endocrinology, 2008. **149**(8): p. 3890-9.

29. Mead, T.J. and K.E. Yutzey, *Notch pathway regulation of chondrocyte differentiation and proliferation during appendicular and axial skeleton development.* Proc Natl Acad Sci U S A, 2009. **106**(34): p. 14420-5.

30. Dong, Y., et al., *RBPjkappa-dependent Notch signaling regulates mesenchymal progenitor cell proliferation and differentiation during skeletal development.* Development, 2010. **137**(9): p. 1461-71.

31. Kohn, A., et al., *Cartilage-specific RBPjkappa-dependent and -independent Notch signals regulate cartilage and bone development.* Development, 2012. **139**(6): p. 1198-212.

32. Tao, J., et al., *Osteosclerosis owing to Notch gain of function is solely Rbpj-dependent.* J Bone Miner Res, 2010. **25**(10): p. 2175-83.

33. Salie, R., et al., *Ubiquitous overexpression of Hey1 transcription factor leads to osteopenia and chondrocyte hypertrophy in bone.* Bone, 2010. **46**(3): p. 680-94.

34. Oldershaw, R.A., et al., *Notch signaling through Jagged-1 is necessary to initiate chondrogenesis in human bone marrow stromal cells but must be switched off to complete chondrogenesis.* Stem Cells, 2008. **26**(3): p. 666-74.

35. Xue, Y., et al., *Embryonic lethality and vascular defects in mice lacking the Notch ligand Jagged1.* Hum Mol Genet, 1999. **8**(5): p. 723-30.

36. Krebs, L.T., et al., *Haploinsufficient lethality and formation of arteriovenous malformations in Notch pathway mutants.* Genes Dev, 2004. **18**(20): p. 2469-73.

37. Gale, N.W., et al., *Haploinsufficiency of delta-like 4 ligand results in embryonic lethality due to major defects in arterial and vascular development.* Proc Natl Acad Sci U S A, 2004. **101**(45): p. 15949-54.

38. Uyttendaele, H., et al., *Vascular patterning defects associated with expression of activated Notch4 in embryonic endothelium.* Proc Natl Acad Sci U S A, 2001. **98**(10): p. 5643-8.

39. Krebs, L.T., et al., *Notch signaling is essential for vascular morphogenesis in mice.* Genes Dev, 2000. **14**(11): p. 1343-52.

40. Limbourg, F.P., et al., *Essential role of endothelial Notch1 in angiogenesis.* Circulation, 2005. **111**(14): p. 1826-32.

41. Benedito, R., et al., *The notch ligands Dll4 and Jagged1 have opposing effects on angiogenesis.* Cell, 2009. **137**(6): p. 1124-35.

42. Kwon, S.M., et al., *Specific Jagged-1 signal from bone marrow microenvironment is required for endothelial progenitor cell development for neovascularization.* Circulation, 2008. **118**(2): p. 157-65.

43. Li, L., et al., *Alagille syndrome is caused by mutations in human Jagged1, which encodes a ligand for Notch1.* Nat Genet, 1997. **16**(3): p. 243-51.

44. Oda, T., et al., *Mutations in the human Jagged1 gene are responsible for Alagille syndrome.* Nat Genet, 1997. **16**(3): p. 235-42.

45. Krantz, I.D., D.A. Piccoli, and N.B. Spinner, *Clinical and molecular genetics of Alagille syndrome.* Curr Opin Pediatr, 1999. **11**(6): p. 558-64.

46. Olsen, I.E., et al., *Deficits in size-adjusted bone mass in children with Alagille syndrome.* J Pediatr Gastroenterol Nutr, 2005. **40**(1): p. 76-82.

47. Bales, C.B., et al., *Pathologic lower extremity fractures in children with Alagille syndrome.* J Pediatr Gastroenterol Nutr, 2010. **51**(1): p. 66-70.

48. Quiros-Tejeira, R.E., et al., *Does liver transplantation affect growth pattern in Alagille syndrome?* Liver Transpl, 2000. **6**(5): p. 582-7.

49. Humphreys, R., et al., *Cranial neural crest ablation of Jagged1 recapitulates the craniofacial phenotype of Alagille syndrome patients.* Hum Mol Genet, 2012. **21**(6): p. 1374-83.

50. Calvi, L.M., et al., *Osteoblastic cells regulate the haematopoietic stem cell niche.* Nature, 2003. **425**(6960): p. 841-6.

51. Weber, J.M., et al., *Parathyroid hormone stimulates expression of the Notch ligand Jagged1 in osteoblastic cells.* Bone, 2006. **39**(3): p. 485-93.

52. Bai, S., et al., *NOTCH1 regulates osteoclastogenesis directly in osteoclast precursors and indirectly via osteoblast lineage cells.* J Biol Chem, 2008. **283**(10): p. 6509-18.

53. Chigurupati, S., et al., *Involvement of notch signaling in wound healing.* PLoS One, 2007. **2**(11): p. e1167.

54. Hayes, S., et al., *Notch signaling regulates regeneration in the avian retina.* Dev Biol, 2007. **312**(1): p. 300-11.

55. Oya, S., et al., *Attenuation of Notch signaling promotes the differentiation of neural progenitors into neurons in the hippocampal CA1 region after ischemic injury.* Neuroscience, 2009. **158**(2): p. 683-92.

56. Tatsumi, K., et al., *Transient activation of Notch signaling in the injured adult brain.* J Chem Neuroanat, 2010. **39**(1): p. 15-9.

57. Gude, N.A., et al., *Activation of Notch-mediated protective signaling in the myocardium.* Circ Res, 2008. **102**(9): p. 1025-35.

58. Okamoto, R., et al., *Requirement of Notch activation during regeneration of the intestinal epithelia.* Am J Physiol Gastrointest Liver Physiol, 2009. **296**(1): p. G23-35.

59. Kobayashi, T., et al., *Expression and function of the Delta-1/Notch-2/Hes-1 pathway during experimental acute kidney injury.* Kidney Int, 2008. **73**(11): p. 1240-50.

60. Gupta, S., et al., *Effect of Notch activation on the regenerative response to acute renal failure.* Am J Physiol Renal Physiol, 2010. **298**(1): p. F209-15.

61. Su, Y., et al., *Pancreatic regeneration in chronic pancreatitis requires activation of the notch signaling pathway.* J Gastrointest Surg, 2006. **10**(9): p. 1230-41; discussion 1242.

62. Conboy, I.M., et al., *Notch-mediated restoration of regenerative potential to aged muscle.* Science, 2003. **302**(5650): p. 1575-7.

63. Androutsellis-Theotokis, A., et al., *Notch signalling regulates stem cell numbers in vitro and in vivo.* Nature, 2006. **442**(7104): p. 823-6.

64. Varnum-Finney, B., et al., *Immobilization of Notch ligand, Delta-1, is required for induction of notch signaling.* J Cell Sci, 2000. **113 Pt 23**: p. 4313-8.

65. Vas, V., et al., *Soluble Jagged-1 is able to inhibit the function of its multivalent form to induce hematopoietic stem cell self-renewal in a surrogate in vitro assay.* J Leukoc Biol, 2004. **75**(4): p. 714-20.

66. Beckstead, B.L., D.M. Santosa, and C.M. Giachelli, *Mimicking cell-cell interactions at the biomaterial-cell interface for control of stem cell differentiation.* J Biomed Mater Res A, 2006. **79**(1): p. 94-103.

67. Beckstead, B.L., et al., *Methods to promote Notch signaling at the biomaterial interface and evaluation in a rafted organ culture model.* J Biomed Mater Res A, 2009. **91**(2): p. 436-46.

68. Goncalves, R.M., et al., *Induction of notch signaling by immobilization of jagged-1 on self-assembled monolayers.* Biomaterials, 2009. **30**(36): p. 6879-87.

69. Nobta, M., et al., *Critical regulation of bone morphogenetic protein-induced osteoblastic differentiation by Delta1/Jagged1-activated Notch1 signaling.* J Biol Chem, 2005. **280**(16): p. 15842-8.

70. Kramer, H., *RIPping notch apart: a new role for endocytosis in signal transduction?* Sci STKE, 2000. **2000**(29): p. pe1.

71. Anderson, T., Hossain, Navarro, Brey, Van Vliet, Langer, Burdick, *A Combinatorial Library of Photocrosslinkable and Degradable Materials.* Advanced Materials, 2006.

72. Brey, D.M., I. Erickson, and J.A. Burdick, *Influence of macromer molecular weight and chemistry on poly(beta-amino ester) network properties and initial cell interactions.* J Biomed Mater Res A, 2008. **85**(3): p. 731-41.

73. Brito, L.A., et al., *In vitro and in vivo studies of local arterial gene delivery and transfection using lipopolyplexes-embedded stents.* J Biomed Mater Res A, 2010. **93**(1): p. 325-36.

74. Anderson, D.G., et al., *A polymer library approach to suicide gene therapy for cancer.* Proc Natl Acad Sci U S A, 2004. **101**(45): p. 16028-33.

75. Shen, Y., et al., *Degradable poly(beta-amino ester) nanoparticles for cancer cytoplasmic drug delivery.* Nanomedicine, 2009. **5**(2): p. 192-201.

76. Brey, D.M., et al., *Identification of osteoconductive and biodegradable polymers from a combinatorial polymer library.* J Biomed Mater Res A, 2010. **93**(2): p. 807-16.

CHAPTER 2

Specific Aims and Hypotheses

Bone fractures can exhibit delayed healing or develop into non-unions. Autologous bone grafts and growth factor therapies such as bone morphogenetic proteins are common therapeutic strategies to treat such severe injuries. However, they have well-documented limitations and safety concerns. Furthermore, although the physiological mechanisms of fracture healing are well characterized, the molecular mechanisms that regulate the complex spatiotemporal progression of events required for healing are poorly understood. Therefore, a need persists for the identification of novel signaling pathways that regulate fracture healing, and the development of new therapies targeting these pathways to enhance bone regeneration.

Notch signaling regulates mesenchymal cell behavior and embryological bone formation, and many aspects of bone formation are recapitulated during bone fracture healing. Furthermore, Notch signaling has been shown to be required for successful wound healing, and targeting the pathway can promote tissue regeneration. However, the role of Notch signaling during bone fracture healing and the ability of the pathway to enhance regeneration has not been investigated.

Therefore, the overall objective of this thesis is to determine the role of Notch signaling during bone fracture healing, and to create a clinically translatable therapy targeting the pathway to enhance healing.

2.1 Specific Aim I (Chapter 3)

Characterize and compare activation of the Notch signaling pathway during endochondral and intramembranous fracture healing using murine tibial fracture healing as a model of endochondral bone repair and murine calvarial defect healing as a model of intramembranous bone repair.

2.1.1 Hypothesis I

Notch signaling components are active during murine tibial fracture and calvarial defect healing.

Gene and protein expression of Notch signaling components will be quantified and localized to specific cell populations.

2.2 Specific Aim II (Chapter 4)

Determine the importance of Notch signaling in regulating bone fracture healing by using a temporally controlled inducible transgenic mouse model to impair canonical Notch signaling in all cells during murine tibial fracture and calvarial defect healing

2.2.1 Hypothesis II

Inhibition of Notch signaling will alter murine tibial fracture and calvarial defect healing.

A floxed GFP-tagged dnMAML transgene will be activated in all cell types just prior to injury using the inducible Mx1-Cre model. dnMAML expression inhibits the Notch signaling pathway just prior to transcription of target genes. Multiple stages of healing will be evaluated, including cartilage formation, callus vascularization, bone formation and remodeling, and inflammation, as well as other cell behaviors such as proliferation and apoptosis.

2.3 Specific Aim III (Chapter 5)

Determine the direct role of Jagged1 during bone formation.

2.3.1 Hypothesis III

Jagged1 expression in the mesenchymal lineage regulates bone formation through paracrine cell-to-cell signaling.

Jagged1 will be conditionally deleted in two skeletal-specific mouse models; first in a mesenchymal progenitor cell population by using the Prx1-Cre model and then in a committed osteoblast population by using the Col2.3-Cre model. Trabecular and cortical bone formation will be analyzed as well as gene expression of Notch components and markers of osteoblast and osteoclast differentiation and proliferation.

2.4 Specific Aim IV (Chapter 6)

Develop a clinically translatable biomaterial construct comprised of Jagged1 and an osteoconductive scaffold, and evaluate its ability to induce bone tissue formation.

2.4.1 Hypothesis IV

Delivery of Jagged1 immobilized to a poly(B-amino ester) polymer will activate the Notch signaling pathway and promote osteoblast differentiation.

The ability of direct and indirect Jagged1 immobilization strategies to activate the Notch signaling pathway and promote an osteogenic phenotype will be evaluated in standard growth media. Then, the ability of the ideal immobilization strategy to induce osteoblast differentiation and calcified mineral deposition will be evaluated in osteogenic media. Finally, translatable biomaterial constructs will be evaluated in murine calvarial defects and tibial fractures.

This thesis aims to uncover the role of the Notch signaling pathway during bone fracture healing, and to develop a clinically translatable therapy targeting the pathway to improve bone repair. In all, this thesis serves as the foundation for Notch signaling-based translational research in regenerative orthopaedic medicine, and represents a model approach to uncover additional novel signaling pathways that regulate – and therefore could potentially enhance – bone fracture healing.

CHAPTER 3

Notch Signaling Components Are Upregulated During Endochondral and Intramembranous Bone Regeneration

3.1 Introduction

Bone regeneration occurs through a series of spatiotemporal events that recapitulate many aspects of embryological development [1, 2]. Long bones such as the tibia develop and heal primarily through endochondral ossification (indirect bone formation on a cartilage intermediate), whereas bones such as the calvarium develop and heal through intramembranous ossification (direct bone formation) [3]. A number of growth factor pathways, including bone morphogenetic protein (BMP) and Wnt signaling, have been widely demonstrated to be required for fracture healing and have also been shown to promote regeneration [4-9]. However, despite the importance of these pathways, the significance of other growth factor pathways that regulate bone healing is not as well described.

Notch signaling is a developmentally conserved pathway that mediates the development of stem and progenitor cell populations in many tissues. Activation of the canonical Notch signaling pathway occurs through direct cell-to-cell contact. When one of four Notch ligands, Jagged (Jag) 1,2 and Delta-like (Dll) 1,4, interacts with one of four Notch receptors, Notch1-4, a two-stage proteolytic event liberates the Notch intracellular domain (NICD) which then translocates to the nucleus and binds with co-activators to initiate transcription of Notch target gene families Hes and Hey.

Notch gain of function mutations in the murine mesenchymal lineage result in enhanced cell proliferation while inhibiting differentiation, which prevents mature endochondral and intramembranous bone development [10, 11]. Alternatively, loss of Notch signaling in the mesenchymal lineage results in enhanced osteoprogenitor differentiation and early endochondral bone formation, which is rapidly lost during aging due to depletion of the progenitor pool [12, 13].

Notch signaling in osteoblasts has also been shown to negatively regulate osteoclast behavior [10, 13-15]. Collectively, these studies demonstrate that the Notch signaling pathway regulates endochondral and intramembranous bone formation.

Although Notch signaling has been shown to regulate tissue repair in a variety of tissues [16-21], an extensive characterization of Notch signaling during bone fracture healing has not been reported. Therefore, the objective of this study was to rigorously characterize and compare activation of the Notch signaling pathway during endochondral and intramembranous bone regeneration, using tibial fracture healing (TF) as a model of endochondral bone repair and calvarial defect healing (CD) as a model of intramembranous bone repair. We hypothesize that Notch signaling components are active during murine tibial fracture and calvarial defect healing.

3.2 Methods

3.2.1 Experimental Design

All *in vivo* protocols were approved by the IACUC. Bilateral tibial fractures or bilateral calvarial defects were created in 8-11 week old male C57Bl/6 mice to evaluate Notch signaling during endochondral and intramembranous bone healing, respectively. Specimens were harvested at 0, 5, 10 and 20 days post-fracture (dpf). Quantitative real-time polymerase chain reaction (QPCR) was used to quantify gene expression of Notch pathway components including ligands (Jag1,2, Dll1,4), receptors (Notch1-4), and target genes (Hes1, Hey1,2,L) (n=4-5). Immunohistochemistry (IHC) was used to identify cell types that express the Jag1 ligand and the activated form of the Notch2 receptor, called the Notch2 intracellular domain (NICD2).

3.2.2 Tibial Fracture (TF) Procedure

Closed, transverse, mid-diaphyseal bilateral tibial fractures were created similar to previously published methods [22]. Briefly, under isoflurane anesthesia, a small incision was made medial to the tuberosity. A canal was punctured through the cortex using a 26-gauge needle, and a 0.009-inch diameter rod was inserted through the length of the intramedullary canal. The incision was closed with surgical glue. Fractures were created using a custom made

three-point bending apparatus. Radiographs were generated to verify correct pin placement and fracture location (Faxitron X-Ray) (Figure 3.1A). 0.05 mg/kg of buprenorphine was administered subcutaneously once after surgery. Mice recovered on heating pads and were fed ad libitum.

3.2.3 Calvarial Defect (CD) Procedure

Bilateral 1.5 mm diameter calvarial defects were created similar to previously published methods [23]. Under isoflurane anesthesia, the mouse was placed into stereotaxic equipment (Stoelting) and a sterile tegaderm drape (3M Health Care) was applied to the cranium after hair removal (Nair, Church & Dwight). A midline incision exposed the parietal bones, and a 1.5 mm diameter biopsy punch (Premier) was used to create a defect in the central portion of each parietal bone, leaving the surrounding periosteum intact (Figure 3.1B). PBS was used to hydrate the tissue. The incision was closed with 5-0 prolene non-absorbable sutures (Ethicon). 0.05 mg/kg of buprenorphine was administered subcutaneously once after surgery. Mice recovered on heating pads and were fed ad libitum.

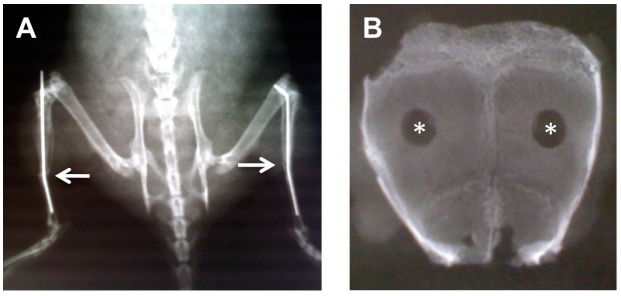

Figure 3.1. Radiographs of closed, transverse, mid-diaphyseal bilateral fractures with intramedullary pin stabilization taken at the time of injury (A), and 1.5 mm diameter bilateral calvarial defects taken at the time of harvest (B). Radiographs were acquired at 15 sec with 25 kV.

3.2.4 Quantitative Real-Time Polymerase Chain Reaction (QPCR)

Fractured tibial calluses were dissected from the surrounding soft tissue at 5, 10 and 20 dpf. Uninjured diaphyseal bone, flushed of marrow, served as 0 dpf controls. Calvarial defects were dissected at 5, 10 and 20 dpf using a 3 mm diameter punch to excise the defect and

surrounding bone tissue. Uninjured calvarial bone was similarly dissected for 0 dpf controls. Tissue was placed in Qiazol lysis reagent (Qiagen) and homogenized using the Tissue Tearor (BioSpec Products). mRNA was extracted using the Qiagen miRNeasy Mini Kit with DNase digestion to remove DNA contamination. RNA yield was determined spectrophotometrically. 1 μg of mRNA was reverse transcribed into cDNA using the Applied Biosystems High Capacity RNA-to-cDNA Kit. Gene expression was quantified from 0.5 μl of cDNA in 10 μl of Power SYBR Green PCR Master Mix (Applied Biosystems) using a 7500 Fast Real-Time PCR system (Applied Biosystems). For each gene of interest, samples were run in duplicate with several controls per primer set to verify that the measured signal was not due to DNA contamination or primer dimer binding. Proper amplicon formulation was confirmed by melt curve analysis.

Fracture healing involves a temporally changing profile of cells derived from different lineages. Although there is no ideal housekeeping gene for normalization across different cell types, a series of genes were identified that show minimal variation in expression [24]. We included three of those genes, run in duplicate and averaged together, as our housekeeping control: β-actin, which regulates cell motility; ornithine decarboxylase antizyme (OAZ1), which regulates polyamine synthesis; and 40S ribosomal protein 29 (RPS29), a component of the 40S ribosomal subunit that regulates protein synthesis. QPCR data is presented as relative gene expression to housekeeping control, calculated using the formula $2^{-\Delta C(t)}$, where $\Delta C(t)$ is the difference in C(t) values between the gene of interest and the average of all three housekeeping genes.

3.2.5 Histology and Immunohistochemistry (IHC)

Tissue was fixed in 4% paraformaldehyde at 4°C for 2-3 days, decalcified in a 4% hydrochloric acid 4% formic acid solution, paraffin embedded, and sectioned into 5 μm longitudinal slices. For Jag1 and NICD2 IHC, sections were deparaffinized and gradually hydrated. Sections were treated with blocking serum (5% donkey, 4% BSA, 0.1% Triton-X 100, 0.05% Tween 20) for 60 minutes at room temperature. Primary antibodies goat Jag1 (Santa Cruz

sc-6011, 1:100) and rabbit cleaved NICD2 (Millipore 07-1234, 1:100) were incubated in a dilution buffer (2% BSA, 0.25% Triton-X 100) overnight at 4°C in a humidified chamber. Control sections were treated with goat IgG (Santa Cruz sc-2028, 1:200) or rabbit IgG (Santa Cruz sc-2027, 1:200) to match the concentration of the appropriate antibody. Sections were then treated with 3% H_2O_2 for 30 minutes at room temperature, followed by biotinylated secondary antibody donkey anti-goat (Santa Cruz sc-2043, 1:200) or donkey anti-rabbit (Santa Cruz sc-2089, 1:200) for 30 minutes at room temperature, and finally streptavidin-HRP (Abcam ab7403, 1:500) for 30 minutes at room temperature. Sections were developed with DAB (Vector SK-4100) and counterstained with Hematoxylin. Additional sections were stained with Hematoxylin and Eosin (H&E) for 15 and 2.5 minutes, respectively, or 0.1% Safranin O and 0.03% Fast Green (SafO) for 5 minutes each to visualize tissue structure and cell morphology. Slides were imaged in brightfield with an Olympus BX51. Color images were acquired with a Spot RT3 2 megapixel camera.

3.2.6 Statistical Analysis

Significance was assessed by one-way ANOVAs comparing the effect of time on gene expression during TF and CD separately, followed by Tukey's post-hoc test. Pairwise t-tests were made to evaluate the level of gene expression during TF vs. CD at each time point.

3.3 Results

3.3.1 Validation of TF and CD Models for EO and IO, Respectively

Stabilized tibial fractures have been shown to heal primarily through endochondral ossification, whereas calvarial defects have been shown to heal via intramembranous ossification. We further set out to verify these injuries as appropriate models to study endochondral and intramembranous bone repair by quantifying gene expression of collagen type II (Col2), a marker of cartilage formation, and osteocalcin (Ocn), a marker of bone formation, and by analyzing SafO histology for cartilage formation.

During tibial fracture healing (TF), Col2 was transiently upregulated, whereas Ocn was initially downregulated and then upregulated later (Figure 3.2). Histology confirmed extensive cartilage in the callus at 10 dpf, which was replaced with bone through endochondral ossification by 20 dpf. During calvarial defect healing (CD), Col2 expression did not change, whereas Ocn was upregulated. The absence of cartilage formation confirmed by histology verifies healing through intramembranous ossification.

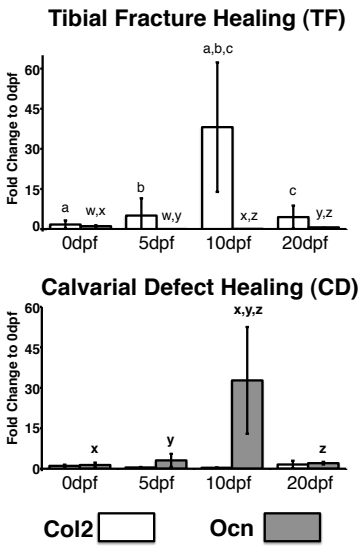

Figure 3.2. Col2 and Ocn gene expression during TF and CD. Col2 is up-regulated during TF but not CD. Ocn is up-regulated during CD, and also during TF between 10dpf and 20dpf. A common letter above any two bars indicates a significant difference between those time points ($p<0.05$). Data presented as fold change to 0dpf, calculated by $2^{-\Delta\Delta C(t)}$.

3.3.2 Comparison of Notch Gene Expression Over Time During TF and CD

Tissue was collected at 0, 5, 10 and 20 dpf for quantitation of Notch ligand, receptor and target gene expression. All Notch genes examined were upregulated over time during TF (Figure 3.3). Generally, the most highly expressed ligand, receptor and target gene during TF (relative to each other) were Jag1, Notch2 and Hes1, whereas the least expressed were Dll4, Notch4 and Hey2. The ligand, receptor and target gene that showed the greatest change (upregulation) during TF (relative to 0 dpf) were Jag2 (71-fold, 10 dpf), Notch4 (19-fold, 10 dpf) and Hes1 (172-fold, 10 dpf).

Only Jag1, Notch2 and Notch4 were upregulated over time during CD. However, consistent with TF, the most highly expressed ligand, receptor and target gene during CD (relative to each other) were Jag1, Notch2 and Hes1, whereas the least expressed were Dll1, Notch4 and Hey2. The ligand, receptor and target gene that showed the greatest change (upregulation) during CD (relative to 0 dpf) were Jag1 (4.2-fold, 10 dpf), Notch4 (11-fold, 20 dpf) and HeyL (2.4-fold, 10 dpf).

3.3.3 Comparison of Notch Gene Expression During TF vs. CD at Each Time Point

We next compared the level of expression for each gene (relative to housekeeping gene expression) during TF vs. CD at each time point (0, 5, 10 and 20 dpf). Basal expression levels (0 dpf) of Jag1, Dll4, Notch1, Notch2, Notch3, Hes1, Hey1, Hey2, and HeyL were higher in uninjured calvaria. No genes were expressed higher in uninjured tibiae (Figure 3.3).

After injury (5, 10, 20 dpf), a greater number of genes were more highly expressed (relative to housekeeping gene expression) during TF compared to CD. Jag2, Dll1, Notch1, Notch3 and Notch4 were greater during TF, whereas Notch2 and Hey2 were greater during CD. Hes1 was the only gene to show variable expression during both CD and TF at different time points.

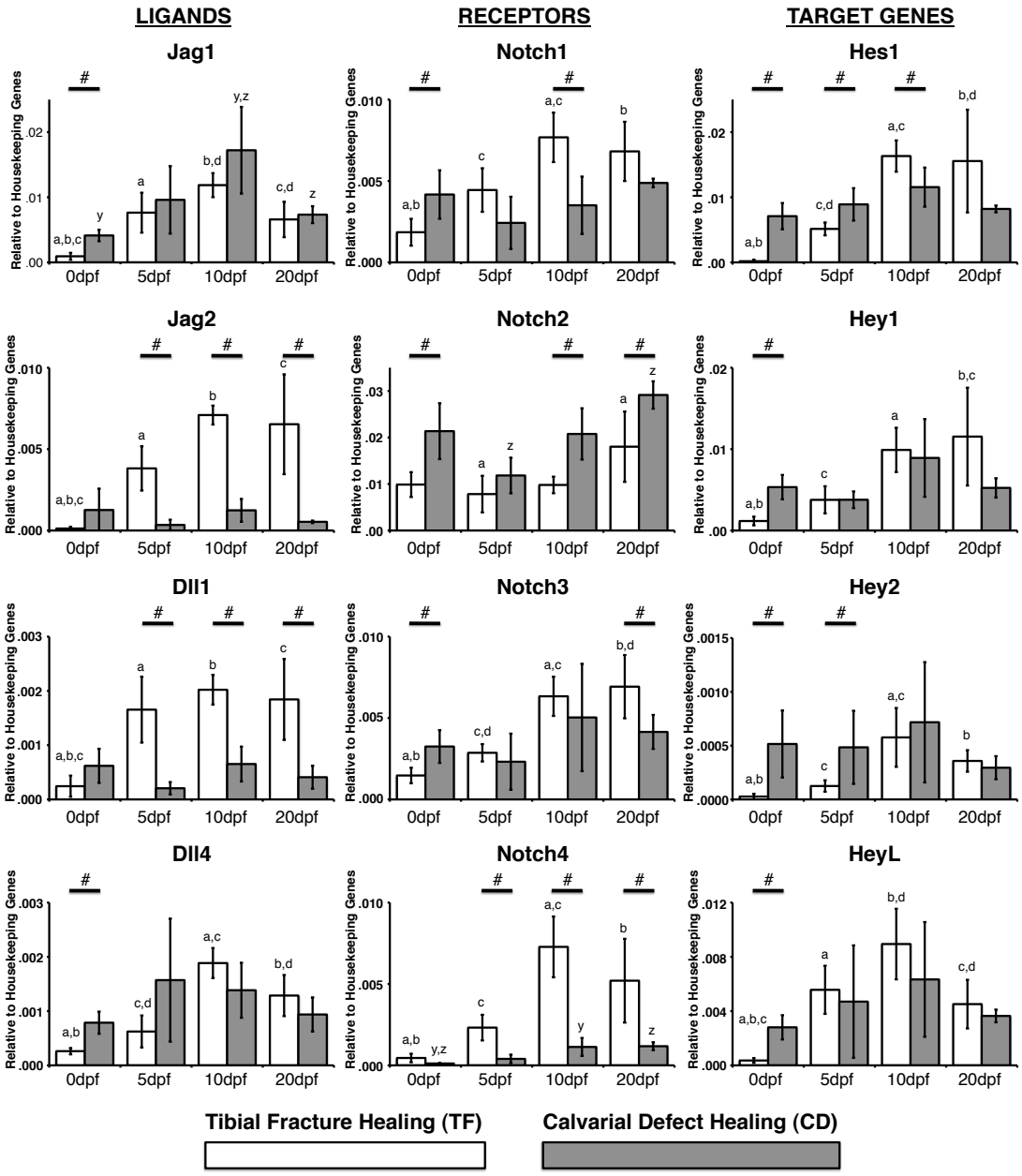

Figure 3.3. Gene expression of Notch ligands (left), receptors (middle) and target genes (right) during TF (white bars) and CD (grey bars). # indicates a significant difference between TF vs. CD at a given time point ($p<0.05$). A common letter above any two bars indicates a significant difference between those time points during TF (a,b,c) or CD (x,y,z) ($p<0.05$). Data is presented as relative gene expression to the housekeeping genes, calculated using the formula $2^{-\Delta C(t)}$ (arbitrary units).

3.3.4 Identification of Cells That Express Jagged1 and NICD2 During TF

Consistent with previous studies investigating mesenchymal tissues [12, 13, 25], Jag1 and Notch2 were the predominantly expressed ligand and receptor during both TF and CD at all time points. Therefore, using IHC, we identified cells that express the Jag1 ligand and the activated form of the Notch2 receptor, called the Notch2 intracellular domain (NICD2), which is indicative of activated Notch signaling.

Jag1 and NICD2 were expressed in identical cell populations that participate in endochondral bone repair during TF (Figure 3.4). Interestingly, it appears that more cells stain positive for NICD2 than Jag1 (non-statistical comparison). At 5 dpf, undifferentiated mesenchymal cells undergo rapid proliferation to produce a fibrovascular callus. These cells are largely Jag1 and NICD2 positive (Figure 3.4A, black arrows), though isolated cells appear negative (white arrows). By 10 dpf, these progenitors gradually lose Jag1 and NICD2 expression as they differentiate into proliferative (Figure 3.4B), pre-hypertrophic (Figure 3.4C), and finally hypertrophic chondrocytes (Figure 3.4D) when they become largely Jag1 and NICD2 negative. During the cartilage-to-bone transition at 10 dpf, mineralized cartilage is resorbed allowing for vascular invasion of the callus. Many vascular endothelial cells that penetrate the matrix are Jag1 and NICD2 positive (Figure 3.5). Surprisingly, terminal hypertrophic chondrocytes that populate the chondro-osseous junction and border the invading vasculature appear to re-express Jag1 and NICD2 (Figures 3.4E and 3.5). The vascular network mediates an influx of Jag1 and NICD2 positive osteoprogenitor cells that lay the initial osteoid matrix on top of the resorbing cartilage (Figure 3.4F). By 20 dpf, these cells differentiate into immature and mature osteoblasts to produce primary (Figure 3.4G) and remodeled bone (Figure 3.4H), and continue to overwhelmingly, but not completely, express Jag1 and NICD2. Osteocytes embedded in remodeled bone are both positive and negative for Jag1 and NICD2 (Figure 3.4H). IgG control slides show no positive staining (Figure 3.4 bottom two rows). Figure 3.6 provides further evidence of these observations during TF. Localization of Jag1 and NICD2 to terminal hypertrophic chondrocytes, areas of vascular invasion, and immature osteoblasts was also

observed in growth plates of uninjured adult mice (Figure 3.7). However, pre-hypertrophic chondrocytes appear to stain more negative in the growth plate than in the fracture callus.

3.3.5 Identification of Cells That Express Jagged1 and NICD2 During CD

Jag1 and NICD2 were also expressed in identical cell populations that participate in intramembranous bone repair during CD (Figure 3.8). Following injury, periosteal-derived osteoprogenitors rapidly proliferate to re-establish a fibrous layer surrounding the defect (Figure 3.8A). At the same time, undifferentiated mesenchymal cells within the defect proliferate to produce fibrovascular tissue that initially fills the defect (Figure 3.8B). Cells that line the defect appear to have initiated early stages of osteogenesis. Consistent with TF, these cell populations are overwhelmingly, though not completely, Jag1 and NICD2 positive. Also consistent with TF, cells at various stages of osteogenic maturity continue to stain positive for Jag1 and NICD2 in areas of new (Figure 3.8C) and remodeled bone (Figure 3.8D). Furthermore, osteocytes embedded in remodeled bone are both positive and negative for Jag1 and NICD2 (Figure 3.8D). IgG control slides show no positive staining (Figure 3.8 bottom two rows). Figure 3.9 provides further evidence of these observations during CD. Localization of Jag1 and NICD2 was also observed in osteoblasts lining uninjured calvarial bone, and to a lesser extent periosteal-derived cells (Figure 3.7). However, more osteocytes appear to stain negative in uninjured bone than in healing calvarium.

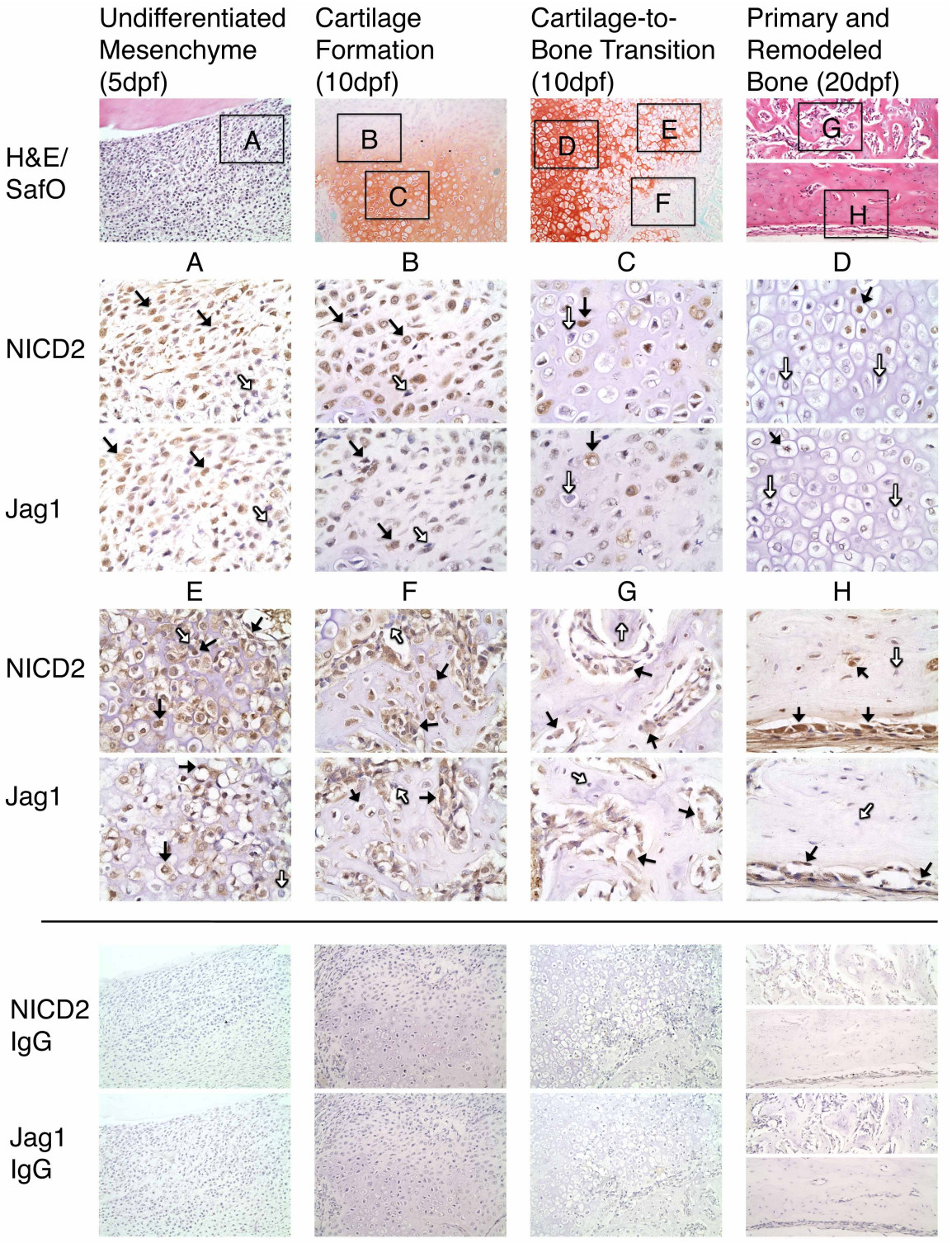
Undifferentiated Mesenchyme (5dpf)
Cartilage Formation (10dpf)
Cartilage-to-Bone Transition (10dpf)
Primary and Remodeled Bone (20dpf)
H&E/ SafO
A
B
C
D
E
F
G
H
NICD2
Jag1
NICD2 IgG
Jag1 IgG

Figure 3.4 (above). Jag1 and NICD2 are expressed in identical cell populations that participate in endochondral bone repair during TF. Undifferentiated mesenchymal cells (A) are largely positive (brown staining, black arrows), but expression gradually decreases as cells differentiate into proliferative (B), pre-hypertrophic (C), and hypertrophic chondrocytes (D), and then is re-expressed in terminal hypertrophic chondrocytes (E). Alternative to chondrogenesis, osteogenic cells at various stages of maturity, located in osteoid (F), primary (G) and remodeled bone formation (H) are mostly positive. Note that varying amounts of Jag1 and NICD2 negative cells are present in distinct cell population (white arrows). H&E and SafO images acquired at 200X magnification. Jag1 and NICD2 images acquired at 600X magnification. IgG control sections show no positive staining (bottom two rows, 200X magnification)

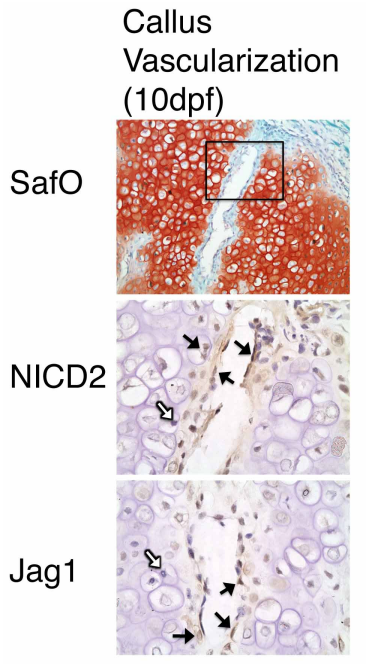

Figure 3.5. Jag1 and NICD2 are expressed in vascular endothelial cells invading the cartilage matrix, as well as terminal hypertrophic chondrocytes adjacent to the invading vasculature. Black arrows and brown staining indicate positive cells. White arrows indicate negative cells. SafO image acquired at 200X magnification. Jag1 and NICD2 images acquired at 600X magnification

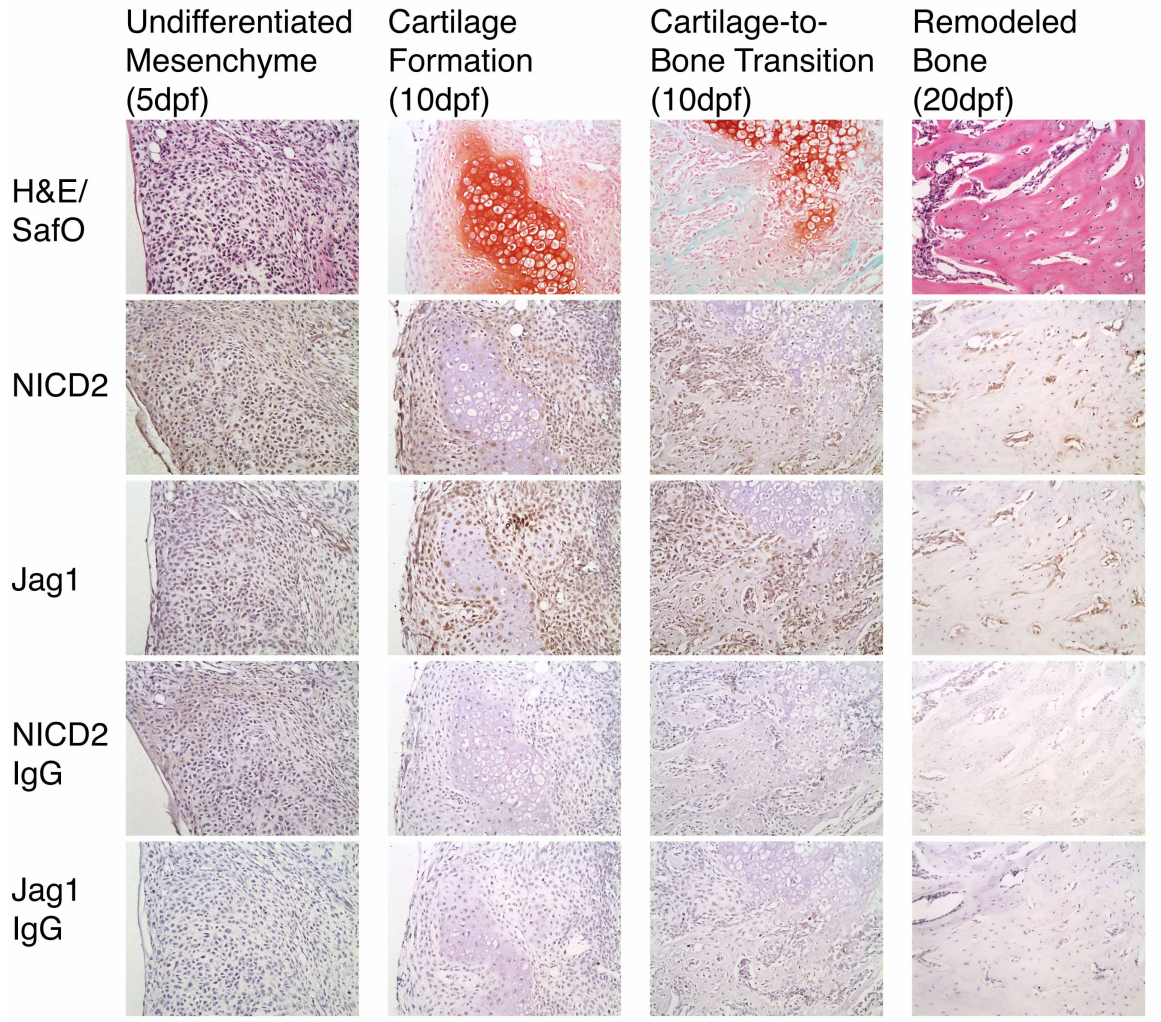

Figure 3.6. Another example of Jag1 and NICD2 immunolocalization during TF with IgG control sections (related to Figure 3.4). Images acquired at 200X magnification.

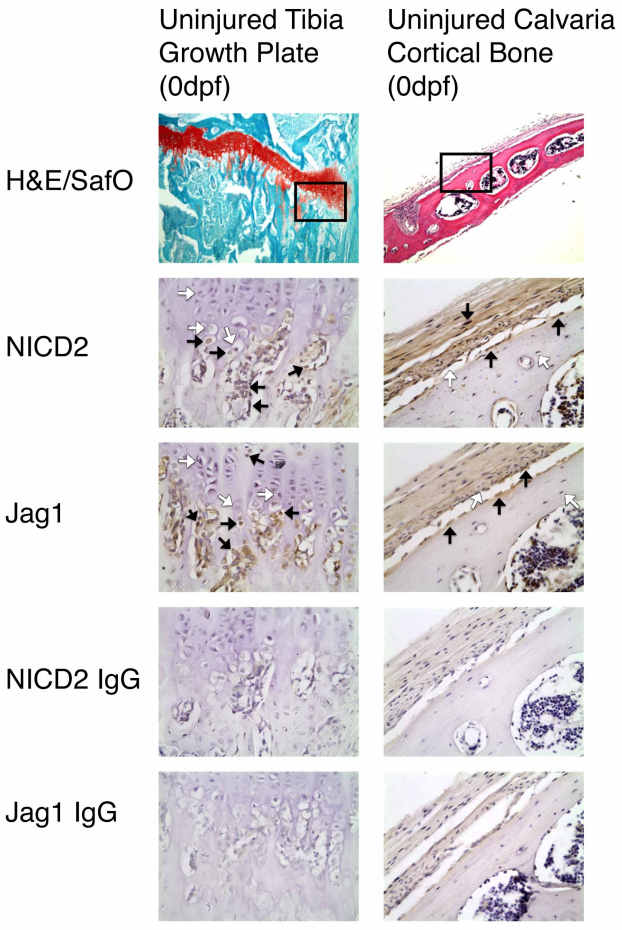

Figure 3.7. Jag1 and NICD2 expression in uninjured tibial growth plate and calvarium. In growth plates, Jag1 and NICD2 are mostly not expressed in pre-hypertrophic and hypertrophic chondrocytes (white arrows). However, at the chondro-osseus junction, terminal hypertrophic chondrocytes express Jag1 and NICD2, as do areas of vascular invasion and immature osteoblasts lining the trabecular spongiosa (black arrows). In calvarium, osteoblasts lining cortical bone as well as some periosteal-derived mesenchymal cells are Jag1 and NICD2 positive. Osteocytes are mostly Jag1 and NICD2 negative. H&E and SafO images acquired at 100X magnification. Jag1 and NICD2 images acquired at 400X magnification.

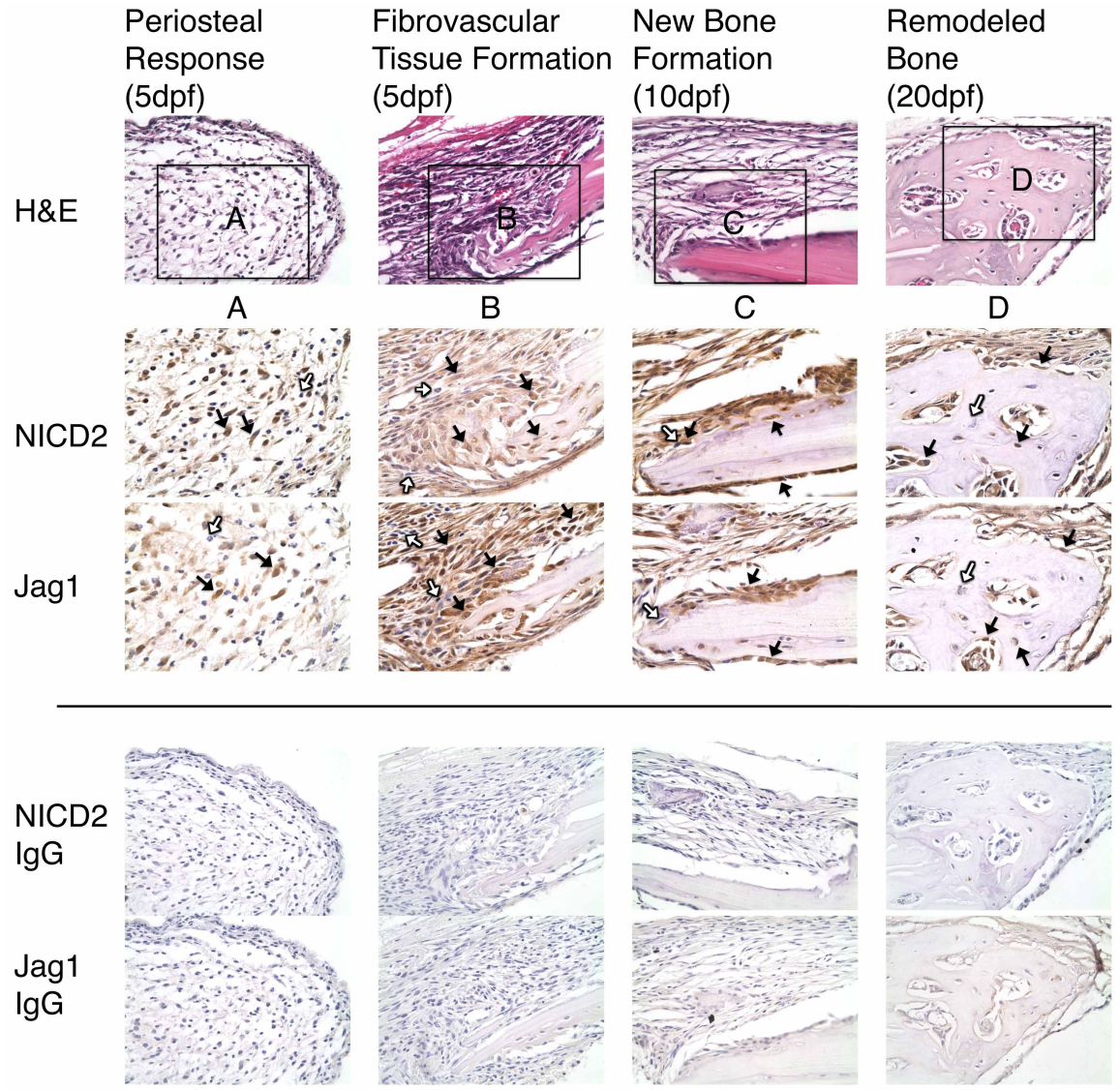

Figure 3.8. Jag1 and NICD2 are expressed in identical cell populations that participate in intramembranous bone repair during CD. Undifferentiated mesenchymal cells located in the periosteum (A) and adjacent to the defect site (B) are largely positive (brown staining, black arrows). As osteogenesis progresses, cells at various stages of maturity continue to stain positive in areas of new (C) and remodeled bone (D). Osteocytes (D) are both positive and negative. Note that Jag1 and NICD2 negative cells (white arrows) are present in each area. H&E images acquired at 400X magnification. Jag1 and NICD2 images acquired at 600X magnification. IgG control sections show no positive staining (bottom two rows, 200X magnification).

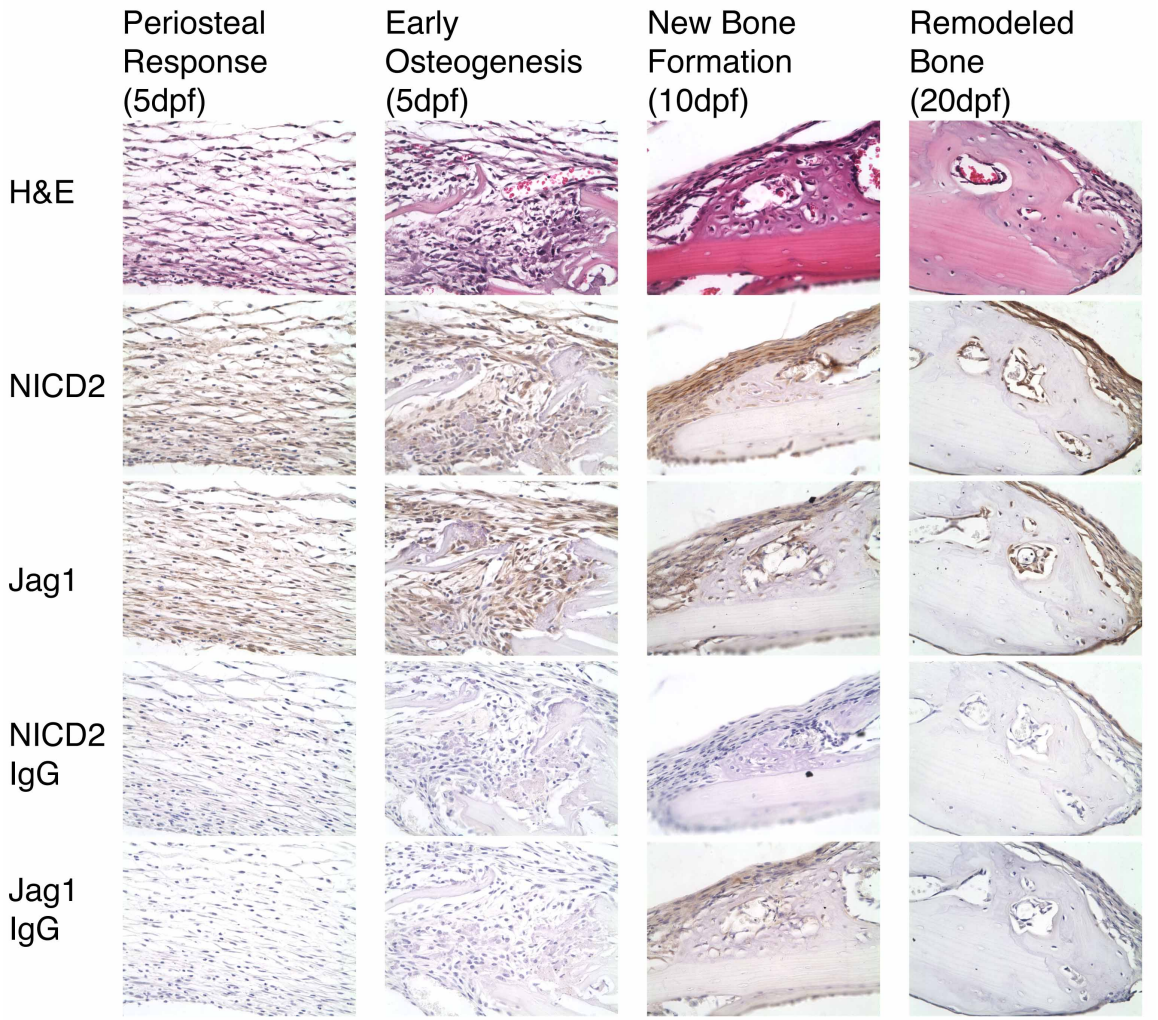

Figure 3.9. Another example of Jag1 and NICD2 immunolocalization during CD with IgG control sections (related to Figure 3.8). Images acquired at 200X magnification.

3.4 Discussion

This is the first study to extensively characterize the Notch signaling pathway during endochondral and intramembranous bone fracture healing, which has previously been shown to be required for proper embryological bone development [10-13, 26]. Our results demonstrate that Notch signaling components are actively regulated during both endochondral and intramembranous fracture healing.

Consistent with previous studies, we identified Jag1 and Notch2 as the predominantly expressed ligand and receptor during TF and CD [12-14, 25]. This Notch ligand-receptor pair has been shown to primarily interact with one another in a variety of cell types [27]. We further identified Jag1 and activated Notch2 (NICD2) to be expressed in the same cell populations during endochondral and intramembranous repair. Jag1 and NICD2 expression is strong in undifferentiated mesenchymal cells, but gradually decreases during chondrogenesis. Previous studies have shown that transient activation of Notch components, including Jag1, is required in uncommitted mesenchymal progenitor cells both *in vivo* and *in vitro*, but must downregulate in order to initiate chondrogenesis [25, 28]. Furthermore, sustained activation of Notch signaling in committed chondrocytes (cells that express the Col2a1 promoter) inhibits both proliferation and differentiation [26]. Many studies have specifically shown that Notch negatively regulates the pre-hypertrophic to hypertrophic chondrocyte transition [13, 26, 28, 29]. NICD and its downstream target genes Hes1 and Hey1 are known to inhibit chondrogenic differentiation by binding to a Sox9 binding site on the Col2a1 promoter [26, 30]. Collectively, the data suggests decreased Notch signaling occurs during chondrogenic lineage commitment and hypertrophic maturation.

This is the first study to show that terminal hypertrophic chondrocytes have the ability to re-express Jag1 and NICD2 in areas that have been infiltrated by Jag1 and NICD2 positive vascular endothelial cells. This applies to the chondro-osseous junction in both the callus during endochondral fracture healing, and in the growth plate during endochondral bone formation. This is consistent with a previous study, which showed that although Notch signaling negatively regulates hypertrophic chondrocyte differentiation, it positively regulates the progression of

hypertrophic chondrocytes to their terminal differentiation, identified by Mmp-13 expression, at the chondro-osseous junction in the growth plate [13]. The Notch signaling pathway is initiated through direct cell-to-cell contact. It is plausible that this re-activation is initiated by endothelial-mesenchymal cell interactions, whereas prior activation of Notch signaling was initiated by mesenchymal-mesenchymal cell interactions. However, more research is required to understand the mechanism of this re-activation as well as the functional significance of Notch signaling in terminal hypertrophic chondrocytes.

Alternative to chondrogenesis, Jag1 and NICD2 are expressed in osteogenic cells at all stages of differentiation. Although this is the first study to show this via histology *in vivo*, Notch signaling has previously been shown to perform pro-osteogenic functions in osteoblasts at all stages of differentiation. Activation of Notch signaling in uncommitted mesenchymal progenitors (cells that express the Prx1 promoter [31]) maintains cells in an undifferentiated state while stimulating proliferation [12, 13]. However, alternative to chondrogenesis, activation of Notch signaling in osteoprogenitors (Col3.6 promoter [32]) and committed but immature osteoblasts (Col2.3 promoter [32]) continues to promote proliferation while inhibiting differentiation [10, 11, 14]. Notch pathway components have been shown to prevent early and late osteoblast differentiation by binding to Runx2 (NICD1, Hes1, Hey1) [10, 13, 33] and the Ocn promoter (Hes1) [34]. Interestingly, instead of directly regulating bone formation, activation of Notch signaling in mature osteoblasts (Ocn promoter) reduces bone resorption by inhibiting osteoclast differentiation [13-15]. Collectively, the data suggests that during endochondral and intramembranous fracture healing, elevated levels of Notch signaling in undifferentiated cells may serve to increase the number of progenitors available to differentiate and produce a mature tissue matrix, and that Notch signaling in mature osteoblasts maintains the tissue matrix through a negative feed-back of osteoclast-mediated bone resorption.

In addition to regulating osteoblast and chondrocyte behavior, Notch signaling also regulates angiogenesis, which is critical for fracture healing. Dll4 signaling through Notch1 has been shown to restrict angiogenesis [35], whereas Jag1 is pro-angiogenic [36]. Not surprisingly Jag1 was the only ligand upregulated during both TF and CD, whereas Dll4 was the least

expressed ligand during TF. Notch4 has been shown to have a redundant angiogenic function to Notch1 [37]. Consistent with this, our data showed that Notch4 was the least expressed receptor during both TF and CD. However, Notch4 was one of only two receptors to be upregulated during both TF and CD, and also demonstrated the greatest fold change among all receptors relative to 0 dpf, suggesting that while redundant, it still may play an active role in the Notch-mediated angiogenic response during bone repair.

When considered in total, Notch ligands demonstrated a higher magnitude of change during healing than receptors, suggesting that downstream target gene activation may be more regulated by ligand rather than receptor activity. Manipulations of Notch signaling to enhance fracture healing could possibly target ligand expression for the most potent therapeutic effect.

Previous studies have shown that bones derived from different embryological germ layers have distinct tissue matrix compositions [38]. The calvarium and tibia originate from the ectoderm and mesoderm, respectively [39], which may explain the difference in basal expression levels of Notch genes in those tissues. There are injury models that would allow for comparison of endochondral and intramembranous fracture healing using a single long bone, which would control for factors intrinsic to the tissue. It is possible that Notch signaling may not be equivalent during intramembranous ossification in all types of bone. However, in this study we show that expression of Notch components are equivalently localized in osteogenic cells regardless of germ layer origin, embryological development, or method of healing, which may suggest that similar results would be expected in all models of bone repair. Importantly, we chose our injury models in order to develop a broader understanding of Notch signaling with applications to both craniofacial and long bone skeletal regeneration.

In conclusion, this study demonstrates that Notch signaling is upregulated during endochondral and intramembranous bone repair, with expression generally greater during endochondral repair. Furthermore, Jag1 and NICD2 are expressed in identical cell populations during healing, with expression gradually decreasing during chondrogenesis, but remaining present at multiple stages of osteoblastogenesis. Targeting the Notch signaling pathway may ultimately provide a mechanism to enhance bone repair; however, much more research is

required to understand the spatiotemporal effects of Notch signaling in mesenchymal, hematopoietic and vascular cells.

3.5 References

1. Vortkamp A, Pathi S, Peretti GM, et al., Recapitulation of signals regulating embryonic bone formation during postnatal growth and in fracture repair. Mech Dev, 1998. 71(1-2): p. 65-76.
2. Ferguson C, Alpern E, Miclau T, et al., Does adult fracture repair recapitulate embryonic skeletal formation? Mech Dev, 1999. 87(1-2): p. 57-66.
3. Einhorn TA, The cell and molecular biology of fracture healing. Clin Orthop Relat Res, 1998(355 Suppl): p. S7-21.
4. Tsuji K, Bandyopadhyay A, Harfe BD, et al., BMP2 activity, although dispensable for bone formation, is required for the initiation of fracture healing. Nat Genet, 2006. 38(12): p. 1424-9.
5. Yu YY, Lieu S, Lu C, et al., Bone morphogenetic protein 2 stimulates endochondral ossification by regulating periosteal cell fate during bone repair. Bone, 2010. 47(1): p. 65-73.
6. Friedlaender GE, Perry CR, Cole JD, et al., Osteogenic protein-1 (bone morphogenetic protein-7) in the treatment of tibial nonunions. J Bone Joint Surg Am, 2001. 83-A Suppl 1(Pt 2): p. S151-8.
7. Govender S, Csimma C, Genant HK, et al., Recombinant human bone morphogenetic protein-2 for treatment of open tibial fractures: a prospective, controlled, randomized study of four hundred and fifty patients. J Bone Joint Surg Am, 2002. 84-A(12): p. 2123-34.
8. Minear S, Leucht P, Jiang J, et al., Wnt proteins promote bone regeneration. Sci Transl Med, 2010. 2(29): p. 29ra30.
9. Komatsu DE, Mary MN, Schroeder RJ, et al., Modulation of Wnt signaling influences fracture repair. J Orthop Res, 2010. 28(7): p. 928-36.
10. Engin F, Yao Z, Yang T, et al., Dimorphic effects of Notch signaling in bone homeostasis. Nat Med, 2008. 14(3): p. 299-305.

11. Tao J, Chen S, Yang T, et al., Osteosclerosis owing to Notch gain of function is solely Rbpj-dependent. J Bone Miner Res, 2010. 25(10): p. 2175-83.

12. Dong Y, Jesse AM, Kohn A, et al., RBPjkappa-dependent Notch signaling regulates mesenchymal progenitor cell proliferation and differentiation during skeletal development. Development, 2010. 137(9): p. 1461-71.

13. Hilton MJ, Tu X, Wu X, et al., Notch signaling maintains bone marrow mesenchymal progenitors by suppressing osteoblast differentiation. Nat Med, 2008. 14(3): p. 306-14.

14. Zanotti S, Smerdel-Ramoya A, Stadmeyer L, et al., Notch inhibits osteoblast differentiation and causes osteopenia. Endocrinology, 2008. 149(8): p. 3890-9.

15. Bai S, Kopan R, Zou W, et al., NOTCH1 regulates osteoclastogenesis directly in osteoclast precursors and indirectly via osteoblast lineage cells. J Biol Chem, 2008. 283(10): p. 6509-18.

16. Gude NA, Emmanuel G, Wu W, et al., Activation of Notch-mediated protective signaling in the myocardium. Circ Res, 2008. 102(9): p. 1025-35.

17. Oya S, Yoshikawa G, Takai K, et al., Attenuation of Notch signaling promotes the differentiation of neural progenitors into neurons in the hippocampal CA1 region after ischemic injury. Neuroscience, 2009. 158(2): p. 683-92.

18. Okamoto R, Tsuchiya K, Nemoto Y, et al., Requirement of Notch activation during regeneration of the intestinal epithelia. Am J Physiol Gastrointest Liver Physiol, 2009. 296(1): p. G23-35.

19. Hayes S, Nelson BR, Buckingham B, et al., Notch signaling regulates regeneration in the avian retina. Dev Biol, 2007. 312(1): p. 300-11.

20. Chigurupati S, Arumugam TV, Son TG, et al., Involvement of notch signaling in wound healing. PLoS One, 2007. 2(11): p. e1167.

21. Conboy IM, Conboy MJ, Smythe GM, et al., Notch-mediated restoration of regenerative potential to aged muscle. Science, 2003. 302(5650): p. 1575-7.

22. Taylor DK, Meganck JA, Terkhorn S, et al., Thrombospondin-2 influences the proportion of cartilage and bone during fracture healing. J Bone Miner Res, 2009. 24(6): p. 1043-54.

23. Aalami OO, Nacamuli RP, Lenton KA, et al., Applications of a mouse model of calvarial healing: differences in regenerative abilities of juveniles and adults. Plast Reconstr Surg, 2004. 114(3): p. 713-20.

24. de Jonge HJ, Fehrmann RS, de Bont ES, et al., Evidence based selection of housekeeping genes. PLoS One, 2007. 2(9): p. e898.

25. Oldershaw RA, Tew SR, Russell AM, et al., Notch signaling through Jagged-1 is necessary to initiate chondrogenesis in human bone marrow stromal cells but must be switched off to complete chondrogenesis. Stem Cells, 2008. 26(3): p. 666-74.

26. Mead TJ and Yutzey KE, Notch pathway regulation of chondrocyte differentiation and proliferation during appendicular and axial skeleton development. Proc Natl Acad Sci U S A, 2009. 106(34): p. 14420-5.

27. Shimizu K, Chiba S, Kumano K, et al., Mouse jagged1 physically interacts with notch2 and other notch receptors. Assessment by quantitative methods. J Biol Chem, 1999. 274(46): p. 32961-9.

28. Watanabe N, Tezuka Y, Matsuno K, et al., Suppression of differentiation and proliferation of early chondrogenic cells by Notch. J Bone Miner Metab, 2003. 21(6): p. 344-52.

29. Crowe R, Zikherman J and Niswander L, Delta-1 negatively regulates the transition from prehypertrophic to hypertrophic chondrocytes during cartilage formation. Development, 1999. 126(5): p. 987-98.

30. Grogan SP, Olee T, Hiraoka K, et al., Repression of chondrogenesis through binding of notch signaling proteins HES-1 and HEY-1 to N-box domains in the COL2A1 enhancer site. Arthritis Rheum, 2008. 58(9): p. 2754-63.

31. Logan M, Martin JF, Nagy A, et al., Expression of Cre Recombinase in the developing mouse limb bud driven by a Prxl enhancer. Genesis, 2002. 33(2): p. 77-80.

32. Kalajzic I, Kalajzic Z, Kaliterna M, et al., Use of type I collagen green fluorescent protein transgenes to identify subpopulations of cells at different stages of the osteoblast lineage. J Bone Miner Res, 2002. 17(1): p. 15-25.

33. Zamurovic N, Cappellen D, Rohner D, et al., Coordinated activation of notch, Wnt, and transforming growth factor-beta signaling pathways in bone morphogenic protein 2-induced osteogenesis. Notch target gene Hey1 inhibits mineralization and Runx2 transcriptional activity. J Biol Chem, 2004. 279(36): p. 37704-15.

34. Zhang Y, Lian JB, Stein JL, et al., The Notch-responsive transcription factor Hes-1 attenuates osteocalcin promoter activity in osteoblastic cells. J Cell Biochem, 2009. 108(3): p. 651-9.

35. Hellstrom M, Phng LK, Hofmann JJ, et al., Dll4 signalling through Notch1 regulates formation of tip cells during angiogenesis. Nature, 2007. 445(7129): p. 776-80.

36. Benedito R, Roca C, Sorensen I, et al., The notch ligands Dll4 and Jagged1 have opposing effects on angiogenesis. Cell, 2009. 137(6): p. 1124-35.

37. Krebs LT, Xue Y, Norton CR, et al., Notch signaling is essential for vascular morphogenesis in mice. Genes Dev, 2000. 14(11): p. 1343-52.

38. van den Bos T, Speijer D, Bank RA, et al., Differences in matrix composition between calvaria and long bone in mice suggest differences in biomechanical properties and resorption: Special emphasis on collagen. Bone, 2008. 43(3): p. 459-68.

39. Chung UI, Kawaguchi H, Takato T, et al., Distinct osteogenic mechanisms of bones of distinct origins. J Orthop Sci, 2004. 9(4): p. 410-4.

CHAPTER 4

Inhibition of Canonical Notch Signaling Results in Sustained Callus Inflammation and Alters Multiple Phases of Fracture Healing

4.1 Introduction

Bone fracture healing occurs through a series of carefully regulated spatiotemporal events. Following injury, inflammation and hematoma formation mediates an influx of undifferentiated mesenchymal cells to the site of injury. During endochondral fracture healing, these cells undergo chondrogenesis to produce a cartilaginous callus that mineralizes and is resorbed permitting vascular invasion of the callus. The vascular network mediates an influx of osteoprogenitor cells that differentiate to produce immature bone on top of the resorbing cartilage matrix. Callus bone matures and is remodeled over time through osteoblast-mediated bone formation and osteoclast-mediated bone resorption [1].

Bone fractures are a significant clinical and economic problem. While the majority of fractures restore original structure and function in a scarless manner, some fractures result in delayed or non-union healing [2]. This increases the cost of care, necessitates additional surgeries, and results in a prolonged period of convalescence, which is associated with increased mortality in an aged population [3]. Common therapeutic strategies such as autologous bone grafts and bone morphogenetic proteins have well-documented limitations [4, 5]. Therefore, a clinical need persists for the development of new methods to enhance healing. Although the spatiotemporal progressions of fracture healing are well-characterized [1], the signaling pathways that regulate these events required for healing are not as well understood. Identifying and elucidating the roles of signaling pathways that regulate fracture healing will allow us to identify novel therapeutic targets for improved regeneration of bone.

Notch signaling is a developmentally conserved pathway that regulates stem cell proliferation, fate determination, and differentiation [6]. Activation of the cell-to-cell signaling pathway occurs when a Notch ligand (Jagged 1,2 and Delta-like 1,4) expressed on the surface of

a signaling cell interacts with a Notch receptor (Notch 1-4) expressed on the surface of a receiving cell. A two-stage proteolytic event liberates the Notch intracellular domain (NICD), which translocates to the nucleus and binds to RBPjκ and Mastermind-like proteins (MAML). MAML serves as a scaffold to recruit other co-activators required to initiate transcription of canonical Notch target gene families Hes and Hey.

The Notch signaling pathway regulates multiple cell lineages that participate in bone formation. Notch signaling in mesenchymal progenitor cells promotes proliferation while inhibiting differentiation [7, 8]. In committed chondroprogenitors, Notch inhibition promotes differentiation, but is reactivated for terminal hypertrophic maturation [8-12]. In osteoprogenitors, Notch inhibition also promotes differentiation [7, 13]. However, Notch components are endogenously expressed at various stages of osteogenic differentiation [12], where expression in mature osteoblasts indirectly inhibits osteoclast differentiation [7, 13, 14]. Notch signaling also inhibits osteoclast differentiation directly through expression in macrophage precursors [15]. Finally, Notch signaling both positively and negatively regulates endothelial cell behavior [16, 17]. These studies have collectively demonstrated that the Notch signaling pathway regulates embryological bone development.

Bone fracture healing recapitulates many aspects of embryological bone development [18-20]. In Chapter 3, we demonstrated that the Notch signaling pathway was upregulated during bone fracture healing, and that Notch signaling components were active in mesenchymal and endothelial lineage cells [12]. Furthermore, Notch signaling has also been shown to regulate tissue repair of other injuries [21]. Collectively, the data suggests that Notch signaling also likely regulates bone fracture healing. However, the precise role is unknown. Therefore, the objective of this study was to determine the importance of Notch signaling in regulating bone fracture healing by using a temporally controlled inducible transgenic mouse model to impair RBPjκ-mediated canonical Notch signaling in all cells during repair. We hypothesize that inhibition of Notch signaling will alter murine tibial fracture and calvarial defect healing.

4.2 Methods

4.2.1 Generation of mice

dnMAML (Mx1-Cre+; dnMAML$^{f/-}$) and WT (Mx1-Cre-; dnMAML$^{f/-}$) mice generated on a C57Bl/6 background were included in this study. The GFP-tagged dominant negative MAML (dnMAML) transgene is a truncated version of MAML, and contains only the NICD binding domain that allows it to bind to the NICD-RBPjκ complex, but lacks the binding domain necessary to recruit other co-activators that are required to initiate transcription of Notch target genes. Therefore, dnMAML inhibits canonical Notch signaling at the level of transcriptional complex assembly just prior to gene transcription [22, 23]. The dnMAML-GFP transgene is preceded by a floxed transcriptional stop sequence allowing it to be conditionally regulated by Cre recombinase expression [24-26]. The inducible Mx1-Cre promoter was used in this study to activate dnMAML expression in all cell types just prior to fracture [27], allowing both dnMAML and WT mice to undergo unaltered embryological development and skeletal maturation. The Mx1 promoter is normally silent, but can be induced by intraperitoneal (IP) injection of polyinosinic-polycytidylic acid (polyI:C). Resulting expression of Cre recombinase deletes the upstream transcriptional stop sequence allowing for systemic dnMAML expression on the ROSA26 locus.

4.2.2 Experimental Design

All *in vivo* protocols were approved by the institutional animal care and use committee. At the onset of skeletal maturity at 3 months of age [28, 29], dnMAML and WT mice were IP injected with 500 μg of polyI:C 10 times over 20 days. This protocol induces dnMAML-GFP expression in greater than 95% of total bone marrow cells [25] and 90% of bone marrow-derived mesenchymal progenitor cells.

After polyI:C injections, closed bilateral tibial fractures were created according to previously published methods using a custom-made three-point bending apparatus with intramedullary pin fixation of the tibia, resulting primarily in endochondral bone repair (also see Chapter 3) [12, 30, 31]. Radiographs were generated to verify correct pin placement and fracture (Faxitron X-Ray). 0.05 mg/kg of buprenorphine was administered subcutaneously twice for four days following injury, including a pre-operative dose. Mice recovered on heating pads and were

allowed to ambulate freely. Fracture calluses were harvested for quantitative real-time polymerase chain reaction (QPCR) analysis of gene expression at 5, 10 and 20 days post fracture (dpf) (n=6-9), quantitative histology and immunohistochemistry (IHC) at 10 and 20dpf (n=4-7), and micro-computed tomography (μCT) at 10 and 20dpf (n=7-13). Both males and females were included in this experiment to decrease the number of animals used, and because several studies have reported similar responsivity of both sexes to manipulations of Notch signaling [7, 14, 32, 33]. However, because male and female skeletons present with different quantities of bone during aging [29], the sexes were separated into different time points for histological and μCT analysis of bone and cartilage. Females were harvested at 10dpf, males at 20dpf, and mixed gender at 5dpf for gene expression analysis only prior to bone or cartilage formation.

3 mm diameter bilateral calvarial defects were also created in a separate group of 3-month-old mice following polyI:C injections according to previously published protocols (also see Chapter 3) [12] to evaluate intramembranous bone repair. dnMAML$^{f/f}$ and dnMAML$^{f/-}$ mice were utilized in this experiment in both dnMAML and WT groups. Defects were harvested at 4 weeks (males, n=11-12) and 16 weeks (females, n=8) post injury for μCT analysis.

4.2.3 Histology and Immunohistochemistry (IHC)

Tissue was fixed in 4% paraformaldehyde at 4°C for 2-3 days, decalcified in 15% formic acid, paraffin embedded, and sectioned at 5 μm. For IHC, sections were deparaffinized and gradually rehydrated. Heat-mediated antigen retrieval via the microwave method was performed using Sodium Citrate Buffer at pH 6.0 for 20 minutes on high (for PCNA antibody) or Citra Plus (Biogenex) for 2 minutes on high followed by 15 minutes at 20% (for GFP antibody), and then cooled in buffer to room temperature. Sections were incubated in serum blocking solution (5% donkey serum, 4% BSA, 0.1% Triton-X 100, 0.05% Tween 20 in PBS) for 60 minutes, and then with primary antibody (see below) diluted in buffer solution (0.5% donkey serum, 2.4% BSA, 0.26% Triton-X 100, 0.005% Tween 20 in PBS) overnight at 4°C in a humidified chamber. Control

sections were incubated in buffer solution only. Sections were then treated with 3% H_2O_2 for 30 minutes, followed by biotinylated secondary antibody Donkey anti-Rabbit (Santa Cruz sc-2089, 1:200 diluted in 0.5% donkey serum, 0.4% BSA, 0.01% Triton-X 100, 0.055% Tween 20 in PBS) for 30 minutes, and finally streptavidin-HRP (Abcam ab7403, 1:500 diluted in PBS) for 30 minutes. Sections were developed with DAB (Vector Laboratories) and counterstained with Hematoxylin. All incubations other than antigen retrieval and primary antibody were done at room temperature. Sections were washed in 0.02% Tween 20 in PBS after each step except between serum blocking and primary antibody incubation.

To identify cells that express the dnMAML-GFP transgene, sections were stained with Rabbit anti-GFP antibody (Abcam ab6556, 1:100). To quantify cell proliferation, sections were stained with Rabbit anti-Proliferating Cell Nuclear Antigen (PCNA) antibody (Abcam ab2426, 1:100), which is expressed in cells undergoing DNA synthesis. To quantify cartilage formation, sections were stained with Safranin O and Fast Green (SafO), which stain proteoglycans red. To quantify osseous tissue formation, sections were stained with Masson's Trichrome (Sigma HT15-1KT), which stains collagenous tissue blue. Sections were also stained with Hematoxylin and Eosin (H&E) for semi-quantitative analysis of inflammation and Gram stain.

4.2.4 Histomorphometric Analysis

Slides were imaged in bright field with an Olympus BX51. Color images were acquired with a Spot RT3 2 megapixel camera. ImageJ (National Institutes of Health) was used to quantify all histological data.

20x SafO images of the entire callus were acquired and stitched together as needed for analysis of cartilage formation. Contours were manually drawn around the total callus area excluding original cortical bone, marrow and muscle tissue. A fixed, global, color threshold was used for automated quantitation of cartilage area for all specimens. For 10dpf specimens, cartilage components were further broken down into immature, mature, and hypertrophic cartilage using semi-automated analysis based on cell morphology and intensity of SafO staining. 400x

images were acquired in areas of immature, mature, and hypertrophic cartilage for automated analysis of chondrocyte cell density and size.

20x Masson's Trichrome images were similarly acquired for analysis of osseous tissue formation. Total callus area and osseous tissue area were similarly quantified. High-resolution images were acquired in areas of immature bone and mature bone for manual analysis of active osteoblast density (400x) and osteoclast density (200x). Active osteoblasts were defined as mononuclear cells aligning the bone surface with a cuboidal or columnar morphology. Osteoclasts were defined as cells aligning the bone surface with greater than two nuclei.

400x PCNA images of 10dpf specimens were acquired in areas of undifferentiated mesenchymal cells and mature cartilage for automated analysis of percent PCNA positive cells at each stage of differentiation. Similar analysis was conducted for area of PCNA staining in areas of immature bone.

For semi-quantitative analysis of inflammation at 10dpf, H&E sections were graded for neutrophil and mononuclear cell (macrophages and leukocytes) inflammation individually. A score of 1-5 was given based on the level of inflammatory cell infiltration within each of the intramedullary cavity, the callus surrounding cortical bone, and the periosteal callus, and the scores were added together for a maximum of 15. For neutrophil inflammation, a score >12 indicated high inflammation (30-50%), 9-12 indicated micro abscess formation, 6-9 indicated moderate inflammation (10-30%), 3-6 indicated mild inflammation (<10%), and 3 indicated no inflammation. Similarly, for mononuclear cell inflammation, a score >12 indicated severe, 9-12 moderate, 6-9 mild, 3-6 minimal, and 3 no inflammation.

4.2.5 Micro-computed Tomography (μCT)

Tibial fracture calluses were scanned using a Scanco vivaCT40 (Scanco Medical) with the following parameters: 21 μm isotropic voxel size, 55 kVp. 145 μA, 500 projections per 180°, 650 millisecond integration time, 2D transverse reconstructed 1024x1024 pixel images. User-defined contours were drawn every 10 images (0.210 mm) or less around the callus for inclusion, with automated morphing used to interpolate the contours for all images in between. Similarly,

user-defined contours were drawn around the original cortical bone and marrow cavity for exclusion with automated morphing in between. This semi-automated segmentation method analyzes the callus outside the pre-existing cortical bone. The entire length of the callus was analyzed. A fixed, global threshold of 16% of the maximum gray value, which corresponds to a mineral density of 169.8 mg HA/cm^3 was applied to distinguish mineralized from unmineralized tissue. The following parameters were quantified: total callus volume, callus bone volume, bone volume fraction, tissue mineral density, trabecular number, trabecular thickness, trabecular separation, connectivity density, and structure model index.

Calvarial defects were scanned using the same machine with the following parameters: 10.5 μm isotropic voxel size, 55 kVp. 145 μA, 1000 projections per 180°, 381 millisecond integration time, 2D reconstructed 2048x2048 pixel images. Reconstructed images were reoriented transverse to the depth of the defect such that 2D reconstructed images presented with a circular defect surrounded by calvarial bone. 3.6 mm diameter cylindrical contours were drawn within the entire depth of the defect to evaluate bone formation within and adjacent to the defect. Bone volume and tissue mineral density were quantified.

4.2.6 Quantitative Real-Time Polymerase Chain Reaction (QPCR)

Fracture calluses were dissected from the surrounding tissue, placed in Qiazol lysis reagent (Qiagen) and stored at -80°C until further processing. Tissue was then homogenized using the Tissue Tearor (BioSpec Products) and mRNA was extracted using the Qiagen miRNeasy Mini Kit with DNase digestion to remove DNA contamination. RNA yield was determined using a NanoDrop 1000 spectrophotometer (ThermoScientific). 1 μg of mRNA was reverse transcribed into 20 μl of cDNA using the Applied Biosystems High Capacity RNA-to-cDNA Kit, and then diluted with RNase- and DNase-free H_2O to a 40 μl volume. Gene expression was quantified using a 7500 Fast Real-Time PCR system (Applied Biosystems) from a total of 10 ul of Master Mix per well, which included 1x Fast SYBR Green (Applied Biosystems), forward and reverse primers (0.45 μM), and 0.5 μl of cDNA. For each gene of interest, samples were run in

duplicate and control wells were run to rule out DNA contamination and primer dimer amplification. Proper amplicon formulation was confirmed by melt curve analysis. qPCR data is presented as relative gene expression to β-actin housekeeping control, calculated using the formula $2^{-\Delta C(t)}$.

4.2.7 Statistical Analysis

For parameters quantified at multiple time points, two-way ANOVAs were performed to test the main effects of dnMAML expression and time, and the interaction between the two. The main objective of this study is to evaluate how dnMAML expression affects fracture healing. Therefore, post-hoc student's t-tests were performed to compare dnMAML to WT at each time point if there was a significant ($*p<0.050$) or trend ($^{\#}p<0.100$) effect of either dnMAML expression or the interaction between dnMAML expression and time. For parameters quantified at only one time point, a student's t-test was used to compare dnMAML to WT. For neutrophil and mononuclear cell inflammation, a Mann-Whitney non-parametric test was used to compare dnMAML to WT. Data is presented as mean ± standard deviation.

4.3 Results

4.3.1 dnMAML Expression During Bone Fracture Healing

The dnMAML transgene is tagged with GFP. GFP gene expression was highly upregulated in dnMAML mice relative to WT mice at 5, 10 and 20dpf (Figure 4.1A). GFP IHC demonstrated that it was also widely expressed in multiple cell populations present during fracture healing in dnMAML mice including undifferentiated mesenchymal cells, chondrocytes, osteoblasts, endothelial cells, hematopoietic cells, and inflammatory cells (Figure 4.1B), verifying that dnMAML was expressed during fracture healing. Expression was undetectable in WT mice.

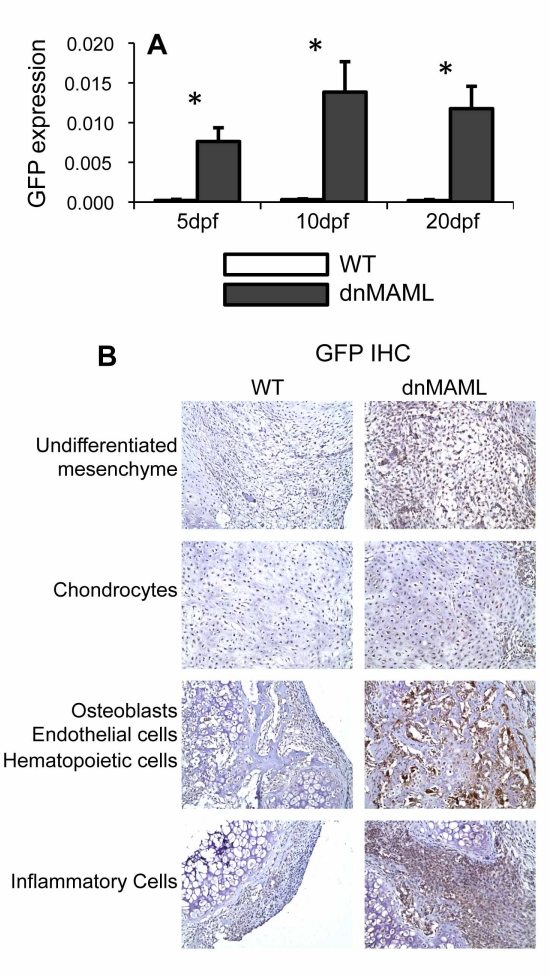

Figure 4.1. GFP-tagged dnMAML is expressed in dnMAML mice during fracture healing. (A) GFP gene expression is upregulated in dnMAML fractures. (B) GFP is expressed in undifferentiated mesenchymal cells, chondrocytes, osteoblasts, endothelial cells, hematopoietic cells and inflammatory cells in dnMAML fractures. There is no expression in WT mice. GFP IHC images were acquired at 200x magnification. Gene expression data is presented as relative expression to β-actin, calculated using the formula. $2^{-\Delta C(t)}$. *p<0.050 (dnMAML vs WT)

4.3.2 dnMAML Decreases Cartilage Formation During Fracture Healing

During the endochondral phase of fracture healing, undifferentiated mesenchymal cells condense at the fracture site and undergo chondrogenesis to produce an initial cartilaginous callus matrix. To evaluate cartilage formation, sections were stained with SafO at 10 and 20dpf and chondrogenic gene expression was assessed at 5, 10 and 20dpf. dnMAML fractures had decreased percent cartilage area within the callus (CA/TA) at 10dpf (Figure 4.2A). Almost all cartilage was resorbed in both groups by 20dpf. Consistent with these histological results, dnMAML fractures had decreased Col2a1 (Figure 4.2B) and Sox9 (Figure 4.2C) gene expression at 10dpf, but were not different from WT at 5 or 20dpf. A two-way ANOVA showed decreased ColX gene expression in dnMAML fractures, though post-hoc analysis did not uncover time-point specific differences (Figure 4.2D). Collectively, the data demonstrates that dnMAML expression decreases cartilage formation during endochondral fracture healing.

The cartilage matrix develops from immature cartilage (IC) populated by proliferating chondrocytes, which develops first into mature cartilage (MC) populated by pre-hypertrophic chondrocytes and then finally into hypertrophic cartilage (HC) populated by hypertrophic chondrocytes. To evaluate differences in relative cartilage maturation, the specific components of the cartilage matrix were quantified based on maturity at 10dpf when peak formation occurs. There were no differences between dnMAML and WT mice in the percent of IC, MC, or HC to total cartilage area within the callus (CA), demonstrating that the rate of cartilage maturation was not delayed or enhanced by dnMAML expression (Figure 4.2E). Chondrocyte density within each of these regions was also not affected by dnMAML expression, indicating that dnMAML expression did not affect individual chondrocyte function, specifically matrix production (Figure 4.2F).

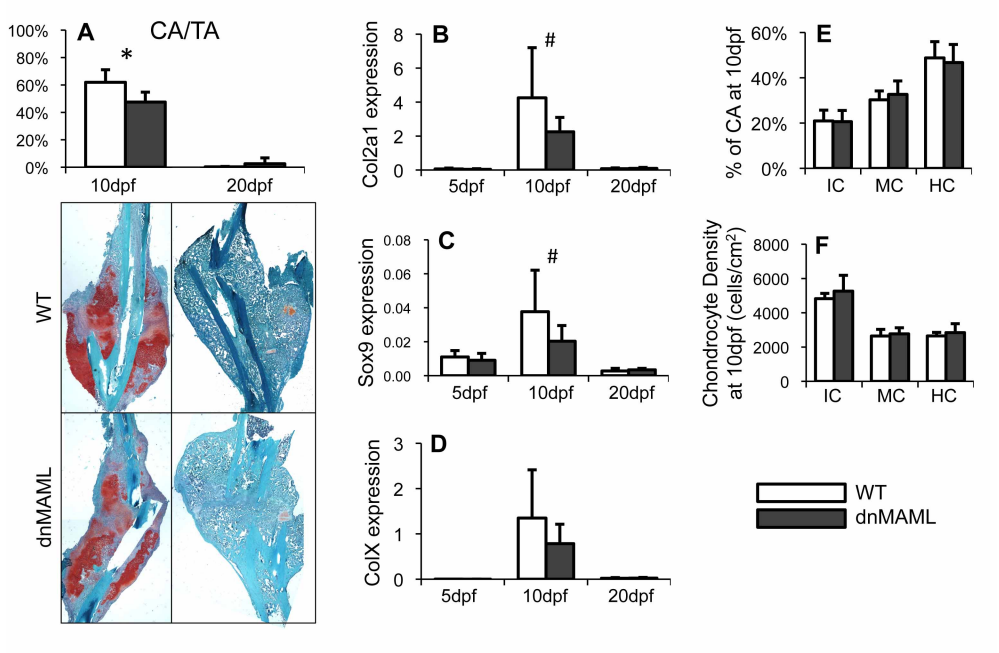

Figure 4.2. dnMAML decreases cartilage formation during fracture. (A) Percent of cartilage area to total callus area (CA/TA) via SafO histomorphometric analysis is decreased in dnMAML fractures at 10dpf. (B) Col2a1 and (C) Sox9 gene expression are decreased in dnMAML fractures at 10dpf. (D) ColX gene expression is non-significantly decreased in dnMAML fractures at 10dpf. (E) There are no differences between WT and dnMAML fractures in percent of immature (IC), mature (MC) or hypertrophic cartilage (HC) to cartilage area (CA) at 10dpf. (F) There are no differences in chondrocyte density within these areas at 10dpf. SafO images were acquired at 20x magnification. Gene expression data is presented as relative expression to β-actin, calculated using the formula. $2^{-\Delta C(t)}$. *p<0.050 #p<0.100 (dnMAML vs WT)

4.3.3 dnMAML Inhibits Expression of Vascular Endothelial Cell Markers During Fracture Healing

Bone formation during fracture healing requires vascularization of the callus mediated by endothelial cells. PECAM gene expression, an endothelial cell marker, is decreased in dnMAML fractures at 20dpf, indicating that dnMAML activation impairs callus vascularization (Figure 4.3A). VEGFα gene expression, a marker of angiogenesis, was not statistically altered due to dnMAML expression, though it was increased by 28% at 20dpf (Figure 4.3B).

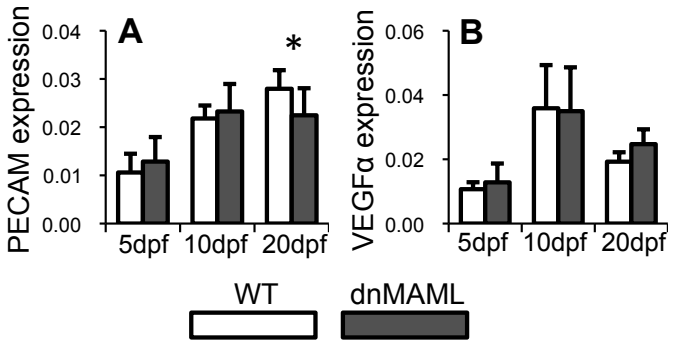

Figure 4.3. dnMAML inhibits expression of vascular endothelial cell markers during fracture healing. (A) PECAM gene expression is decreased in dnMAML fractures at 20dpf. (B) There are no differences in VEGFα gene expression. Gene expression data is presented as relative expression to β-actin, calculated using the formula. $2^{-\Delta C(t)}$. *p<0.050

4.3.4 dnMAML Alters Bone Remodeling During Fracture Healing

During endochondral bone formation that occurs during fracture healing, immature bone is produced on top of a resorbing cartilage callus. Maturation and remodeling occurs over time through osteoblast-mediated bone formation and osteoclast-mediated bone resorption. To evaluate bone mass within the callus, fractures were analyzed via three-dimensional μCT and two-dimensional Masson's Trichrome histology at 10 and 20dpf. Osteogenic gene expression was also assessed at 5, 10 and 20dpf.

dnMAML fractures presented with an increased proportion of bone mass during the remodeling phase (20dpf), indicated by increased bone volume fraction (BV/TV) (Figure 4.4A). Percent osseous tissue area within the callus (OA/TA) was also non-statistically increased at 20dpf (Figure 4.4B). This appears to be the result from a moderate decrease in callus size (TV and Avg TA), with no difference in total bone mass (BV and Avg OA) (Figure 4.5). Osteocalcin (Ocn) gene expression was also increased in dnMAML fractures at 20dpf (Figure 4.4C). However, Osterix (Osx) and Collagen type I (Col1a1) were not changed (Figure 4.4D,E).

Trabecular bone morphometry was altered in dnMAML fractures at 20dpf, with increased trabecular thickness (Tb.Th), but decreased structural model index (SMI) characteristic of

concave trabeculae (negative value) and trabecular connectivity density (Conn.D) (Table 4.1). Trabecular number (Tb.N), trabecular separation (Tb.Sp), and tissue mineral density (TMD) were not different.

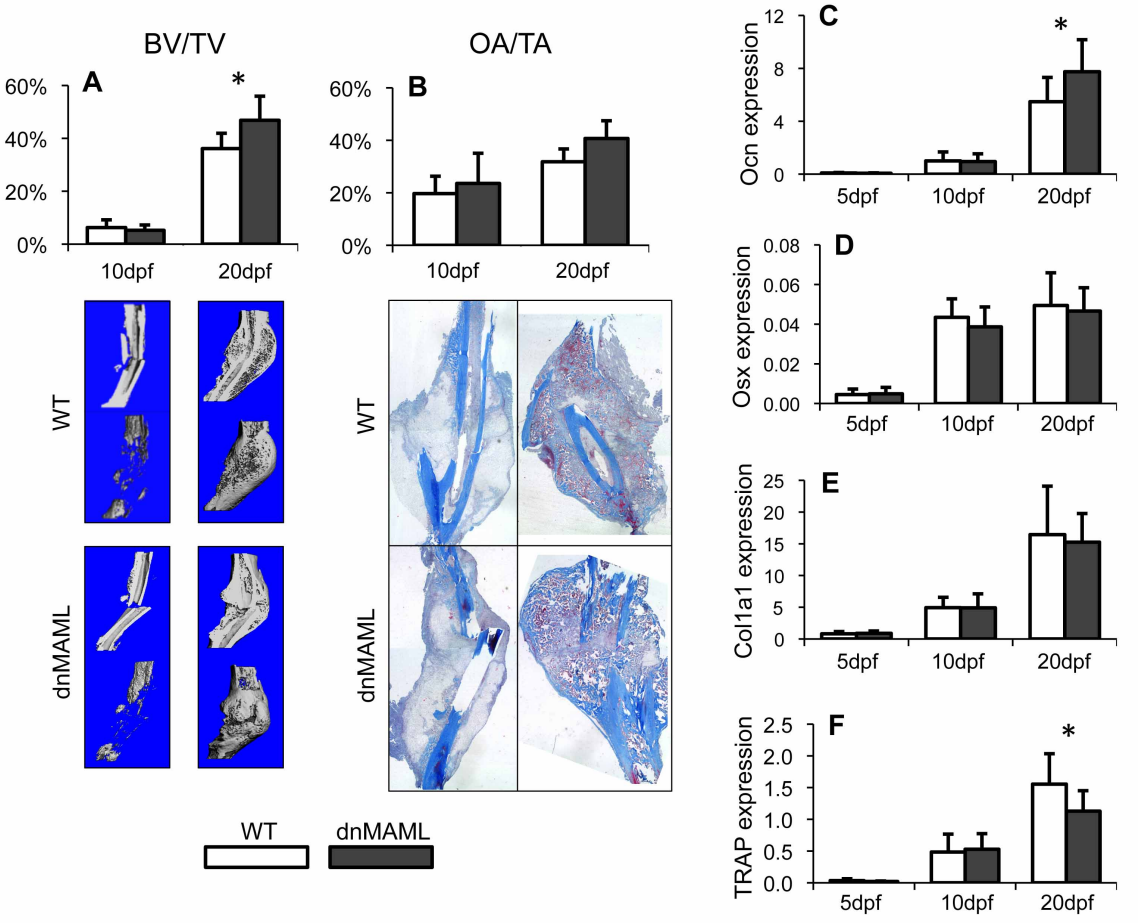

Figure 4.4. dnMAML alters bone remodeling during fracture healing. (A) Bone volume fraction (BV/TV) via μCT analysis is increased in dnMAML fractures at 20dpf. (B) There are no differences in percent osseous tissue area to total callus area (OA/TA) via Masson's Trichrome histomorphometric analysis. (C) Osteocalcin (Ocn) gene expression is increased in dnMAML fractures at 20dpf. There are no differences in (D) Osterix (Osx) or (E) Collagen type I (Col1a1) gene expression. (F) TRAP gene expression is decreased in dnMAML fractures at 20dpf. μCT images were acquired at a 21 μm voxel size. Masson's Trichrome images were acquired at 20x magnification. Gene expression data is presented as relative expression to β-actin, calculated using the formula. $2^{-\Delta C(t)}$. *p<0.050 (dnMAML vs WT)

Table 4.1. μCT morphometric analysis of WT and dnMAML fractures at 10 and 20dpf.

	10dpf		20dpf	
	WT	dnMAML	WT	dnMAML
Tb.N (1/mm)	1.13 ± 0.19	1.05 ± 0.22	6.08 ± 0.43	6.37 ± 0.42
Tb.Th (mm)	0.110 ± 0.013	0.111 ± 0.017	0.099 ± 0.013	0.137 ± 0.033 *
Tb.Sp (mm)	0.98 ± 0.13	1.05 ± 0.22	0.17 ± 0.02	0.16 ± 0.02
TMD (mg HA/cm^3)	347 ± 19	344 ± 18	420 ± 22	438 ± 27
SMI	2.0 ± 0.4	2.2 ± 0.7	1.1 ± 0.7	-0.3 ± 1.5 *
Conn.D (1/mm^3)	15.1 ± 10.9	9.9 ± 3.5	175 ± 19	150 ± 21 *

Trabecular number (Tb.N), trabecular thickness (Tb.Th), trabecular separation (Tb.Sp), tissue mineral density (TMD), structural model index (SMI) and connectivity density (Conn.D) were quantified via μCT. Results are presented at mean ± standard deviation. * p<0.050 (WT vs dnMAML)

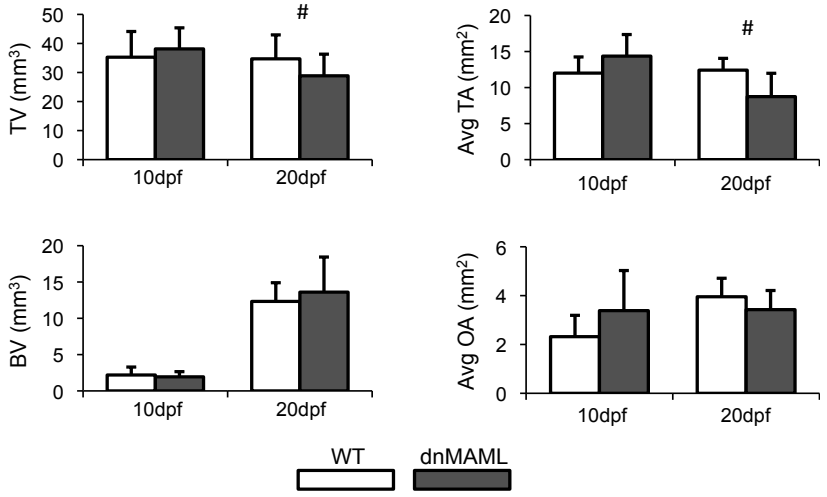

Figure 4.5. dnMAML decreases callus size at 20dpf but not bone mass during fracture healing. Total callus volume (TV, top left) via μCT analysis and average total callus area (Avg TA, top right) via Masson's Trichrome histomorphometric analysis are decreased in dnMAML fractures at 20dpf. Bone volume (BV, bottom left) and average bone area (Avg BA, bottom right) are not different. μCT images were acquired at a 21 μm voxel size. Masson's Trichrome images were acquired at 20x magnification. #p<0.100 (dnMAML vs WT)

Surprisingly, despite increases in BV/TV and Tb.Th, both osteoblast density (normalized to bone perimeter and area) in immature and mature bone and osteoclast density in mature bone were decreased in dnMAML fractures at 20dpf (Table 4.2). Consistent with decreased osteoclast density, TRAP gene expression was decreased in dnMAML fractures at 20dpf (Figure 4.4F). These molecular and phenotypic changes to bone occurred only during the late stage of repair, at early time points, there was no indication of an alteration in bone volume or osteoblast-related gene expression suggesting that dnMAML expression alters bone remodeling, but does not affect early bone formation.

Bone formation and remodeling during intramembranous fracture healing was also evaluated using a calvarial defect model. dnMAML expression significantly decreased BV 4 weeks post injury (Figure 4.6A). Similar results persisted at 16 weeks but were not significant. TMD was increased at 16 weeks. (Figure 4.6B).

Table 4.2. Osteoblast and osteoclast density in immature bone at 10 and 20dpf and mature bone at 20dpf.

	10dpf		20dpf			
	Immature Bone		Immature Bone		Mature Bone	
	WT	dnMAML	WT	dnMAML	WT	dnMAML
Obl/BP (1/mm)	55 ± 6	53 ± 4	58 ± 9	47 ± 2 *	63 ± 10	45 ± 5 *
Obl/BA ($1/mm^2$)	4029 ± 671	4279 ± 1244	6114 ±1487	3898 ± 1115 *	3819 ± 1098	2197 ± 368 *
Ocl/BP (1/mm)	1.1 ± 0.5	1.1 ± 0.3	0.8 ± 0.2	0.7 ± 0.2	1.0 ± 0.3	0.5 ± 0.3 *
Ocl/BA ($1/mm^2$)	59 ± 24	63 ± 23	67 ± 19	45 ± 18	41 ± 10	19 ± 14 *

Osteoblast density is normalized to bone perimeter (Obl/BP) and bone area (Obl/BA). Osteoclast density is also normalized to bone perimeter (Ocl/BP) and bone area (Ocl/BA). Results are presented at mean ± standard deviation. * $p<0.050$ (WT vs dnMAML)

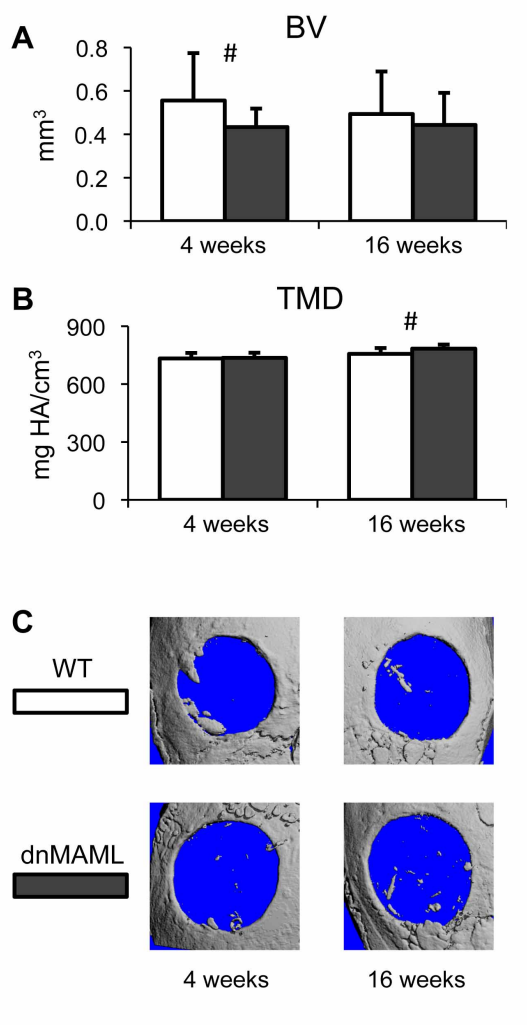

Figure 4.6. dnMAML decreases bone mass during calvarial defect healing. (A) Bone volume (BV) is decreased in dnMAML defects 4 weeks post injury. (B) Tissue mineral density (TMD) is decreased in dnMAML defects at 16 weeks post injury. (C) μCT images were acquired at a 10.5 μm voxel size. $^{\#}p<0.100$ (dnMAML vs WT)

4.3.5 dnMAML Prolongs Inflammation During Fracture Healing

The area of non-cartilage and non-osseous tissue, known as the void area within the callus, includes undifferentiated mesenchymal cells, hematopoietic cells and unstained empty space [34]. The percent void space within the callus (Void/TA) was significantly increased in dnMAML mice at 10dpf (Figure 4.7A). To further characterize this area, semi-quantitative analysis of inflammatory cells was performed at 10dpf, and inflammatory cytokine gene expression was evaluated at 5, 10 and 20dpf. Neutrophil inflammation was characterized as high for dnMAML fractures (>12) and moderate for WT fractures (6-9) (Figure 4.7B). These values were

significantly different. Mononuclear cell inflammation was characterized as mild for both dnMAML and WT fractures (6-9) (Figure 4.7C). Gram staining showed no bacterial infection in any fracture (data not shown). Consistent with neutrophil inflammation, TNFα (Figure 4.7D) and IL-1β (Figure 4.7E) were upregulated in dnMAML mice at 10dpf. Collectively, the data demonstrates that dnMAML expression results in enhanced prolonged inflammatory cell infiltration and cytokine expression during fracture healing.

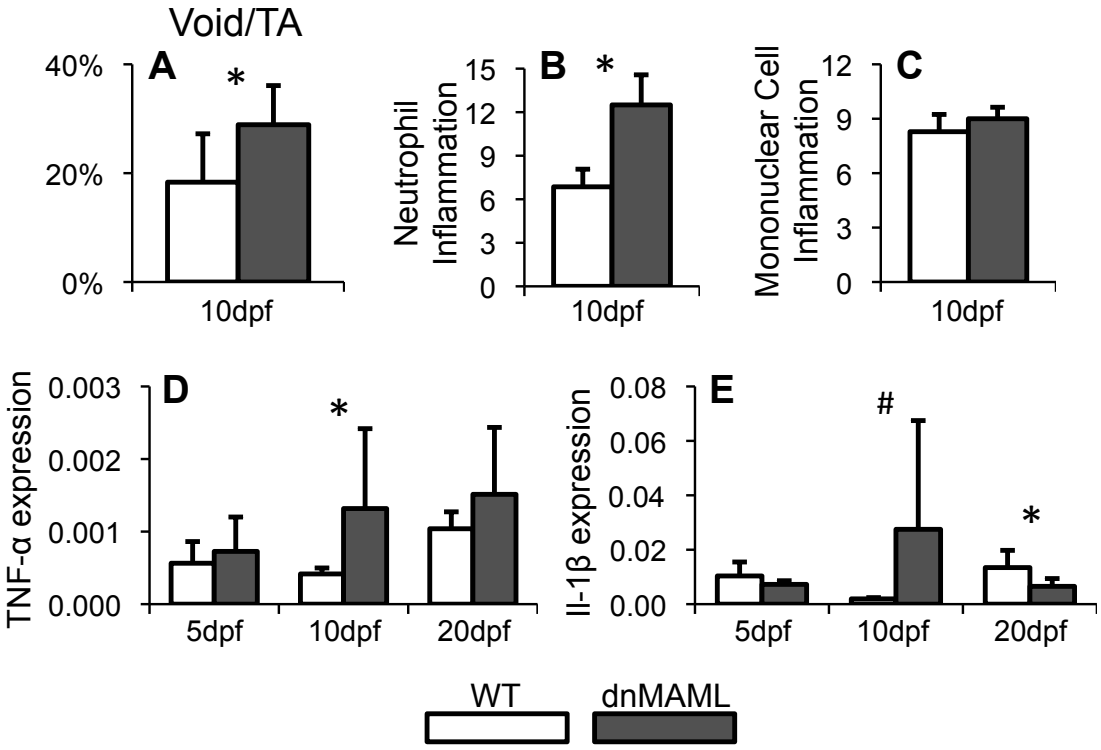

Figure 4.7. dnMAML prolongs inflammation during fracture healing. (A) Percent void area to total callus area (Void/TA) via histomorphometric analysis is increased in dnMAML fractures at 10dpf. (B) Neutrophil inflammation via semi-quantitative analysis of H&E images is increased in dnMAML fractures at 10dpf. (C) There is no difference in mononuclear cell inflammation. (D) TNF-α and (E) IL-1β gene expression are increased in dnMAML fractures at 10dpf. IL-1β is decreased at 20dpf. Gene expression data is presented as relative expression to β-actin, calculated using the formula. $2^{-\Delta C(t)}$. *$p<0.050$ #$p<0.100$ (dnMAML vs WT)

4.3.6 dnMAML Does Not Alter Cell Proliferation or Apoptosis During Fracture Healing

In addition to regulating differentiation, Notch signaling has been shown to control cell proliferation and apoptosis. However, dnMAML expression did not affect proliferation or apoptosis during fracture healing. Specifically, PCNA (Figure 4.8A), Cyclin D1 (Figure 4.8B), and Caspase 3 (Figure 4.8C) gene expression were not different at any of the time points. Furthermore, PCNA IHC staining at 10dpf (Figure 4.8D) revealed no difference in the % of PCNA+ staining cells in undifferentiated mesenchymal cells (UDM) or mature chondrocytes (MC) (Figure 4.8E), nor in the PCNA+ staining area normalized to bone perimeter in areas of immature bone (IB) formation, which primarily includes osteoblasts, but also endothelial cells, osteoclasts, and other hematopoietic cells (Figure 4.8F).

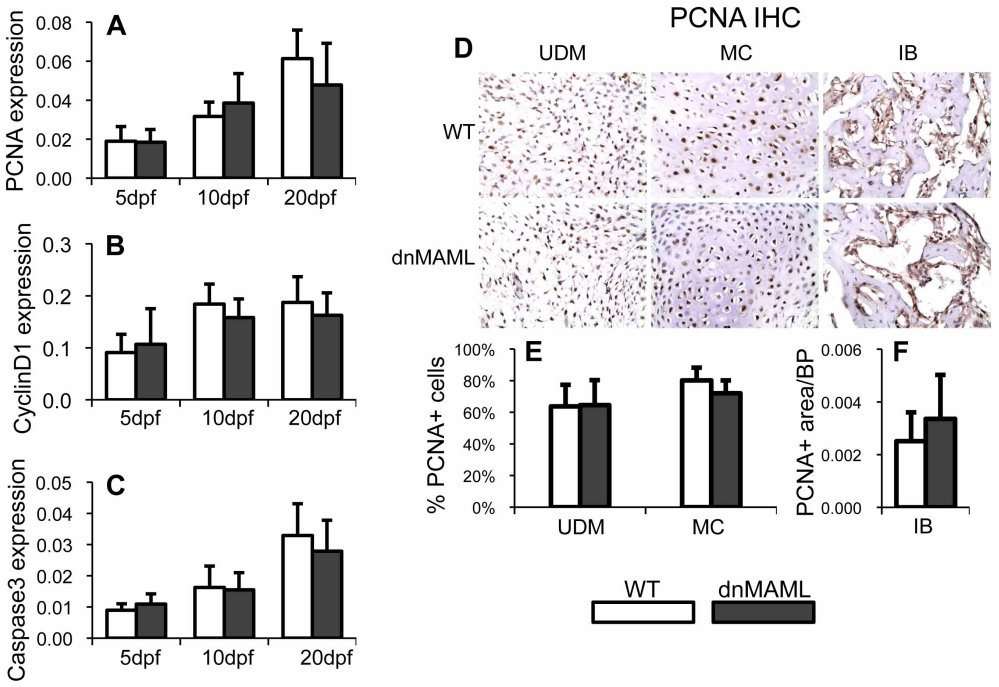

Figure 4.8. dnMAML does not alter cell proliferation or apoptosis during fracture healing. There are no differences in (A) PCNA, (B) Cyclin D1, and (C) Caspase 3 gene expression during fracture healing. (D) PCNA IHC staining shows no differences in (E) % PCNA+ cells in undifferentiated mesenchymal cells (UDM) or in mature chondrocytes, and no differences in (F) PCNA+ area per bone perimeter (PCNA+ area/BP) in immature bone (IB). PCNA IHC images were acquired at 400x magnification. Gene expression data is presented as relative expression to β-actin, calculated using the formula. $2^{-\Delta C(t)}$.

4.4 Discussion

The Notch signaling pathway regulates embryological bone development [7, 8, 10, 11, 13, 14, 32, 33], and because many aspects of development are recapitulated during repair [18-20], we set out to identify the role of Notch signaling during bone fracture healing. To do this, we crossed heterozygous dnMAML mice with inducible Mx1-Cre promoter mice. A series of polyI:C injections just prior to injury activated the Mx1 promoter and Cre expression in all cell types, resulting in systemic dnMAML expression, which inhibits the Notch signaling pathway at the level of transcriptional complex assembly (NICD- RBPjκ-MAML) just prior to gene transcription [22-27]. It is important to note that there are other functions of the Notch pathway that dnMAML is not known to affect, including direct binding of NICD to Runx2 [13], RBPjκ-independent Notch cell autonomous and non-autonomous functions [10], and potential reverse ligand intracellular domain signaling in the signaling cell [35, 36]. Heterozygous dnMAML mice were chosen as a more clinically relevant model since any potential therapeutic applications that would attempt to inhibit Notch signaling would likely achieve partial but not complete Notch ablation.

Our results demonstrate that Notch signaling is required for the spatiotemporal cascade of healing, where systemic inhibition of canonical Notch signaling alters inflammation, cartilage formation and callus vascularization, which in turn secondarily affect bone formation and remodeling. Our results also indicate that Notch signaling primarily regulates processes governing the cell-types present, and in turn tissue types, in callus, but doesn't appear to affect cell proliferation or apoptosis during repair.

The acute inflammatory phase is required to initiate the repair cascade by promoting mesenchymal cell recruitment to the fracture site and initiating early angiogenesis [37]. However, chronic inflammatory diseases that occur in mouse models such as type I diabetes impair fracture healing [38]. Our results show that systemic Notch inhibition prolongs the inflammatory phase, increasing cytokine gene expression and neutrophil but not mononuclear cell inflammation. Neutrophils and macrophages (a primary component of identifiable mononuclear cells) are the

dominant inflammatory cell types present during fracture healing [37, 39]. Previous studies have also shown that Notch inhibition prolongs inflammation and delays dermal wound closure [21], results in severe airway inflammation [40], and mice with conditional Notch inhibition in the developing skeleton died prematurely and presented with severe ulcerative dermatitis possibly due to excessive inflammation [7]. Collectively, these studies demonstrate the requirement of Notch signaling to resolve the inflammatory phase and prevent chronic inflammation.

During endochondral fracture healing, mesenchymal cells recruited to the fracture site condense and undergo chondrogenesis to produce an initial cartilaginous callus [1]. Systemic Notch inhibition reduced cartilage formation during fracture healing. Previous studies have shown that Notch inhibition in fact enhances chondrogenesis [7, 8, 11]. However, transient activation of Notch is required to initiate chondrocyte differentiation [9]. In our model, Mx1-Cre mediated Notch inhibition occurred prior to injury, which prevented the transient Notch activation required for chondrogenic induction of mesenchymal cells at the fracture site. Alternatively, prolonged inflammation due to Notch inhibition could also be responsible for reduced cartilage formation. Previous studies have shown that inflammatory cytokines inhibit chondrogenesis and that chronic inflammation destroys articular cartilage [41-43].

Concomitant with cartilage resorption, callus vascularization mediates an influx of osteogenic cells to the fracture. Systemic Notch inhibition reduced vascularization of the callus, specifically endothelial cell expression, during bone formation and remodeling. Notch inhibition has also shown to impair vascularization during dermal wound healing [21] and craniofacial development [44]. Interestingly, Notch regulation of vascularization appears to be ligand dependent, with Jagged1 beneficial and Dll4 inhibitory [16]. Jagged1 is the most highly expressed ligand during fracture healing [12] suggesting that dnMAML inhibition of Jagged1-initiated Notch signaling may be responsible for decreased vascularization of the callus. Alternatively, it could also be hypothesized that Notch inhibition in tissues with high Dll4 expression would in fact promote vascularization.

Bone formation and remodeling during endochondral fracture healing requires the proper spatiotemporal progression of inflammation, cartilage formation, and callus vascularization, all of

which were altered due to dnMAML expression. Downstream effects from these tissues may be primarily responsible for the observed bone remodeling phenotype, as opposed to direct effects of Notch on osteoblasts and osteoclasts. For example, Notch inhibition in mesenchymal cells enhances osteogenic differentiation. However, our model of systemic Notch inhibition had no effect on bone formation at early time points, and in fact decreased osteoblast density during later stage bone remodeling. Enhanced expression of inflammatory cytokines, which inhibits osteogenesis [45], may be primarily responsible for the observed osteoblast phenotype in dnMAML fractures. Similarly, Notch inhibition promotes osteoclast differentiation directly through expression in macrophage precursors [15] and indirectly through expression in osteoblasts [7, 13, 14]. Inflammatory cytokines also promote osteoclast differentiation [46]. Thus, at this point the dominant mechanism behind systemic Notch regulation of osteoclast activity is unknown, as there were no differences within the cartilaginous callus and decreased osteoclast activity during bone remodeling in dnMAML fractures.

Interestingly, bone remodeling during intramembranous repair of calvarial defects was also impaired due to systemic Notch inhibition. However, this injury model presented with decreased bone mass. These injury models differ in that direct bone formation without a cartilage precursor occurs during calvarial defect healing. Furthermore, adult wild type murine calvarial defects as small as 1.8 mm in diameter do not heal within one year [47], whereas closed transverse tibial fractures normally regenerate completely. This suggests that inhibiting the Notch pathway for the duration of healing is not an ideal therapeutic to enhance repair via direct bone formation, or to promote healing in fractures that are at high risk of non-union. Note that bone formation is not much different between 16-week injuries in females and 4-week injuries in males. This is likely due to a combination of the lack of bone formation that occurs during the later stages of non-union healing and the fact that female mice naturally have decreased bone mass during aging [29].

Because of the complexity of the spatiotemporally changing population of cells and tissues during healing, we were unable to assess the role of Notch signaling in distinct cell populations, including osteoblasts and osteoclasts. To address this limitation, future studies could

utilize tissue-specific models of Cre recombinase expression to activate dnMAML in specific lineages. Utilizing Prx1, Col3.6 or Col2.3 promoters would inhibit Notch signaling in undifferentiated mesenchymal progenitors, osteoprogenitors, or committed osteoblasts, respectively. Similarly, TRAP promoters would inhibit Notch signaling in osteoclast lineage cells, and expressing Cre in lineage-restricted inflammatory cells would be useful for exploring the contribution of inflammatory cells. Alternatively, the use of gamma secretase inhibitors (GSI) would allow temporal control of Notch signaling to isolate or exclude the role of Notch signaling in specific phases of healing. For example, GSI injections following the conclusion of the acute inflammatory phase could exclude any secondary effects of altered inflammation on the rest of healing, providing a model to better understand the direct role of Notch signaling in cartilage formation, callus vascularization, and bone formation and remodeling. Similarly, GSI injections starting at the cartilage-to-bone transition would isolate the role of Notch signaling during bone formation and remodeling.

In conclusion, our results demonstrate that the Notch signaling pathway is required for the proper temporal cascade of bone fracture healing, and that systemic inhibition of the pathway for the duration of healing is not an ideal therapeutic to improve regeneration. However, more research is required to understand the role of Notch signaling in individual cell populations during repair.

4.5 References

1. Einhorn, T.A., *The cell and molecular biology of fracture healing.* Clin Orthop Relat Res, 1998(355 Suppl): p. S7-21.
2. Audige, L., et al., *Path analysis of factors for delayed healing and nonunion in 416 operatively treated tibial shaft fractures.* Clin Orthop Relat Res, 2005. **438**: p. 221-32.
3. Braithwaite, R.S., N.F. Col, and J.B. Wong, *Estimating hip fracture morbidity, mortality and costs.* J Am Geriatr Soc, 2003. **51**(3): p. 364-70.
4. Dimitriou, R., et al., *Bone regeneration: current concepts and future directions.* BMC Med, 2011. **9**: p. 66.
5. Carragee, E.J., et al., *Future directions for The spine journal: managing and reporting conflict of interest issues.* Spine J, 2011. **11**(8): p. 695-7.
6. Artavanis-Tsakonas, S., M.D. Rand, and R.J. Lake, *Notch signaling: cell fate control and signal integration in development.* Science, 1999. **284**(5415): p. 770-6.
7. Hilton, M.J., et al., *Notch signaling maintains bone marrow mesenchymal progenitors by suppressing osteoblast differentiation.* Nat Med, 2008. **14**(3): p. 306-14.
8. Dong, Y., et al., *RBPjkappa-dependent Notch signaling regulates mesenchymal progenitor cell proliferation and differentiation during skeletal development.* Development, 2010. **137**(9): p. 1461-71.
9. Oldershaw, R.A., et al., *Notch signaling through Jagged-1 is necessary to initiate chondrogenesis in human bone marrow stromal cells but must be switched off to complete chondrogenesis.* Stem Cells, 2008. **26**(3): p. 666-74.
10. Kohn, A., et al., *Cartilage-specific RBPjkappa-dependent and -independent Notch signals regulate cartilage and bone development.* Development, 2012. **139**(6): p. 1198-212.

11. Mead, T.J. and K.E. Yutzey, *Notch pathway regulation of chondrocyte differentiation and proliferation during appendicular and axial skeleton development.* Proc Natl Acad Sci U S A, 2009. **106**(34): p. 14420-5.

12. Dishowitz, M.I., et al., *Notch signaling components are upregulated during both endochondral and intramembranous bone regeneration.* J Orthop Res, 2012. **30**(2): p. 296-303.

13. Engin, F., et al., *Dimorphic effects of Notch signaling in bone homeostasis.* Nat Med, 2008. **14**(3): p. 299-305.

14. Zanotti, S., et al., *Notch inhibits osteoblast differentiation and causes osteopenia.* Endocrinology, 2008. **149**(8): p. 3890-9.

15. Bai, S., et al., *NOTCH1 regulates osteoclastogenesis directly in osteoclast precursors and indirectly via osteoblast lineage cells.* J Biol Chem, 2008. **283**(10): p. 6509-18.

16. Benedito, R., et al., *The notch ligands Dll4 and Jagged1 have opposing effects on angiogenesis.* Cell, 2009. **137**(6): p. 1124-35.

17. Kwon, S.M., et al., *Specific Jagged-1 signal from bone marrow microenvironment is required for endothelial progenitor cell development for neovascularization.* Circulation, 2008. **118**(2): p. 157-65.

18. Vortkamp, A., et al., *Recapitulation of signals regulating embryonic bone formation during postnatal growth and in fracture repair.* Mech Dev, 1998. **71**(1-2): p. 65-76.

19. Ferguson, C., et al., *Does adult fracture repair recapitulate embryonic skeletal formation?* Mech Dev, 1999. **87**(1-2): p. 57-66.

20. Gerstenfeld, L.C., et al., *Fracture healing as a post-natal developmental process: molecular, spatial, and temporal aspects of its regulation.* J Cell Biochem, 2003. **88**(5): p. 873-84.

21. Chigurupati, S., et al., *Involvement of notch signaling in wound healing.* PLoS One, 2007. **2**(11): p. e1167.

22. Weng, A.P., et al., *Growth suppression of pre-T acute lymphoblastic leukemia cells by inhibition of notch signaling.* Mol Cell Biol, 2003. **23**(2): p. 655-64.

23. Maillard, I., et al., *Mastermind critically regulates Notch-mediated lymphoid cell fate decisions.* Blood, 2004. **104**(6): p. 1696-702.

24. Maillard, I., et al., *The requirement for Notch signaling at the beta-selection checkpoint in vivo is absolute and independent of the pre-T cell receptor.* J Exp Med, 2006. **203**(10): p. 2239-45.

25. Maillard, I., et al., *Canonical notch signaling is dispensable for the maintenance of adult hematopoietic stem cells.* Cell Stem Cell, 2008. **2**(4): p. 356-66.

26. Tu, L., et al., *Notch signaling is an important regulator of type 2 immunity.* J Exp Med, 2005. **202**(8): p. 1037-42.

27. Kuhn, R., et al., *Inducible gene targeting in mice.* Science, 1995. **269**(5229): p. 1427-9.

28. Buie, H.R., C.P. Moore, and S.K. Boyd, *Postpubertal architectural developmental patterns differ between the L3 vertebra and proximal tibia in three inbred strains of mice.* J Bone Miner Res, 2008. **23**(12): p. 2048-59.

29. Glatt, V., et al., *Age-related changes in trabecular architecture differ in female and male C57BL/6J mice.* J Bone Miner Res, 2007. **22**(8): p. 1197-207.

30. Bonnarens, F. and T.A. Einhorn, *Production of a standard closed fracture in laboratory animal bone.* J Orthop Res, 1984. **2**(1): p. 97-101.

31. Taylor, D.K., et al., *Thrombospondin-2 influences the proportion of cartilage and bone during fracture healing.* J Bone Miner Res, 2009. **24**(6): p. 1043-54.

32. Tao, J., et al., *Osteosclerosis owing to Notch gain of function is solely Rbpj-dependent.* J Bone Miner Res, 2010. **25**(10): p. 2175-83.

33. Salie, R., et al., *Ubiquitous overexpression of Hey1 transcription factor leads to osteopenia and chondrocyte hypertrophy in bone.* Bone, 2010. **46**(3): p. 680-94.

34. Gerstenfeld, L.C., et al., *Application of histomorphometric methods to the study of bone repair.* J Bone Miner Res, 2005. **20**(10): p. 1715-22.

35. D'Souza, B., A. Miyamoto, and G. Weinmaster, *The many facets of Notch ligands.* Oncogene, 2008. **27**(38): p. 5148-67.

36. Bray, S.J., *Notch signalling: a simple pathway becomes complex.* Nat Rev Mol Cell Biol, 2006. **7**(9): p. 678-89.

37. Mountziaris, P.M., et al., *Harnessing and modulating inflammation in strategies for bone regeneration.* Tissue Eng Part B Rev, 2011. **17**(6): p. 393-402.

38. Alblowi, J., et al., *High levels of tumor necrosis factor-alpha contribute to accelerated loss of cartilage in diabetic fracture healing.* Am J Pathol, 2009. **175**(4): p. 1574-85.

39. Bastian, O., et al., *Systemic inflammation and fracture healing.* J Leukoc Biol, 2011. **89**(5): p. 669-73.

40. Ostroukhova, M., et al., *Treg-mediated immunosuppression involves activation of the Notch-HES1 axis by membrane-bound TGF-beta.* J Clin Invest, 2006. **116**(4): p. 996-1004.

41. Keffer, J., et al., *Transgenic mice expressing human tumour necrosis factor: a predictive genetic model of arthritis.* EMBO J, 1991. **10**(13): p. 4025-31.

42. Niki, Y., et al., *Macrophage- and neutrophil-dominant arthritis in human IL-1 alpha transgenic mice.* J Clin Invest, 2001. **107**(9): p. 1127-35.

43. Lubberts, E., et al., *IL-1-independent role of IL-17 in synovial inflammation and joint destruction during collagen-induced arthritis.* J Immunol, 2001. **167**(2): p. 1004-13.

44. Humphreys, R., et al., *Cranial neural crest ablation of Jagged1 recapitulates the craniofacial phenotype of Alagille syndrome patients.* Hum Mol Genet, 2012. **21**(6): p. 1374-83.

45. Caparbo, V.F., et al., *Serum from children with polyarticular juvenile idiopathic arthritis (pJIA) inhibits differentiation, mineralization and may increase apoptosis of human osteoblasts "in vitro".* Clin Rheumatol, 2009. **28**(1): p. 71-7.

46. Cappellen, D., et al., *Transcriptional program of mouse osteoclast differentiation governed by the macrophage colony-stimulating factor and the ligand for the receptor activator of NFkappa B.* J Biol Chem, 2002. **277**(24): p. 21971-82.

47. Cooper, G.M., et al., *Testing the critical size in calvarial bone defects: revisiting the concept of a critical-size defect.* Plast Reconstr Surg, 2010. **125**(6): p. 1685-92.

CHAPTER 5

The Role of the Notch Ligand Jagged1 During Bone Development and Aging

5.1 Introduction

Embryological development of long bones utilizes endochondral ossification. Mesenchymal cells form condensations and then differentiate into chondrocytes to produce an initial cartilage matrix that is eventually replaced by bone. Cells at the periphery of the condensations elongate and form a layer of connective tissue known as the perichondrium and periosteum. These cells ultimately differentiate into osteoblasts forming the bone collar, which is the precedent to cortical bone. Chondrocytes in the center of the condensations continue to differentiate and produce the cartilage matrix, eventually becoming enlarged hypertrophic chondrocytes. The hypertrophic cartilage matrix mineralizes and cells begin to undergo apoptosis. The invading vasculature from the surrounding bone collar mediates an influx of osteoblasts, which forms the initial bone matrix on top of resorbing cartilage. This initial bone is known as the primary spongiosa, which is the prequel to trabecular bone. Chondrocytes either proximally or distally to this primary site of ossification continue to proliferate and arrange into columns of avascular cartilage known as the growth plate, which is found at each end of expanding bone. The growth plate is responsible for longitudinal bone growth through the sequence of chondrocyte proliferation, which effectively expands the growth plate towards the bone center, followed by differentiation, hypertrophy, apoptosis, and replacement of cartilage by bone. A secondary site of ossification forms between the growth plate and the distal ends of the bone. In the trabecular region contained within the cortical compartment, hematopoietic elements form the marrow cavity. During post-natal growth, long bones continue to elongate through endochondral ossification until chondrocytes in the growth plate cease to proliferate and the cartilage is completely replaced by bone in most mammals. Cortical bone growth and remodeling continues throughout adulthood through osteoblast-mediated expansion of the outer periosteal

surface and osteoclast-mediated resorption of the inner endosteal surface, which together regulate thickness of the cortical compartment [1-4].

The Notch signaling pathway is a developmentally conserved cell-to-cell signaling pathway that regulates cell proliferation, differentiation, fate determination, apoptosis, and other behaviors [5]. Activation of this signaling pathway occurs when a Notch ligand (Jagged 1,2 and Delta-like 1,4) expressed on the surface of a signaling cell interacts with a Notch receptor (Notch 1-4) expressed on the surface of a receiving cell. The Notch intracellular domain (NICD) is cleaved via a two-stage proteolytic event mediated first by the ADAM family metalloproteinase tumor necrosis factor α conversion enzyme (ADAM/TACE), and then by the γ-secretase complex comprised of Presenilins (Psen) 1 and 2. Cleaved NICD translocates to the nucleus where it binds to RBPjκ converting it from a transcriptional repressor to an activator. Mastermind-like proteins (MAML) then bind to the NICD-RBPjκ complex and serve as a scaffold to recruit other co-activators necessary to initiate transcription of canonical Notch target gene families Hes and Hey [6-8].

Notch signaling and its components have been shown to regulate embryological bone development and maturation. Deletion of Notch1 and Notch2 in mesenchymal progenitor cells (utilizing Cre recombinase driven by the Prx1 promoter) (Prx1-Cre; Notch1$^{-/f}$ Notch2$^{f/f}$) or similar deletion of Psen1 and Psen2 (Prx1-Cre; Psen1$^{f/f}$ Psen2$^{-/-}$) stimulates osteoblast differentiation and early trabecular bone formation, which is ultimately lost during aging due to depletion of the progenitor pool and increased osteoclast activity [9]. These results demonstrate that early expression of Notch components maintains progenitors in an undifferentiated state. Deletion of Notch receptors or Psens in committed osteoblasts (Col2.3 promoter) or mature osteoblasts (Ocn promoter) does not alter early bone formation, but results in osteopenia during aging, demonstrating that expression of these Notch pathway components in more mature osteogenic cells primarily serves to indirectly inhibit osteoclast activity (Col2.3-Cre; Notch1$^{f/f}$ Notch2$^{f/f}$) [9] (Col2.3-Cre; Psen1$^{f/f}$ Psen2$^{-/-}$) [10] (Ocn-Cre; Notch1$^{f/f}$) [11]. Global deletion of Notch target gene Hey1 also results in osteopenia [12], further demonstrating the role of Notch components to inhibit osteoclast activity. Although the roles of Notch receptors, mediators of NICD cleavage, and

target genes are well-characterized, the roles of Notch ligands, which are the initiators of the pathways, during embryological bone development and maturation are not as well-understood.

Jagged1 (Jag1) is the most highly expressed Notch ligand during skeletal development [13], bone fracture healing [14], and chondrogenesis [15]. High Jag1 expression in osteochondral progenitor cells gradually decreases during chondrogenic differentiation [14, 15], whereas it is expressed at multiple stages of osteoblast differentiation [14]. Jag1 expression in the mesenchymal lineage also regulates hematopoietic cell behavior. Activation of parathyroid hormone and its receptor in osteoblast-lineage cells increases Jag1 expression, which then promotes hematopoietic stem cell expansion [16, 17]. Co-culture of Jag1-expressing stromal cells with bone marrow-derived macrophages inhibits osteoclast differentiation [18]. Collectively, the data suggests that Jag1 regulates bone formation and resorption.

Clinically, loss-of-function mutations to Jag1 are primarily responsible for Alagille Syndrome (ALGS) in humans [19, 20]. ALGS incorporates a vast array of developmental defects, including chronic liver cholestasis, bile duct paucity, particular facial structural abnormalities, cardiovascular disease, kidney and pancreatic disease, and musculoskeletal defects [21]. ALGS patients present with decreased bone mass [22] and increased risk of fracture [23], which is often assumed to be secondary to chronic liver cholestasis, where the resulting malabsorption of fat soluble vitamins and minerals is believed to be primarily responsible for impaired skeletal development. However, liver transplantations, which are common treatments for ALGS patients, have not been able to recover normal bone growth [22, 24]. A recent study demonstrated a direct role for Jag1 in craniofacial development [25]. Furthermore, in Chapter 3 we showed Jag1 to be highly expressed in mesenchymal lineage cells during bone fracture healing [14], suggesting that low bone mass and increased risk of fracture in ALGS patients may be due to direct effects of Jag1 expression in the skeleton, which a liver transplantation would not address. However, the role of Jag1 in mesenchymal lineage cells during skeletal development is unknown.

Therefore, the objective of this study was to determine the direct role of Jag1 during bone formation by using two skeletal-specific conditional Jag1 knockout mouse models; first removing the gene in a mesenchymal progenitor cell population (Prx1 promoter), and then deleting the

gene in a committed osteoblast population (Col2.3 promoter). We hypothesize that Jag1 expression in the mesenchymal lineage regulates bone formation through paracrine cell-to-cell signaling.

5.2 Methods

5.2.1 Generation of Mice

Jag1$^{f/f}$ mice [26] were crossed with mice expressing Cre recombinase on the Prx1 promoter (Prx1-Cre;Jag1$^{f/f}$). The Prx1 promoter is active in undifferentiated osteochondral progenitor cells, and all mesenchymal lineage cells in the developing mouse limb bud are derived from Prx1-expressing cells [27]. Therefore, in this model Jag1 will be conditionally deleted in osteochondral progenitor cells of the limb-bud prior to skeletal development (Figure 5.1). Wild type mice are heterozygous and homozygous Jag1 floxed but Cre-negative (WT). These mice are on a C57Bl/6 background.

Jag1$^{f/f}$ mice were also crossed with mice expressing Cre recombinase from the 2.3 kb fragment of the collagen type I promoter, also known as the Col2.3 promoter (Col2.3-Cre;Jag1$^{f/f}$). The Col2.3 promoter is active in committed osteoblasts that align trabecular and cortical bone, but not in cells in the growth plate or osteoprogenitors in the periosteum [28, 29]. Therefore, in this model Jag1 will be deleted in an osteoblast-specific population later on during differentiation (Figure 5.1). Wild type mice are heterozygous and homozygous Jag1 floxed but Cre-negative (WT). These mice are on a mixed C57Bl/6 and CD1 background.

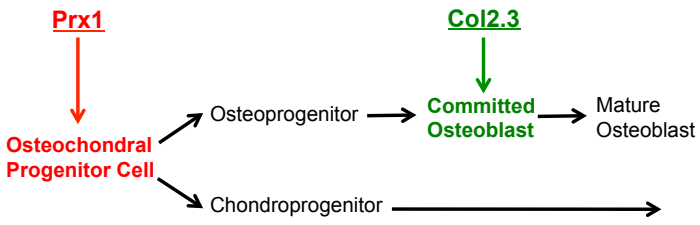

Figure 5.1. Schematic depicting Prx1 and Col2.3 expression during osteochondral lineage differentiation. Prx1 is first expressed in undifferentiated osteochondral progenitor cells [27]. Col2.3 is first expressed in committed osteoblasts [28, 29].

5.2.2 Experimental Design

Femurs were harvested for micro-computed tomography (μCT) analysis of bone formation from Prx1-Cre;Jag1$^{f/f}$ and Col2.3-Cre;Jag1$^{f/f}$ male and female mice with respective WT controls at 8 weeks of age. Additional femurs from Prx1-Cre;Jag1$^{f/f}$ male mice and WT mice were also harvested at 9 months (n=7-12).

RNA from whole tibiae (including cortical bone, trabecular bone, and marrow) was harvested for quantitative real-time polymerase chain reaction (QPCR) analysis of gene expression from Prx1-Cre;Jag1$^{f/f}$ and Col2.3-Cre;Jag1$^{f/f}$ mice with respective WT controls at 8 weeks of age. RNA was also isolated from the tibial cortical bone compartment (excluding trabecular bone and marrow) from Prx1-Cre;Jag1$^{f/f}$ mice and WT control at 8 weeks (n=3-5).

5.2.3 Micro-computed Tomography (μCT)

Femurs were scanned using a Scanco vivaCT40 μCT system (Scanco Medical) with the following parameters: 10.5 μm isotropic voxel size, 55 kVp, 145 μA, 1000 projections per 180°, 200 milliseconds integration time, 2D transverse reconstructed 2,048 x 2,048 pixel images. Cortical bone parameters were measured by analyzing 50 slices (0.525 mm) in the mid-diaphysis. This defined region was the central portion between the proximal and distal ends of the femur. A semi-automated contouring method was used to determine the outer cortical bone perimeter. Briefly, a user-defined contour was drawn around the cortical bone perimeter of the first slice. This initial estimate was then subjected to automated edge detection. This semi-automated contour then served as the initial estimate for the next slice, and the automated contouring process continued for all 50 slices. A fixed, global threshold of 37.2% of the maximum gray value was used to distinguish cortical bone from soft tissue and marrow. Trabecular bone parameters were measured by analyzing 101 slices (1.06 mm) of the distal metaphysis. Briefly, the distal end of the analysis region was chosen to be 0.105 mm proximal to the end of the primary spongiosa in the marrow cavity. This assured that only trabecular bone was analyzed. Starting at this image, a user-defined contour was drawn to include trabecular bone within the marrow cavity and exclude cortical bone. User-defined contours were drawn every 10 slices (0.105 mm) and an

automated morphing program was used to interpolate the contours for all images in between. A fixed, global threshold of 23% of the maximum gray value, which corresponds to 321.6 mg HA/cm^3 was used to distinguish trabecular bone from soft tissue and marrow. A Gaussian low-pass filter (σ = 0.8, support = 1) was used for all analyses.

5.2.4 Quantitative Real-Time Polymerase Chain Reaction (QPCR)

Tissue was placed in RNAlater solution and stored at -80°C until further processing. Specimens were then thawed on ice and placed in Qiazol lysis reagent (Qiagen). Tissue was homogenized using the Tissue Tearor (BioSpec Products) and mRNA was extracted using the Qiagen miRNeasy Mini Kit with DNase digestion to remove DNA contamination. RNA yield was determined using a NanoDrop 1000 spectrophotometer (ThermoScientific). 1 μg of mRNA was reverse transcribed into 20 μl of cDNA using the Applied Biosystems High Capacity RNA-to-cDNA Kit. Gene expression was quantified using a 7500 Fast Real-Time PCR system (Applied Biosystems) from a total of 10 μl of Master Mix per well, which included 1x Fast SYBR Green (Applied Biosystems), forward and reverse primers (0.45 μM), and 0.5 μl of cDNA. For each gene of interest, samples were run in duplicate and control wells were run to rule out DNA contamination and primer dimer binding. Proper amplicon production was confirmed by melt curve analysis. QPCR data was first normalized to β-actin housekeeping control, and then presented as fold change expression to each genotype's respective whole bone (Prx1-Cre;Jag1$^{f/f}$ or Col2.3-Cre;Jag1$^{f/f}$) calculated using the formula $2^{-\Delta\Delta C(t)}$.

5.2.5 Statistical Analysis

A student's t-test was used to compare each Jag1 knockout group to its respective wild type control for all μCT and QPCR parameters (*p<0.050, $^{\#}$p<0.100). For linear regression analysis, genes are presented as relative expression to β-actin calculated using the formula $2^{-\Delta C(t)}$.

5.3 Results

5.3.1 Jag1 Deletion During Early and Late Differentiation Inhibits Trabecular Bone Formation

Jag1 deletion in Prx1 lineage cells decreased trabecular bone volume fraction (BV/TV) and tissue mineral density (TMD) in 8-week-old female mice (Figure 5.2). This phenotype persisted during aging in 9-month-old male mice. Similarly, there was an increase in trabecular number (Tb.N) and decrease in trabecular separation (Tb.Sp) in 8-week-old male mice that persisted to 9 months. There were no differences in trabecular thickness (Tb.Th).

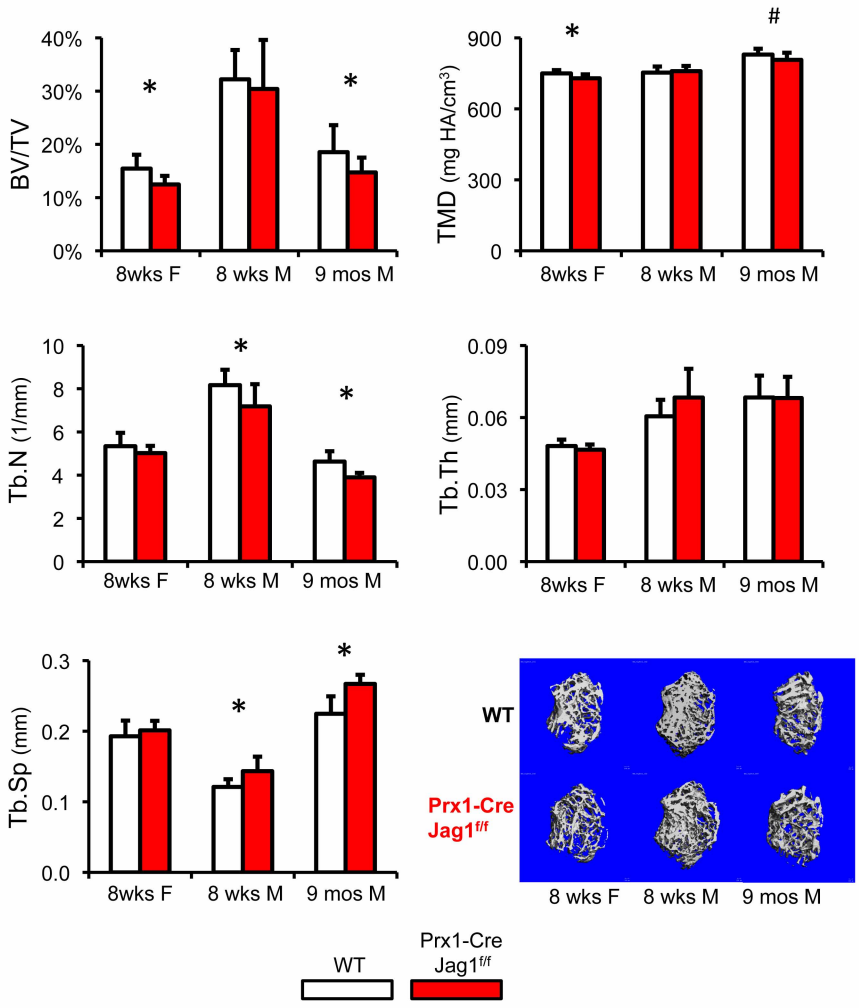

Figure 5.2. μCT analysis of trabecular bone in Prx1 mice at 8 weeks (females and males) and 9 months of age (males): bone volume fraction (BV/TV, top left), tissue mineral density (TMD, top right), trabecular number (Tb.N, middle left), trabecular thickness (Tb.Th, middle right), trabecular separation (Tb.Sp, bottom left), and representative 3D images (bottom right). *p<0.050, #p<0.100

Jag1 deletion on the Col2.3 promoter also decreased trabecular BV/TV, TMD, Tb.N, Tb.Th and increased Tb.Sp at 8 weeks (Figure 5.3). This phenotype was observed in male mice only. Collectively, the data suggests that endogenous Jag1 expression during both early and late differentiation positively regulates trabecular bone mass during development and aging.

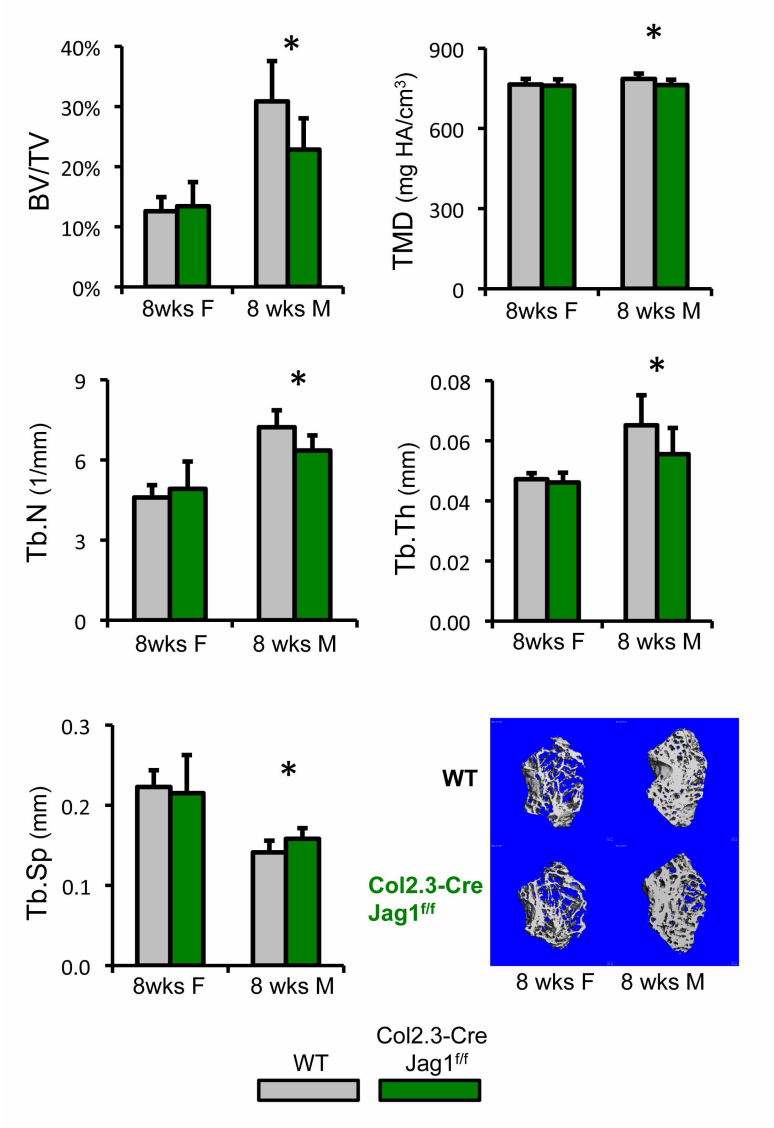

Figure 5.3. μCT analysis of trabecular bone in Col2.3 mice at 8 weeks (females and males) of age: bone volume fraction (BV/TV, top left), tissue mineral density (TMD, top right), trabecular number (Tb.N, middle left), trabecular thickness (Tb.Th, middle right), trabecular separation (Tb.Sp, bottom left), and representative 3D images (bottom right). *p<0.050, #p<0.100

5.3.2 Jag1 Deletion During Early and Late Differentiation Promotes Periosteal Expansion and Endosteal Resorption of Cortical Bone

Jag1 deletion on the Prx1 promoter increased total area (Tt.Ar), marrow area (M.Ar), cortical bone area (Ct.Ar) and cortical bone thickness (Ct.Th) in 8-week-old male and female mice (Figure 5.4). This phenotype largely persisted in 9-month-old males.

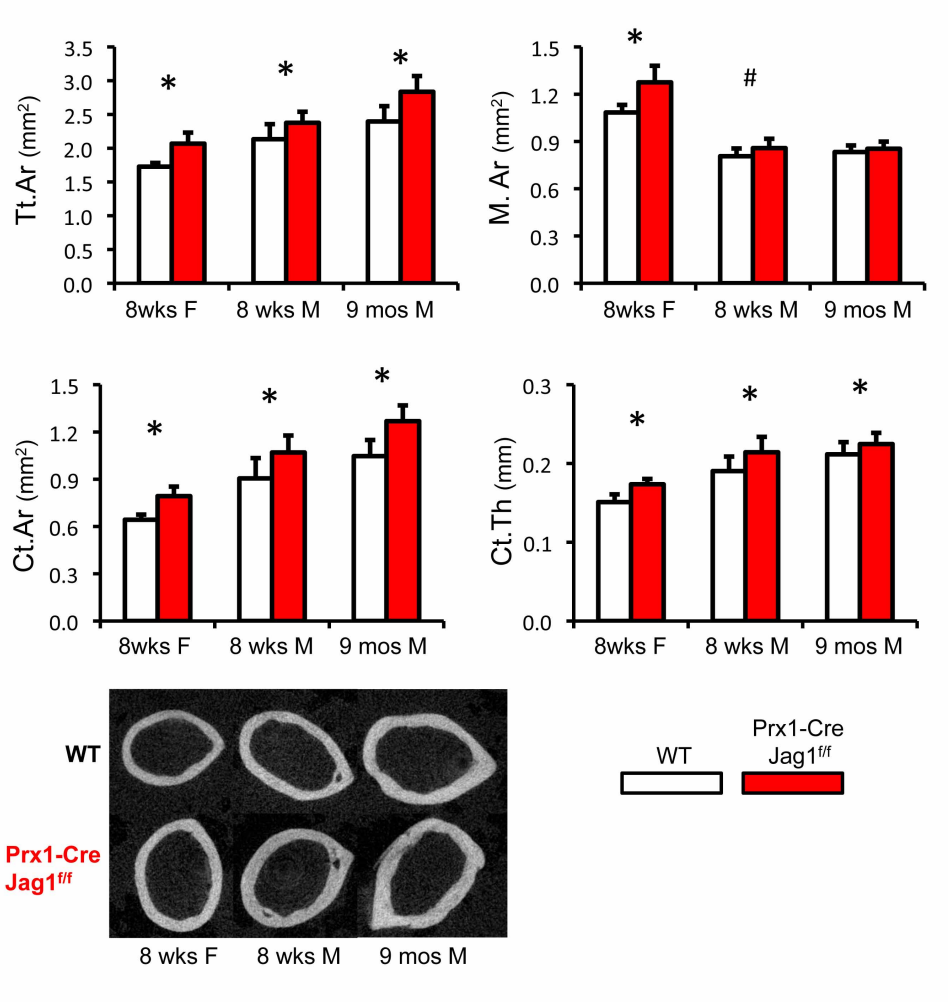

Figure 5.4. μCT analysis of cortical bone in Prx1 mice at 8 weeks (females and males) and 9 months of age (males): total area (Tt.Ar, top left), marrow area (M.Ar, top right), cortical bone area (Ct.Ar, middle left), cortical bone thickness (Ct.Th, middle right), and representative 2D images (bottom left). *p<0.050, #p<0.100

Jag1 deletion on the Col2.3 promoter also increased Tt.Ar and M.Ar in 8-week-old female mice (Figure 5.5). However this did not translate to a difference in Ct.Ar or Ct.Th. No differences were found in male mice. Collectively, the data suggests that endogenous Jag1 expression during early and late differentiation negatively regulates periosteal expansion, indicated by Tt.Ar, and endosteal resorption of cortical bone, indicated by M.Ar. Endogenous Jag1 expression during early differentiation also negatively regulates cortical bone mass, indicated by Ct.Ar and Ct.Th. The observed cortical bone phenotype is in apparent opposition to the trabecular bone phenotype.

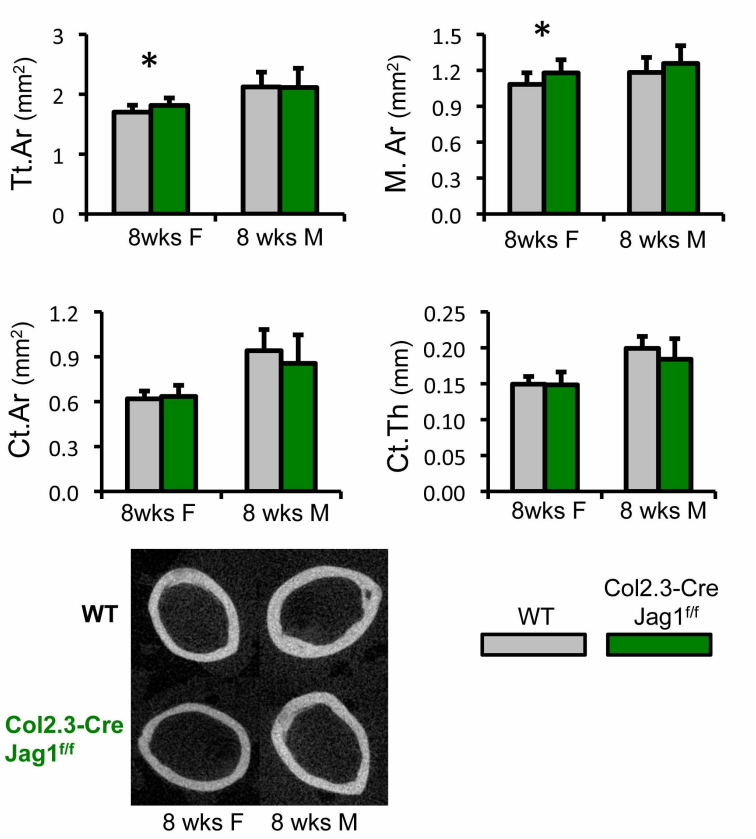

Figure 5.5. μCT analysis of cortical bone in Col2.3 mice at 8 weeks (females and males) of age: total area (Tt.Ar, top left), marrow area (M.Ar, top right), cortical bone area (Ct.Ar, middle left), cortical bone thickness (Ct.Th, middle right), and representative 2D images (bottom left). *p<0.050, #p<0.100

5.3.3 Jag1 regulation of Notch Pathway, Osteoblast, Osteoclast, and Proliferation Gene Expression

To understand the role of Jag1 on gene expression, RNA was harvested from whole bone (tibia) of Prx1-Cre;Jag1$^{f/f}$ female and Col2.3-Cre;Jag1$^{f/f}$ male mice at 8 weeks of age. Because there was an opposite cortical bone phenotype, RNA was also harvested from the diaphyseal cortical compartment from Prx1-Cre;Jag1$^{f/f}$ male mice. Sexes were chosen based on intensity of observed phenotypes via μCT and availability of RNA specimens. β-actin C(t) values were not different between Jag1 deletion and respective WT groups in whole and cortical bone.

Jag1 gene expression is decreased in whole bone of Prx1-Cre;Jag1$^{f/f}$ and Col2.3-Cre;Jag1$^{f/f}$ mice as well as in cortical bone of Prx1-Cre;Jag1$^{f/f}$ mice (Figure 5.6). In whole bone, this resulted in decreased Notch target Hey1 and Hes1 gene expression. However, there was no change in expression in cortical bone, which already had reduced levels of basal Notch target gene expression. This demonstrates that Jag1 deletion inhibits Notch target gene expression in whole bone but not in cortical bone.

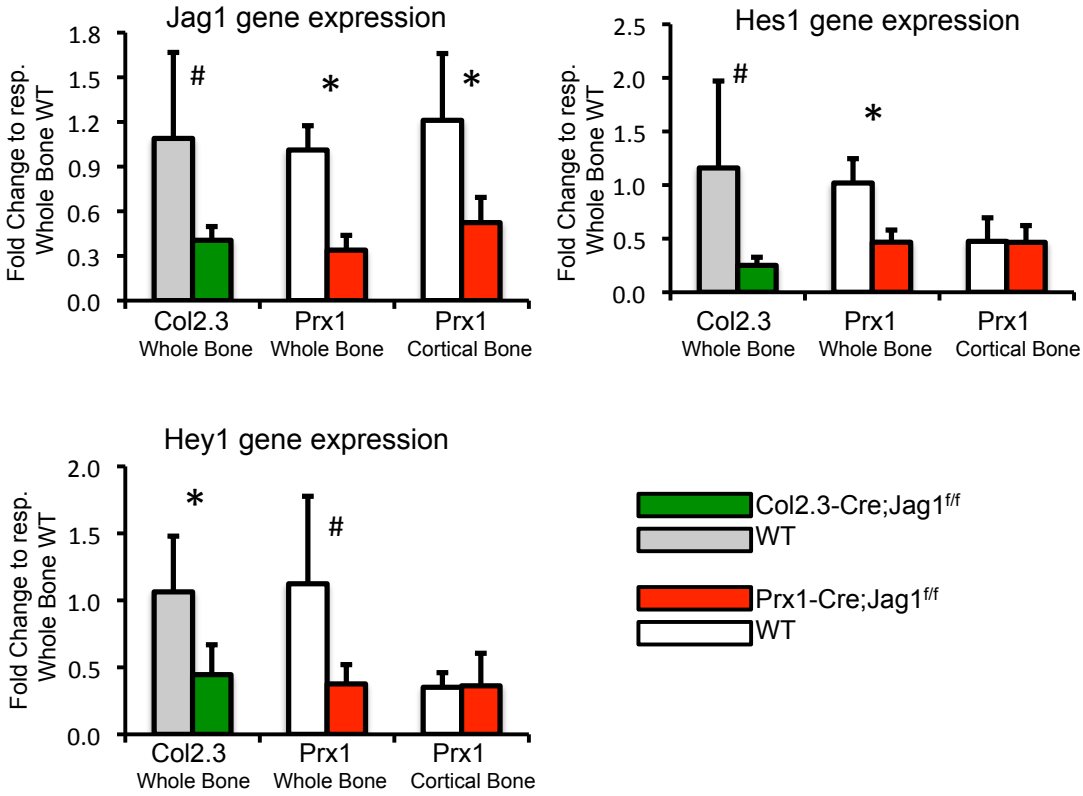

Figure 5.6 (above). Gene expression of Notch pathway components Jag1, Hes1 and Hey1. Data is presented as fold change expression to each genotype's respective whole bone (Prx1-Cre;Jag1$^{f/f}$ or Col2.3-Cre;Jag1$^{f/f}$) calculated using the formula $2^{-\Delta\Delta C(t)}$. *p<0.050, $^{\#}$p<0.100

Jag1 disruption from either Prx1 or Col2.3 promoters decreased expression of osteogenic genes osterix (Osx), osteocalcin (Ocn) and collagen type I (Col1a1) in whole bone (Figure 5.7). However, Jag1 deletion on the Prx1 promoter had no affect on osteogenic gene expression in cortical bone, demonstrating that Jag1 deletion inhibits osteoblast activity in whole bone but not within the cortical bone.

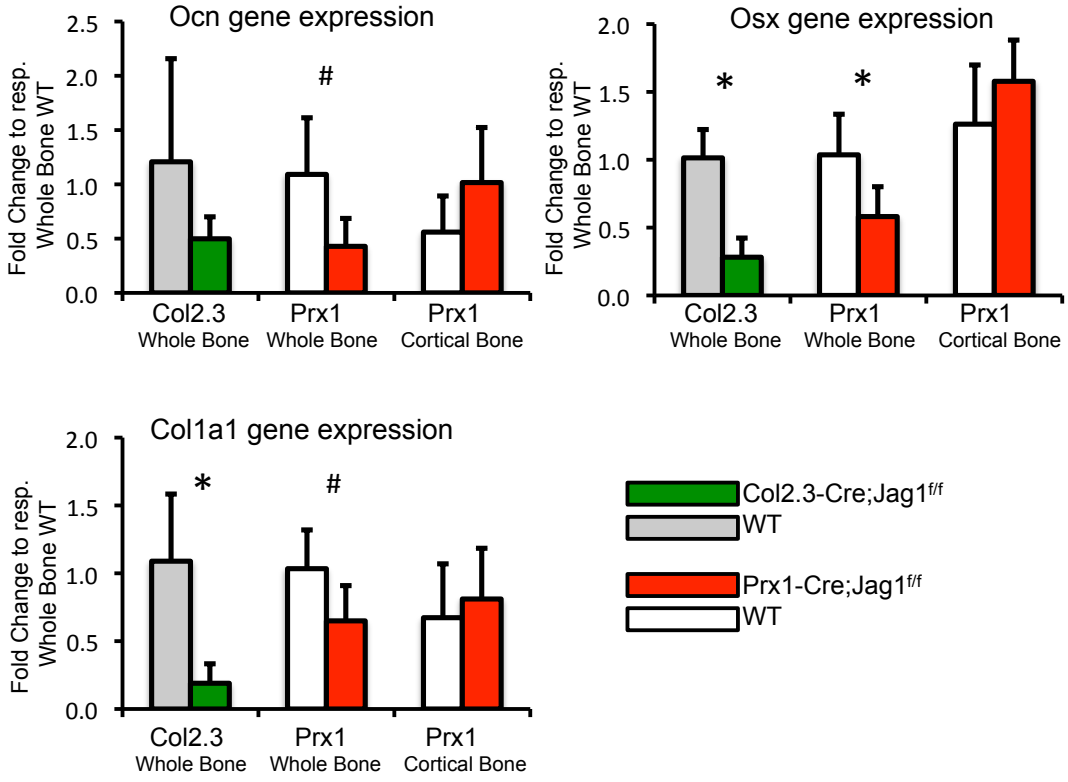

Figure 5.7. Osteogenic gene expression of osteocalcin (Ocn), osterix (Osx) and collagen type I (Col1a1). Data is presented as fold change expression to each genotype's respective whole bone (Prx1-Cre;Jag1$^{f/f}$ or Col2.3-Cre;Jag1$^{f/f}$) calculated using the formula $2^{-\Delta\Delta C(t)}$. *p<0.050, $^{\#}$p<0.100

Prx1 and Col2.3 specimens were pooled together for linear regression analysis. Gene expression of Notch components Jag1, Hes1 and Hey1 were each positively significantly correlated to Col1a1 gene expression regardless of specimen (whole bone and cortical bone combined) (Figure 5.8). Hey1 was further positively significantly correlated to Ocn gene expression within whole bone. This data demonstrates that expression of Notch components are positively correlated with expression of osteogenic markers.

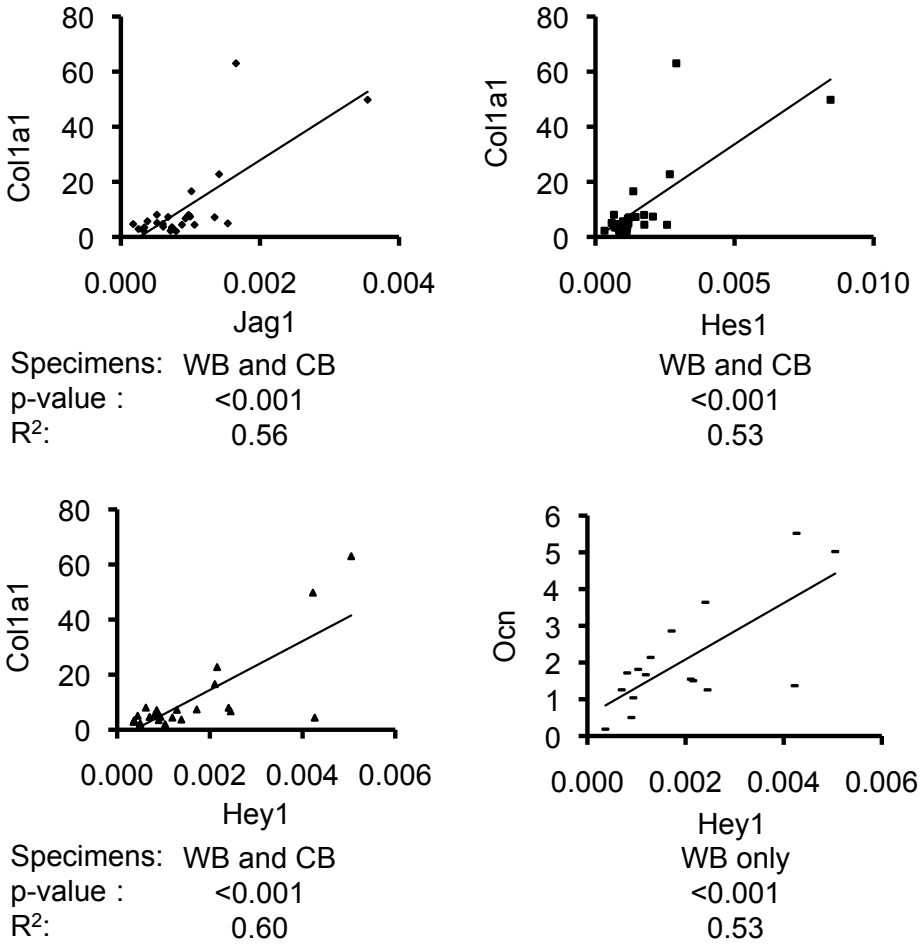

Figure 5.8. Linear correlation of Notch components (Jag1, Hes1, Hey1) with osteogenic markers (Col1a1, Ocn) for whole bone (WB only) or whole bone and cortical bone combined (WB and CB). All data includes both Prx1 and Col2.3 models. Data is presented as relative expression to β-actin calculated using the formula $2^{-\Delta C(t)}$.

Jag1 deletion on the Prx1 and Col2.3 promoters also decreased expression of RankL, a pro-osteoclast ligand expressed by osteoblasts that binds to RANK expressed on the surface of osteoclasts to promote differentiation, as well as osteoprotogerin (OPG), an anti-osteoclast decoy receptor expressed by osteoblasts that binds to RankL to inhibit its activity, in whole bone but not in cortical bone (Figure 5.9). Although the OPG:RankL ratio was unaltered in both compartments, TRAP gene expression, a direct marker of osteoclasts, was increased due to Jag1 deletion on the Prx1 promoter in cortical bone. Collectively, the data suggest that Jag1 deletion does not alter the balance of pro- and anti-osteoclast genes expressed by osteoblasts in whole bone and cortical bone, but does increase expression of direct osteoclast markers in cortical bone only.

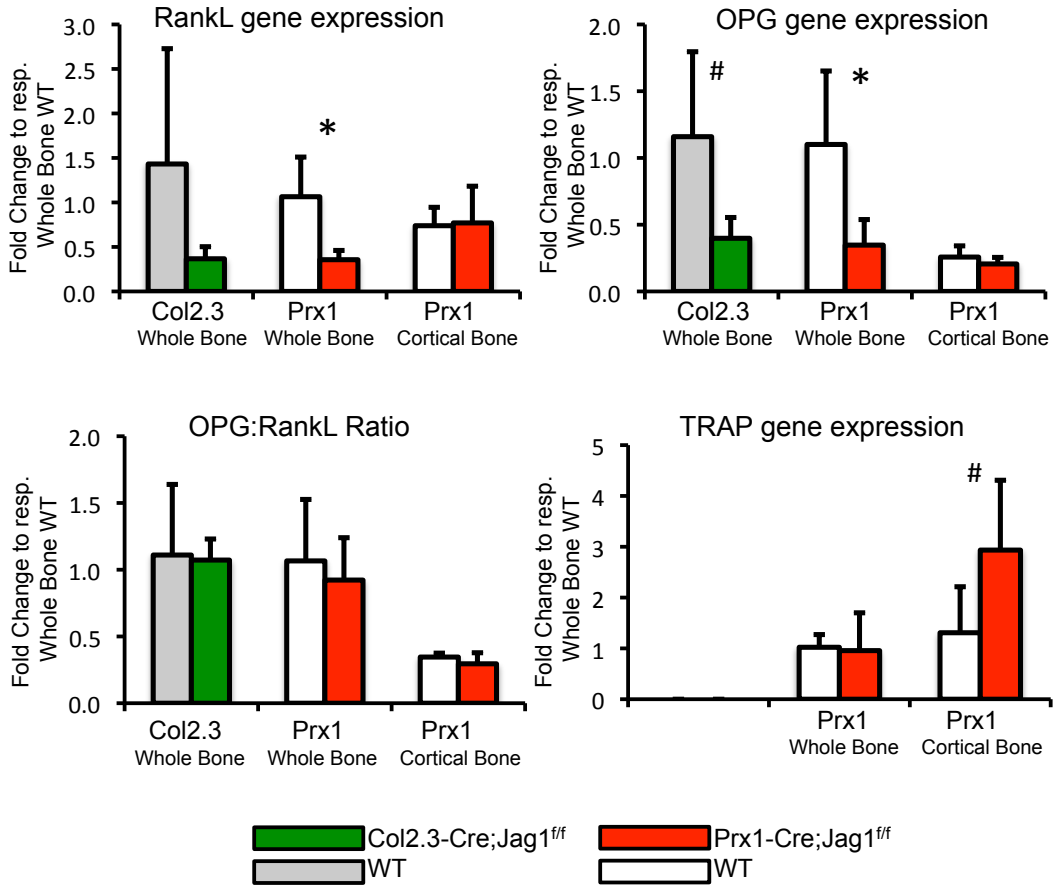

Figure 5.9. Gene expression of osteoblast mediators of osteoclast activity – RankL, osteoprotogerin (OPG) and the ratio between the two (OPG:RankL) – and osteoclast marker TRAP. Data is presented as fold change expression to each genotype's respective whole bone (Prx1-Cre;Jag1$^{f/f}$ or Col2.3-Cre;Jag1$^{f/f}$) calculated using the formula $2^{-\Delta\Delta C(t)}$. *p<0.050, $^{\#}$p<0.100

Jag1 deletion on the Col2.3 promoter decreased expression of Cyclin D1 in whole bone (Figure 5.10). Col2.3 and Prx1 trends were similar but non-significant for PCNA gene expression. Alternatively, Jag1 deletion on the Prx1 promoter increased PCNA expression in cortical bone, suggesting that Jag1 deletion moderately inhibits proliferation gene expression in whole bone, but moderately promotes expression in cortical bone.

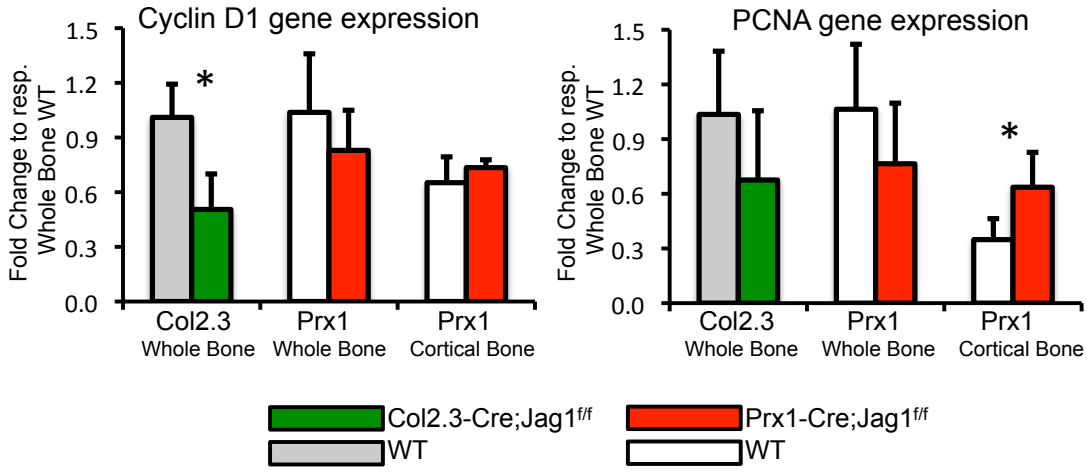

Figure 5.10. Gene expression of proliferation markers Cyclin D1 and PCNA. Data is presented as fold change expression to each genotype's respective whole bone (Prx1-Cre;Jag1$^{f/f}$ or Col2.3-Cre;Jag1$^{f/f}$) calculated using the formula $2^{-\Delta\Delta C(t)}$. *p<0.050, $^{\#}$p<0.100

5.4 Discussion

The objective of this study was to determine the role of Jag1 during bone formation and remodeling. We found a similar role for Jag1 during early (Prx1) and late (Col2.3) osteoblast differentiation. Endogenous Jag1 expression in whole bone positively regulated notch target and osteogenic gene expression, had no effect on osteoclast gene expression, and moderately stimulated proliferation genes. Whole bone gene expression results strongly correlated with increased trabecular bone formation in wild type mice at 8 weeks and 9 months of age. Osteoblast density in trabecular bone is more than two times greater than in cortical bone [30], suggesting that osteogenic components of whole bone gene expression analysis are primarily of trabecular osteoblast origin. Alternatively, it is also possible that there is greater ability to liberate RNA from trabecular bone than from cortical bone. Collectively, the data shows that in trabecular bone Jag1 activates the Notch signaling pathway, and promotes osteoblast differentiation and proliferation, ultimately enhancing bone formation. Furthermore, gene expression analysis of all compartments and animal models demonstrated that Jag1-induced Notch signaling was positively and linearly correlated with osteogenic gene expression. This pro-osteogenic role for Jag1 has not been identified for other Notch ligands, and the results are in contrast to previous results showing that expression of Notch receptors in the mesenchymal lineage primarily serve to maintain mesenchymal progenitors in an undifferentiated state [9] or indirectly inhibit osteoclast activity [9-11]. However, consistent with this finding, Notch ligands have previously demonstrated reciprocal effects on cell function. Dll4 inhibits vascularization, whereas Jag1 promotes it [31]. Furthermore, a recent study demonstrated that Dll1 directly enhances osteoclast differentiation, whereas Jag1 directly inhibits it [32]. Therefore, it is not surprising that Jag1 could function as a discrete positive regulator of osteoblast differentiation and bone formation in opposition to what has been shown for other Notch components.

The differences in bone geometry in Prx1-Cre;Jag1$^{f/f}$ mice present at 8 weeks persisted during aging to 9 months, demonstrating a consistent role for Jag1 during skeletal development,

maturation and aging. Again, this is opposed to other studies that have shown differing phenotypes in young and aged mice due to Notch loss of function [9, 10].

Surprisingly, Jag1 appears to have divergent roles in trabecular and cortical compartments. The loss of Jag1 in cortical bone affected neither notch target nor osteogenic gene expression, enhanced osteoclast gene expression, which is consistent with other Notch components, and moderately promoted proliferation genes. This also strongly correlated with enhanced periosteal expansion, endosteal resorption, and bone mass in the cortical compartment. The mechanism behind this is currently unknown. However, it is of note that Jag1 does not appear to regulate Notch target gene expression in cortical bone. Hey1 and Hes1 are also targets of the BMP/TGF-β signaling pathway [33, 34]. It is possible that the BMP/TGF-β pathway compensated for the loss of Jag1-initiated Notch activity in the cortical compartment only. However, basal expression levels of Notch target genes in the cortical compartment of wild type mice are already at reduced levels relative to whole bone, suggesting that Notch signaling may be decreased in normal mature cortical bone. Alternatively, Jag1 could function non-canonically in cortical bone. There is evidence that Jag1 could signal within its own cell by reverse ligand cleavage of the intracellular domain independent of the Notch signaling pathway [35, 36]. Furthermore, Jag1 expression by cells outside of the cortical compartment could function in a non-paracrine manner acting on cortical bone, such as in a long range cell non-autonomous fashion [37]. Similarly, compensatory effects caused by decreased trabecular bone formation in knockout mice may regulate cortical bone mass independent of the Notch pathway. Finally, the cortical bone phenotype may also be due to changes in gene expression that occurred prior to the earliest 8-week time point analyzed. Regardless, more work is needed to fully elucidate a potential mechanism.

Prx1 trabecular and cortical bone phenotypes were present in both males and females. However, trabecular phenotypes in Col2.3 mice were more pronounced in males, whereas cortical bone phenotypes were more pronounced in females. A previous study showed that using the Col2.3 promoter model, floxing of alleles in the absence of germ-line transmission of the Cre recombinase gene (which would be considered a wild type mouse) could happen in as many as

50% of females but just 15% of males [38]. Thus, aberrant activity of the Col2.3 promoter in female gametes may account for the lack of trabecular phenotypic differences. The presence of a stronger cortical phenotype in Col2.3 females relative to male mice also further suggests that changes to cortical bone may be independent of Jag1 activity.

In conclusion, we demonstrate that Jag1 expression in the skeleton directly and positively regulates bone formation. This suggests liver transplantations for ALGS patients as an incomplete therapeutic strategy. While this will address secondary effects of liver function on bone mass, direct strategies should be taken to target the skeleton and mesenchymal lineage cells to improve Jag1 and ultimately osteogenic function. Our data demonstrated a pro-osteogenic role for Jag1 during bone formation. Delivery of Jag1 to the metaphysis (which includes the growth plate and trabecular bone) of developing long bones may improve bone formation prior to skeletal ALGS phenotypic onset. Jag1 can also be targeted to address other skeletal disorders. For example, delivery of Jag1 could enhance osteogenesis and improve bone formation during fracture healing.

Further characterization of Col2.3-Cre;$Jag1^{f/f}$ and Pr1-Cre;$Jag1^{f/f}$ mice is required to better understand the role of Jag1 on cellular behavior. Future studies will harvest bone marrow-derived mesenchymal progenitor cells to quantify the effect of Jag1 deletion during early and late differentiation on mesenchymal progenitor number (CFU-F assay), cell proliferation (Alamar Blue assay), and osteoblast differentiation (Alizarin Red S staining). Furthermore, histological analysis of bones will help localize the observed changes in gene expression, as well as allow for analysis of the cartilaginous growth plate.

5.5 References

1. Karsenty, G., H.M. Kronenberg, and C. Settembre, *Genetic control of bone formation.* Annu Rev Cell Dev Biol, 2009. **25**: p. 629-48.
2. Kronenberg, H.M., *Developmental regulation of the growth plate.* Nature, 2003. **423**(6937): p. 332-6.
3. Colnot, C., *Cellular and molecular interactions regulating skeletogenesis.* J Cell Biochem, 2005. **95**(4): p. 688-97.
4. Price, C., et al., *Genetic variation in bone growth patterns defines adult mouse bone fragility.* J Bone Miner Res, 2005. **20**(11): p. 1983-91.
5. Artavanis-Tsakonas, S., M.D. Rand, and R.J. Lake, *Notch signaling: cell fate control and signal integration in development.* Science, 1999. **284**(5415): p. 770-6.
6. Iso, T., L. Kedes, and Y. Hamamori, *HES and HERP families: multiple effectors of the Notch signaling pathway.* J Cell Physiol, 2003. **194**(3): p. 237-55.
7. Zanotti, S. and E. Canalis, *Notch and the skeleton.* Mol Cell Biol, 2010. **30**(4): p. 886-96.
8. Engin, F. and B. Lee, *NOTCHing the bone: insights into multi-functionality.* Bone, 2010. **46**(2): p. 274-80.
9. Hilton, M.J., et al., *Notch signaling maintains bone marrow mesenchymal progenitors by suppressing osteoblast differentiation.* Nat Med, 2008. **14**(3): p. 306-14.
10. Engin, F., et al., *Dimorphic effects of Notch signaling in bone homeostasis.* Nat Med, 2008. **14**(3): p. 299-305.
11. Zanotti, S., et al., *Notch inhibits osteoblast differentiation and causes osteopenia.* Endocrinology, 2008. **149**(8): p. 3890-9.
12. Salie, R., et al., *Ubiquitous overexpression of Hey1 transcription factor leads to osteopenia and chondrocyte hypertrophy in bone.* Bone, 2010. **46**(3): p. 680-94.

13. Dong, Y., et al., *RBPjkappa-dependent Notch signaling regulates mesenchymal progenitor cell proliferation and differentiation during skeletal development.* Development, 2010. **137**(9): p. 1461-71.

14. Dishowitz, M.I., et al., *Notch signaling components are upregulated during both endochondral and intramembranous bone regeneration.* J Orthop Res, 2012. **30**(2): p. 296-303.

15. Oldershaw, R.A., et al., *Notch signaling through Jagged-1 is necessary to initiate chondrogenesis in human bone marrow stromal cells but must be switched off to complete chondrogenesis.* Stem Cells, 2008. **26**(3): p. 666-74.

16. Calvi, L.M., et al., *Osteoblastic cells regulate the haematopoietic stem cell niche.* Nature, 2003. **425**(6960): p. 841-6.

17. Weber, J.M., et al., *Parathyroid hormone stimulates expression of the Notch ligand Jagged1 in osteoblastic cells.* Bone, 2006. **39**(3): p. 485-93.

18. Bai, S., et al., *NOTCH1 regulates osteoclastogenesis directly in osteoclast precursors and indirectly via osteoblast lineage cells.* J Biol Chem, 2008. **283**(10): p. 6509-18.

19. Oda, T., et al., *Mutations in the human Jagged1 gene are responsible for Alagille syndrome.* Nat Genet, 1997. **16**(3): p. 235-42.

20. Li, L., et al., *Alagille syndrome is caused by mutations in human Jagged1, which encodes a ligand for Notch1.* Nat Genet, 1997. **16**(3): p. 243-51.

21. Krantz, I.D., D.A. Piccoli, and N.B. Spinner, *Clinical and molecular genetics of Alagille syndrome.* Curr Opin Pediatr, 1999. **11**(6): p. 558-64.

22. Olsen, I.E., et al., *Deficits in size-adjusted bone mass in children with Alagille syndrome.* J Pediatr Gastroenterol Nutr, 2005. **40**(1): p. 76-82.

23. Bales, C.B., et al., *Pathologic lower extremity fractures in children with Alagille syndrome.* J Pediatr Gastroenterol Nutr, 2010. **51**(1): p. 66-70.

24. Quiros-Tejeira, R.E., et al., *Does liver transplantation affect growth pattern in Alagille syndrome?* Liver Transpl, 2000. **6**(5): p. 582-7.

25. Humphreys, R., et al., *Cranial neural crest ablation of Jagged1 recapitulates the craniofacial phenotype of Alagille syndrome patients.* Hum Mol Genet, 2012. **21**(6): p. 1374-83.

26. Kiernan, A.E., J. Xu, and T. Gridley, *The Notch ligand JAG1 is required for sensory progenitor development in the mammalian inner ear.* PLoS Genet, 2006. **2**(1): p. e4.

27. Logan, M., et al., *Expression of Cre Recombinase in the developing mouse limb bud driven by a Prxl enhancer.* Genesis, 2002. **33**(2): p. 77-80.

28. Kalajzic, I., et al., *Use of type I collagen green fluorescent protein transgenes to identify subpopulations of cells at different stages of the osteoblast lineage.* J Bone Miner Res, 2002. **17**(1): p. 15-25.

29. Liu, F., et al., *Expression and activity of osteoblast-targeted Cre recombinase transgenes in murine skeletal tissues.* Int J Dev Biol, 2004. **48**(7): p. 645-53.

30. Dodds, R.A., et al., *Comparative metabolic enzymatic activity in trabecular as against cortical osteoblasts.* Bone, 1989. **10**(4): p. 251-4.

31. Benedito, R., et al., *The notch ligands Dll4 and Jagged1 have opposing effects on angiogenesis.* Cell, 2009. **137**(6): p. 1124-35.

32. Sekine, C., et al., *Differential regulation of osteoclastogenesis by Notch2/Delta-like 1 and Notch1/Jagged1 axes.* Arthritis Res Ther, 2012. **14**(2): p. R45.

33. Larman, B.W., et al., *Distinct bone morphogenetic proteins activate indistinguishable transcriptional responses in nephron epithelia including Notch target genes.* Cell Signal, 2012. **24**(1): p. 257-64.

34. de Jong, D.S., et al., *Regulation of Notch signaling genes during BMP2-induced differentiation of osteoblast precursor cells.* Biochem Biophys Res Commun, 2004. **320**(1): p. 100-7.

35. D'Souza, B., A. Miyamoto, and G. Weinmaster, *The many facets of Notch ligands.* Oncogene, 2008. **27**(38): p. 5148-67.

36. Bray, S.J., *Notch signalling: a simple pathway becomes complex.* Nat Rev Mol Cell Biol, 2006. **7**(9): p. 678-89.

37. Kohn, A., et al., *Cartilage-specific RBPjkappa-dependent and -independent Notch signals regulate cartilage and bone development.* Development, 2012. **139**(6): p. 1198-212.

38. Cochrane, R.L., et al., *Rearrangement of a conditional allele regardless of inheritance of a Cre recombinase transgene.* Genesis, 2007. **45**(1): p. 17-20.

CHAPTER 6

Activation of Notch Signaling by Jagged1 Immobilization to a Poly(β-amino ester) Polymer Induces Osteoblastogenesis

6.1 Introduction

Bone fractures are a significant clinical and economic problem. While the majority of fractures heal with standard care, a considerable number exhibit delayed healing and can develop into non-unions [1, 2]. To treat these injuries, therapeutics have been developed to deliver osteoinductive (biological cues to stimulate osteoblast activity) and osteoconductive (scaffold or other cue to support bone formation) signals. Autologous bone grafts are considered the 'gold standard', but can result in donor site morbidity and yield only a limited amount of graft material. Demineralized bone matrix is more readily available, but has limited osteoinductive potential and can induce immunogenic reactions [3]. More recently, growth factor-based therapies have been developed to induce bone formation. Use of bone morphogenetic proteins (BMPs) has become a common clinical treatment to promote bone repair [4, 5]. However, recent reports suggest that BMPs lack the clinical efficiency and safety that has been widely demonstrated in pre-clinical animal models [6]. Therefore, a need persists for the identification of new targets and development of new therapies to promote bone tissue formation through delivery of osteoinductive and osteoconductive signals.

The Notch signaling pathway has been shown extensively to regulate mesenchymal cell behavior and embryological bone formation [7-14]. Briefly, activation of the cell-to-cell signaling pathway occurs when a membrane-bound ligand (Jagged 1,2 and Delta-like 1,4) from one cell interacts with a membrane-bound receptor (Notch 1-4) on the receiving cell. A two-stage proteolytic event cleaves the Notch intracellular domain (NICD), which translocates to the nucleus and binds with co-activators to initiate transcription of Notch target gene families Hes and Hey.

Jagged1 is the most highly expressed Notch ligand in mesenchymal cells [11, 15]. In Chapter 3, we demonstrated that it is also the most highly upregulated Notch ligand during bone

fracture healing [16]. Furthermore, in Chapter 5, we demonstrated that endogenous Jagged1 activity during early and late osteoblast differentiated promotes trabecular bone formation. Clinically, loss-of-function mutations to Jagged1 are responsible for Alagille Syndrome in humans [17, 18], a genetic disorder characterized by defects to multiple organs including the skeleton, where patients present with decreased bone mass and an increased risk of fracture [19, 20]. Collectively, the data demonstrates that Jagged1 regulates bone formation and may be a potential therapeutic target to improve bone regeneration. Therefore, the objective of this study is to develop a clinically translatable biomaterial construct comprised of Jagged1 and an osteoconductive scaffold, and evaluate its ability to induce bone tissue formation.

Previous studies have demonstrated a requirement for Jagged1 immobilization to a substrate in order to activate the Notch signaling pathway [21-23]. It has been hypothesized that the naturally-occurring immobilized state of a membrane-bound Notch ligand is required to apply a pulling force on the extracellular domain of the Notch receptor, which precedes cleavage of the intracellular domain (NICD) [24]. However, non-immobilized ligands are also able to bind to the Notch receptor and effectively inhibit Notch activity by preventing other immobilized ligands from binding to that receptor [25]. A previous study comparing Jagged1 immobilization strategies demonstrated that indirect immobilization of a recombinant Jagged1/Fc protein to a substrate via anti-Fc antibody binding was more effective than direct Jagged1/Fc adsorption at activating Notch signaling at lower protein concentrations (0.14–1.42 μg/mL [26]). It has been hypothesized that indirect immobilization of Jagged1/Fc bound by the Fc region results in uniformly oriented protein with the Jagged1 extracellular binding domain readily available for receptor binding, whereas direct adsorption results in randomly oriented protein with some binding domains inaccessible [26]. However, the optimal immobilization strategy to induce Notch activation at higher concentrations likely required for *in vivo* therapeutic effects is unknown. Therefore, we first set out to evaluate the ability of direct and indirect Jagged1 immobilization strategies at 2.5 and 10 μg/mL to induce Notch activity. We hypothesize that direct Jagged1 immobilization increases Notch activation relative to indirect at higher protein concentrations. Then we evaluated the

osteoinductive capabilities of the ideal Jagged1 immobilization strategy, with the hypothesis that Jagged1/A6 biomaterial constructs promote osteoblast differentiation.

Poly(β-amino ester)s (PBAEs) are clinically advantageous polymers to use as therapeutics because they are simple to synthesize with no by-products formed, and are inexpensive and commercially available. A combinatorial library of acrylate-terminated photocrosslinkable PBAEs was developed and characterized based on mechanics, degradation rate, and cellular interactions *in vitro* [27, 28]. One PBAE in particular, diethylene glycol diacrylate combined with isobutylamine, known as A6, was shown to promote bone tissue regeneration when used as a carrier for BMP-2 [29]. Based on its osteoconductive capability, A6 was utilized as the biomaterial substrate for Jagged1.

This research aims to develop a clinically translatable therapy to improve bone regeneration by targeting the Notch signaling pathway. The global hypothesis is that delivery of Jagged1 immobilized to A6 [Jagged1/A6] will activate Notch signaling and promote osteoblast differentiation.

6.2 Methods

6.2.1 Macromer Synthesis and Photopolymerization

A6 was synthesized as previously described [27]. Briefly, diethylene glycol diacrylate ('A') (Sigma, St. Louis, MO, USA) and isobutylamine ('6') (Sigma, St. Louis, MO, USA) were mixed together at a 1.2:1 molar ratio for 40 h at 90°C. 0.5 wt% of the photoinitiator 2,2-dimethoxy-2-phenylacetophenone (DMPA) (Sigma, St. Louis, MO, USA) diluted in dichloromethane was then mixed in for 1 h at 90°C.

For *in vitro* experiments, A6 was mixed with an equal volume of ethanol and 30 μL was added to coat the bottom of each 24-well tissue culture plate. Ethanol was allowed to evaporate overnight. The A6 macromer was photopolymerized by exposure to ultraviolet light (~10 mW/cm^2, 365 nm, 15 min) (Omnicure S1000 UV Spot Cure System, Exfo, Ontario, Canada) in a nitrogen-purging environment.

6.2.2 Jagged1 Immobilization Strategies

Recombinant rat Jagged1/Fc (98% homology to human Jagged1, R&D Systems, Minneapolis, MN, USA) was used to evaluate direct and indirect immobilization strategies. For direct immobilization, Jagged1/Fc diluted in PBS was adsorbed to the A6 surface for 2 h followed by two PBS washes.

For indirect immobilization, 15 μg/mL of $F(ab')_2$ fragment rabbi anti-human IgG-Fc specific fragment (anti-Fc antibody, Jackson Immunoresearch, West Grove, PA, USA) diluted in PBS was first adsorbed to the A6 surface for 2 h followed by two PBS washes. Anti-Fc-bound-A6 wells were then blocked in 1% BSA diluted in PBS for 2 h. Finally, Jagged1/Fc diluted in 0.1% BSA in PBS was added for 2 h, allowing for the anti-Fc antibody to bind to the Fc portion of the recombinant Jagged1/Fc protein. In the following sections, recombinant Jagged1/Fc will simply be referred to as Jagged1. All incubations were done at room temperature.

6.2.3 In vitro Experimental Design

Direct and indirect Jagged1 immobilization strategies to A6 [Jagged1/A6] at 0, 2.5 and 10 μg/mL (Direct[0/A6], Direct[2.5/A6], Direct[10/A6], Indirect[0/A6], Indirect[2.5/A6], Indirect [10/A6]) were evaluated in primary human bone marrow-derived mesenchymal stem cells (hMSCs, Lonza, Walkersville, MD, USA) plated at 5000 cells/cm^2 at passage 4 in 24-well plates and cultured in standard growth media (SGM: αMEM, 20% FBS, 1x l-glutamine, 1x pen/strep). Cells were harvested for gene expression analysis of Notch target and osteogenic genes at days 1, 3, 5 and 7 post-plating (n=3). Control tissue culture polystyrene (TCPS) wells with no A6 and no Jagged1 [0/TCPS] were included for gene expression analysis. Cell number was assessed using an Alamar Blue assay at days 1, 3, 5 and 7 (n=5). Alkaline phosphatase, an enzyme produced by osteoblasts during bone formation, was evaluated histochemically at day 7 (n=5). Successfully immobilized Jagged1 to the A6 surface through direct and indirect strategies was quantified using an enzyme-linked immunosorbent assay (ELISA) (n=4). The 40-day release kinetics profile of direct and indirect immobilized Jagged1 was similarly quantified by ELISA (n=1).

Then to evaluate the ability of direct Jagged1/A6 immobilization at 0 and 10 μg/mL (Direct[0/A6], Direct[10/A6]) to induce osteogenesis, hMSCs were plated at 10,000 cells/cm^2 at passage 4 in 24-well plates and cultured in osteogenic media (OGM: αMEM, 10% FBS, 1x l-glutamine, 1x pen/strep, 200 μM ascorbic acid 2-phosphate, 100 mM β-glycerophosphate, 100 nM dexamethasone). Cell number was assessed using Alamar Blue at days 1 (n=9), 7 (n=6), 10 (n=6) and 13 (n=3). Alkaline phosphatase was evaluated using histochemistry 7 (n=3). Calcified mineral tissue deposition by cells, which is indicative of terminal osteoblast differentiation, was assessed by Alizarin Red S staining at days 10 and 13 (n=5). Control TCPS wells with no A6 and no Jagged1 [0/TCPS] were also included for calcified mineral deposition analysis (n=3).

6.2.4 Quantitative Real-Time Polymerase Chain Reaction (QPCR)

mRNA was extracted from cells using the Qiagen RNeasy Mini Kit with DNase digestion to remove DNA contamination. Yield was determined spectrophotometrically. 0.125 μg of mRNA was reverse transcribed into 20 μL of cDNA using the Applied Biosystems High Capacity RNA-to-cDNA Kit. Gene expression was quantified using a 7500 Fast Real-Time PCR system (Applied Biosystems, Foster City, CA, USA) from a total of 10 μL of master mix per well, which included 1x Power SYBR Green (Applied Biosystems, Foster City, CA, USA), forward and reverse primers (0.45 μM), and 0.5 μL of cDNA. For each gene of interest, samples were run in duplicate and control wells were run to rule out DNA contamination and primer dimer amplification. Proper amplicon development was confirmed by melt curve analysis. QPCR data is normalized to β-actin housekeeping control and presented as fold change relative to direct A6 control (Direct[0/A6]) at day 1 for each experiment using the formula $2^{-\Delta\Delta C(t)}$.

6.2.5 Alamar Blue Assay

At each time point, cells were incubated in 500 μL of 10% Alamar Blue solution (Invitrogen, Carlsbad, CA, USA) diluted in media and protected from light. Experiments in SGM comparing direct and indirect immobilization strategies were incubated for 4 h. Experiments in

OGM evaluating the ability of Jagged1 to induce osteogenesis were incubated for 2 h. 100 μL from each well were then transferred to a 96 well plate and fluorescently measured (excitation 570 nm, emission 585 nm). Wells were then refreshed with new media.

6.2.6 Alkaline Phosphatase (AP) Histochemical Staining

Cells were fixed and stained using an Alkaline Phosphatase kit (Sigma, St. Louis, MO, USA) according to the manufacturer's instructions. Plates were scanned and area of alkaline phosphatase staining within each well was quantified using ImageJ (National Institutes of Health).

6.2.7 Alizarin Red S Staining

Cells were fixed in ice cold 70% ethanol for 10 min and then incubated in 0.5% Alizarin Red S diluted in dH_2O (pH adjusted to 4.1-4.3) for 10 min. Alizarin Red S stains calcified mineral tissue red and the A6 background yellow. Multiple images were acquired from each well using an Olympus CKX41 inverted microscope with a Spot Idea 5 megapixel camera. Area of mineral staining within each well was quantified using ImageJ.

6.2.8 ELISA

Jagged1 was immobilized to A6 as described above in 96-well plates in order to quantify the concentration of successfully immobilized Jagged1 through direct and indirect strategies. Wells were then incubated with biotinylated goat anti-rat Jagged1 detection antibody for 2 h followed by streptavidin-HRP for 20 min. H_2O_2 equally mixed with tetramethylbenzidine was used as the substrate for 20 min followed by addition of 2 N H_2SO_4 to stop the reaction. Optical density of each well was read at 450 nm with wavelength correction at 570 nm.

Jagged1 was similarly immobilized to A6 as described above in 48-well plates to evaluate the release kinetics profile of direct and indirect strategies. Following Jagged1 immobilization, wells were incubated in PBS at 37°C. At days 1, 3, 5, 7, 14, 21, 28 and 40, PBS supernatants were removed and saved, and wells were refreshed with new PBS. The amount of Jagged1 released from A6 over time was quantified within the supernatants. 96-well ELISA plates were

coated with goat anti-rat Jagged1 capture antibody overnight. Wells were blocked in 1% BSA. Supernatants were then added to wells for 2 h followed by (as described above) Jagged1 detection antibody, streptavidin-HRP, substrate solution, stop solution, and optical readout. All reagents used were from R&D Systems (Minneapolis, MN, USA).

6.2.9 In vivo Analysis

Directly immobilized Jagged1/A6 scaffolds were evaluated in two injury models with different scaffold fabrication techniques. First, Jagged1/A6 scaffolds were implanted in 3 mm diameter murine calvarial defects. Porous A6 scaffolds were fabricated as previously described [29]. Briefly, poly(methyl methacrylate) (PMMA) beads with an average diameter of 200 μm were sintered together in a 3 mm diameter by 1 mm thick teflon mold overnight at 120°C. A6 was added to the mold, allowed to settle within the void space, and photopolymerized. PMMA beads were then leached out in serial washes of acetone. Resulting 3D porous A6 scaffolds were washed in PBS and sterilized via UV exposure. 10 μg/mL of Jagged1 was directly adsorbed to A6 for 2 h. Bilateral 3 mm diameter murine calvarial defects were created with a dermal punch as previously described [16] (also see Chapters 3 and 4). Scaffolds were press fit into the defects and mid-line skin incisions above the calvarium were sutured closed.

Jagged1/A6 fracture wrap biomaterials were also implanted in intramedullary stabilized, closed transverse murine tibial fractures created by three point bending, as previously described [16] (also see Chapters 3 and 4). 1 mm thick solid A6 biomaterials were crosslinked and cut into 0.5 cm x 1.2 cm rectangular wraps. At 3 days post fracture, incisions were made to expose the fractured tibia, which by then had formed a provisional mesenchymal callus. The surrounding muscle was peeled back and the Jagged1/A6 fracture wrap (Direct[10] and Direct[0], 2 h incubation) was slid underneath the tibia between the fibula. The biomaterial was cut as needed and wrapped around the fracture callus. Normal muscle position was re-established and the skin sutured closed.

6.2.10 Statistical Analysis

Two-way ANOVAs were used to test the effects of Jagged1 dose (0, 2.5, 10) and immobilization strategy (direct vs. indirect) at each time point for SGM experiments, followed by a Tukey's post-hoc test with planned comparisons reported (comparison of Jagged1 doses to each other within direct and indirect strategies, and comparison of direct to indirect strategies for each Jagged1 dose). To evaluate the effect of A6 alone, an additional student's t-test was used to compare A6 to TCPS controls (Direct[0/A6] vs [0/TCPS]) for SGM gene expression data. A student's t-test was also used to evaluate the effects of Jagged1 and A6 for OGM experiments. Data is presented as mean ± standard deviation.

6.3 Results

6.3.1 Direct Jagged1/A6 Is More Effective at Activating Canonical Notch Signaling

To evaluate the ability of each Jagged1/A6 immobilization strategy to activate the Notch signaling pathway, hMSCs were cultured in SGM and harvested at days 1, 3, 5 and 7 for gene expression analysis of Notch target gene Hey1. Overall, Jagged1/A6 upregulated Hey1 gene expression in a dose-dependent manner (Figure 6.1a). Hey1 activation was transient, with expression gradually decreasing over time. Specifically, Direct[10/A6] increased expression relative to Direct[0/A6] at all time points and relative to Direct[2.5/A6] at days 1, 3 and 7. Indirect Jagged1/A6 did not increase Hey1 gene expression for any concentration at any time point. Furthermore, comparing across immobilization strategies, Direct[10/A6] increased expression relative to Indirect[10/A6] at days 3 and 7, demonstrating that the direct immobilization strategy was more effective at activating the Notch signaling pathway.

Direct[0/A6] also increased Hey1 gene expression relative to [0/TCPS] at day 1 (Figure 6.1b), demonstrating that A6 on its own transiently activated the Notch signaling pathway.

6.3.2 More Jagged1 is Successfully Immobilized to A6 via the Direct Method

To determine the mechanism responsible for increased Notch activation via the direct method, the relative surface density of successfully immobilized Jagged1 to A6 was quantified for both strategies. More Jagged1 was immobilized to A6 via the direct method at 10 μg/mL than the indirect method (Figure 6.2a). The direct strategy also increased the amount of Jagged immobilized in a dose-dependent manner, with Direct[10/A6] greater than Direct[2.5/A6]. There was no difference between Indirect[10/A6] and Indirect[2.5/A6].

The release kinetics profile showed that less than 0.2% of successfully immobilized Jagged1 was released into the incubation media over 40 days for both direct and indirect methods. (Figure 6.2b)

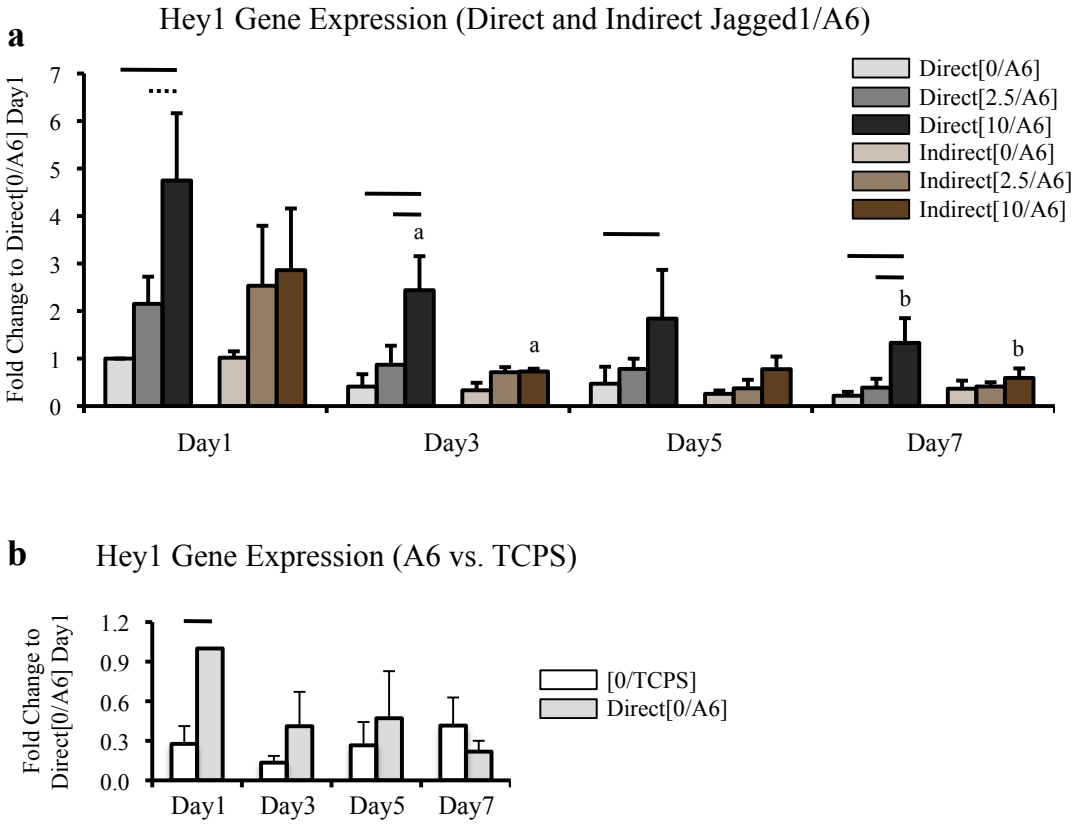

Figure 6.1. Notch target Hey1 gene expression of hMSCs cultured on direct and indirect Jagged1/A6 in SGM (n=3). Jagged1/A6 transiently upregulates Hey1 gene expression, with direct more effective than indirect (a). A6 polymer alone transiently upregulates Hey1 gene expression relative to TCPS (b). Solid lines indicate significance ($p<0.050$) and dashes lines indicate a trend ($p<0.100$) between Jagged1 doses for direct or indirect strategies. A common letter (a,b) above any two bars indicates significance ($p<0.050$) between direct and indirect strategies at that given Jagged1 dose.

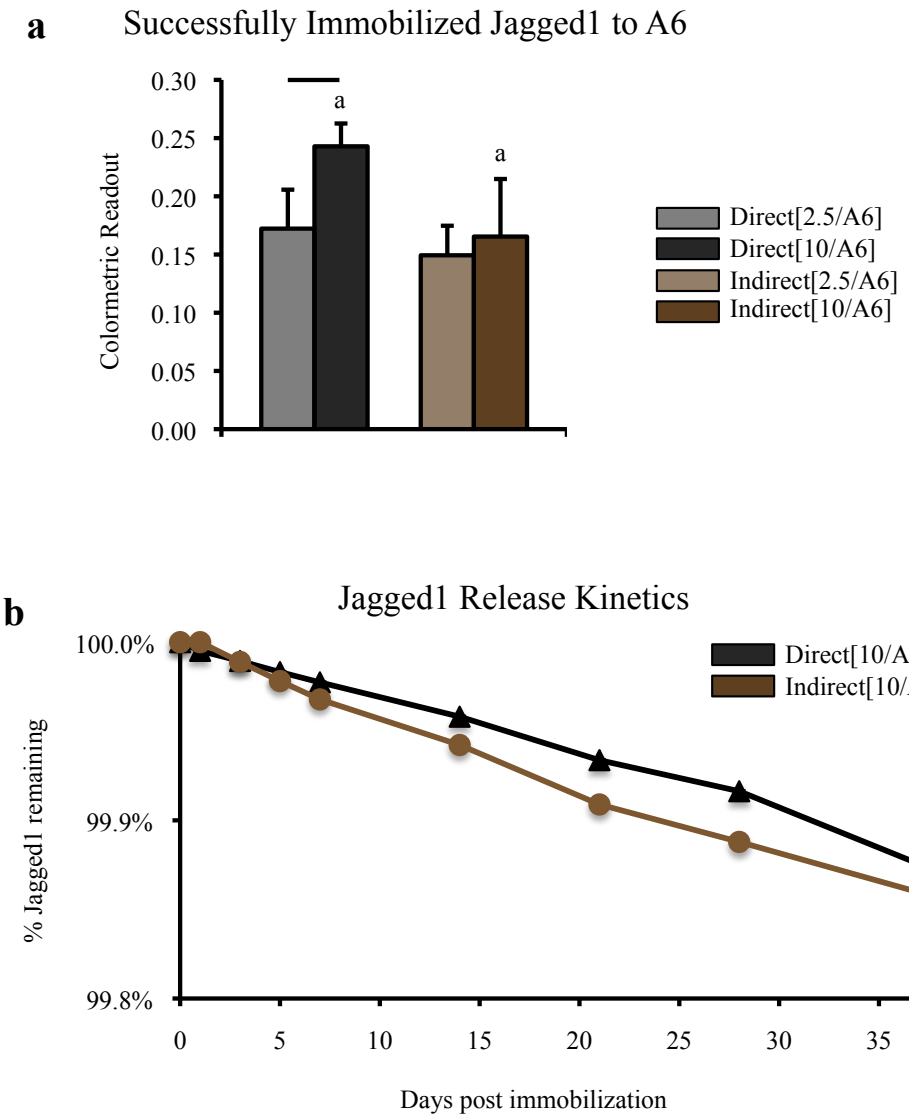

Figure 6.2. Relative surface density of successfully immobilized Jagged1 to A6 via Direct and Indirect strategies, and the release kinetics profile. More Jagged1 is successfully immobilized to A6 via the direct strategy at 10 μg/mL as measured by the colormetric readout (absorbance) (a). The direct strategy also increases the amount of Jagged1 immobilized in a dose-dependent response. Less than 0.2% of successfully immobilized Jagged1 is released over 40 days for both direct and indirect strategies (b). Solid lines indicate significance ($p<0.050$) between Jagged1 doses for direct or indirect strategies. A common letter (a,b) above any two bars indicates significance ($p<0.050$) between direct and indirect strategies at that given Jagged1 dose.

6.3.3 Direct and Indirect Jagged1/A6 Immobilization Does Not Increase Cell Number

The Notch signaling pathway has been shown to increase mesenchymal progenitor cell proliferation. An Alamar Blue assay was used to assess the effects of direct and indirect Jagged1/A6 immobilization strategies on hMSC cell number, indicative of proliferation, at days 1, 3, 5, and 7 during SGM culture. Although hMSC number gradually increased over time for all groups, there was no significant effect of Jagged1 dose or immobilization strategy on cell number at any time point analyzed (Figure 6.3).

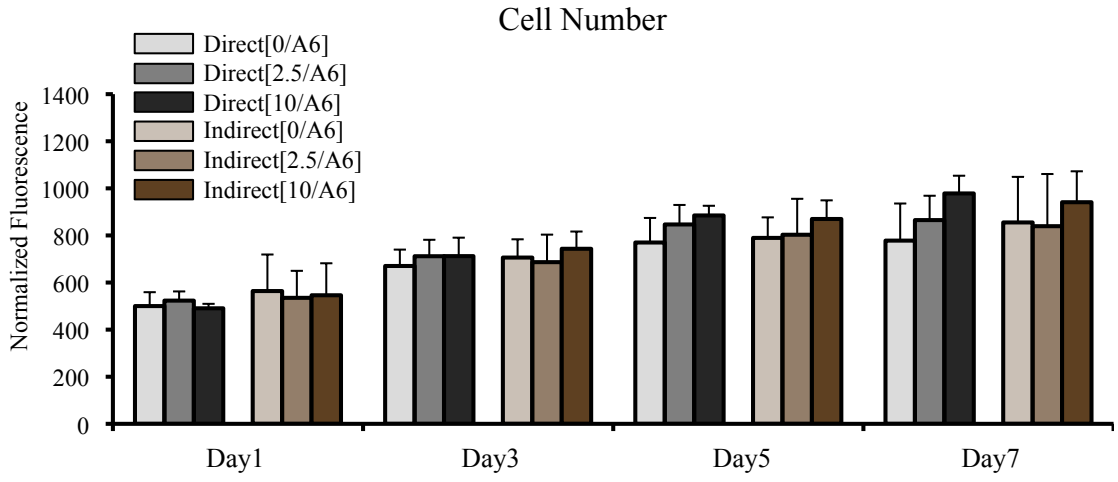

Figure 6.3. Cell number of hMSCs cultured on direct and indirect Jagged1/A6 in SGM (n=5). Direct and indirect Jagged1 immobilization strategies do not increase cell number.

6.3.4 Direct Jagged1/A6 is More Effective at Promoting an Osteogenic Phenotype

To evaluate the ability of direct and indirect Jagged1/A6 immobilization strategies to promote an osteogenic phenotype, bone sialoprotein (BSP) and alkaline phosphatase (AP) gene expression were quantified at days 1, 3, 5 and 7 during SGM culture. Overall, Jagged1/A6 increased BSP gene expression in a dose-dependent response (Figure 6.4a). Similar to Hey1, BSP activation was transient. Specifically, Direct[10/A6] increased BSP expression relative to

Direct[0/A6] at days 1 and 3. Also similar to Hey1, indirect Jagged1/A6 did not increase BSP gene expression for any concentration at any time point.

Overall, Jagged1/A6 also increased AP gene expression, with Direct[10/A6] increased relative to Direct[0/A6] at days 3 and 5, and relative to Direct[2.5/A6] at day 5 (Figure 6.4b). Direct[2.5/A6] was also increased relative to Direct[0/A6] at day 5. Indirect[10/A6] increased AP gene expression relative to Indirect[0/A6] at day 5. However, comparing across immobilization strategies, Direct[10/A6] was increased relative to Indirect[10/A6] at day 5. Collectively, the data demonstrates that the direct immobilization strategy was more effective at inducing osteogenic gene expression.

Direct[0/A6] also increased BSP gene expression relative to [0/TCPS] at day 1 (Figure 6.4c), demonstrating that A6 promotes transient osteogenic gene expression. However, the A6 polymer did not have an effect on AP gene expression (Figure 6.4d).

There was also a significant positive linear correlation between Hey1 and BSP gene expression independent of Jagged1 dose, immobilization strategy, or time post plating (Figure 6.5), demonstrating that expression of Jagged1-induced Notch target genes and mature osteoblast markers are related and have similar expression patterns.

hMSCs were also stained for AP enzymatic activity at day 7 during SGM culture (Figure 6.6a). Overall, Jagged1/A6 increased AP activity in a dose-dependent manner (Figure 6.6b). Direct[10/A6] and Direct[2.5/A6] were increased relative to Direct[0/A6]. Indirect[10/A6] was also increased relative to Indirect[0/A6]. However, comparing across immobilization strategies, Direct[10/A6] increased AP enzymatic activity relative to Indirect[10/A6], demonstrating that the direct immobilization strategy was more effective at inducing osteogenic enzymatic activity. Similar results were also found for AP staining normalized to cell number, demonstrating increased osteogenic activity for direct Jagged1/A6 on a per cell basis (Figure 6.6c).

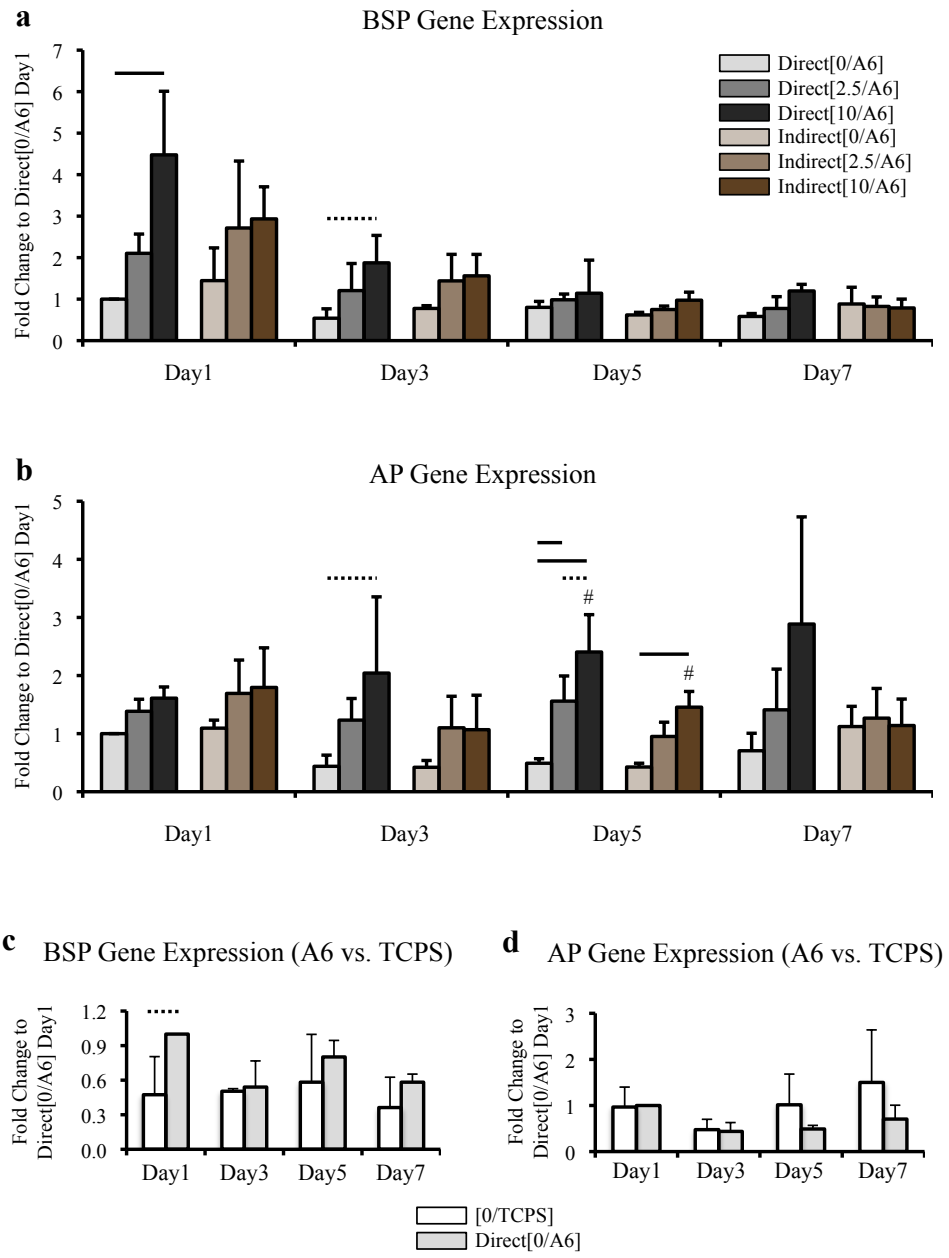

Figure 6.4. Osteogenic gene expression of hMSCs cultured on direct and indirect Jagged1/A6 in SGM (n=3). Jaged1/A6 transiently increases bone sialoprotein (BSP) gene expression, with direct more effective than indirect (a). Jagged1/A6 also increases alkaline phosphatase (AP) gene expression, with direct more effective than indirect (b). A6 polymer alone increases BSP (c) but not AP gene expression (d) relative to TCPS alone. Solid lines indicate significance ($p<0.050$) and dashes lines indicate a trend ($p<0.100$) between Jagged1 doses for direct or indirect strategies. A common letter (a,b) above any two bars indicates significance ($p<0.050$) and a common symbol (#) indicates a trend ($p<0.100$) between direct and indirect strategies at that given Jagged1 dose.

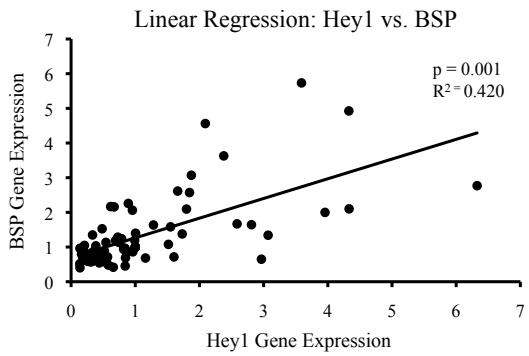

Figure 6.5 (left). There is a significant positive linear correlation between Hey1 and bone sialoprotein (BSP) gene expression. Samples include both direct and indirect immobilization strategies at all Jagged1 doses (0, 2.5, 10) at all time points (days 1, 3, 5, 7) (n=72).

Figure 6.6 (below). Alkaline Phosphatase (AP) enzymatic activity of hMSCs cultured on direct and indirect Jagged1/A6 in SGM at day 7 (n=5). Representative plate scan demonstrating the average amount of AP staining (a). Jagged1/A6 increases AP activity, specifically % area of staining (b) and % area of staining normalized by cell number (c), with direct more effective than indirect. Solid lines indicate significance ($p<0.050$) and dashes lines indicate a trend ($p<0.100$) between Jagged1 doses for direct or indirect strategies. A common letter (a,b) above any two bars indicates significance ($p<0.050$) between direct and indirect strategies at that given Jagged1 dose.

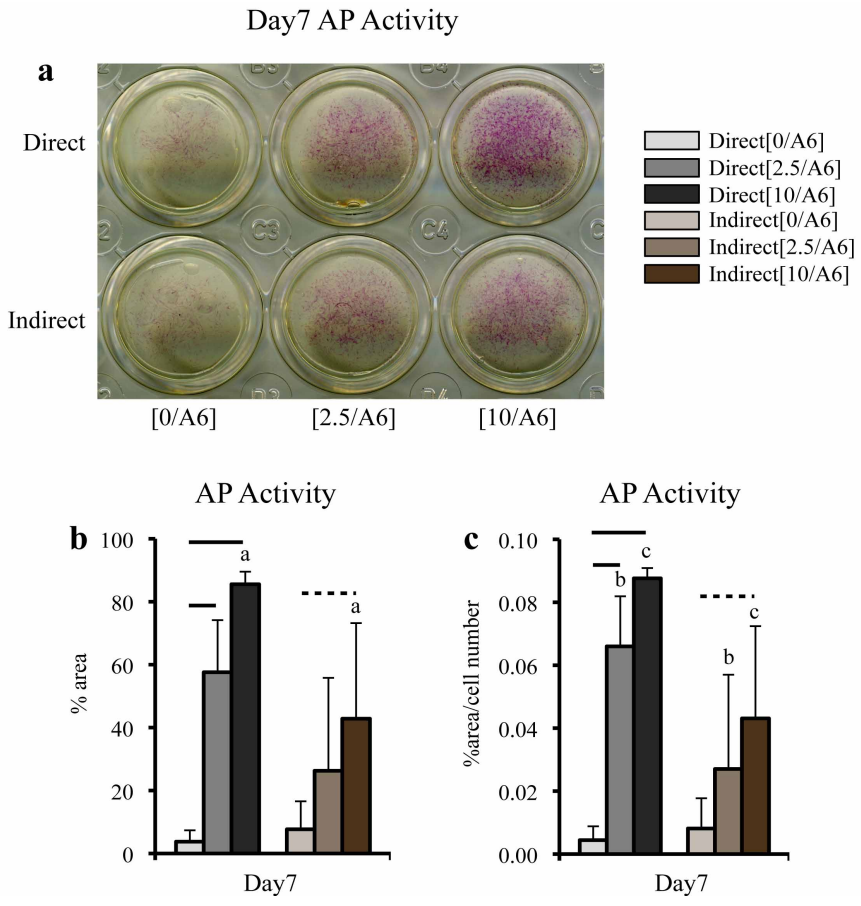

6.3.5 Direct Jagged1/A6 Induces Osteoblast Differentiation and Calcified Mineral Deposition

For SGM experiments, direct Jagged1/A6 was more effective at activating the Notch signaling pathway and inducing an osteogenic phenotype. In general, Jagged1-induced activity was transient and dose-dependent, with maximum expression found in Direct[10/A6]. Furthermore, the direct strategy increased the amount Jagged1 successfully immobilized to A6. Therefore, we next set out to evaluate the ability of Direct[10/A6] and Direct[0/A6] to induce osteogenesis when cultured in OGM.

hMSC number gradually increased over time in OGM culture (Figure 6.7), with Direct[10/A6] increased relative to Direct[0/A6] at day 7. Direct[10/A6] also increased AP enzymatic activity at day 7 (Figure 6.8a,b), though there were no differences when normalized by cell number (Figure 6.8c). Finally, Alizarin Red S staining of calcified mineral tissue deposition by cells was conducted at days 10 and 13 to evaluate the ability of direct Jagged1/A6 and A6 alone to induce terminal osteoblast differentiation. Direct[10/A6] increased calcified mineral deposition relative to Direct[0/A6] at all time points (Figure 6.9a). Direct[0/A6] and Direct[10/A6] also increased calcified mineral deposition relative to [0/TCPS] at all time points. Collectively, the data demonstrates that direct Jagged1/A6 moderately promotes cell proliferation and strongly induces osteoblast differentiation and calcified mineral deposition, with the A6 polymer further demonstrating its osteoconductive properties.

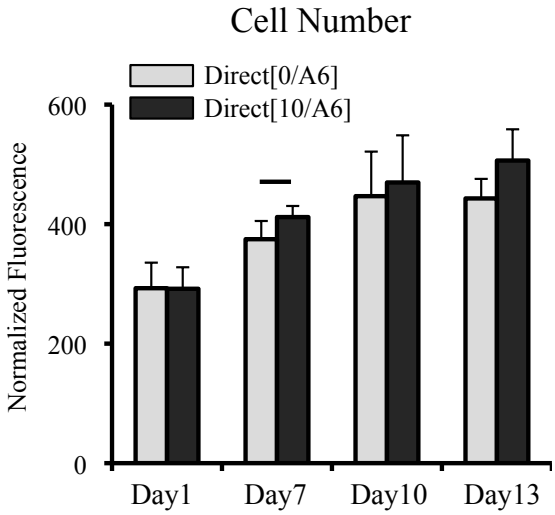

Figure 6.7. Cell number of hMSCs cultured on direct Jagged1/A6 in OGM (n=3-9). Direct[10/A6] increases cell number at Day 7. Solid line indicates significance ($p<0.050$).

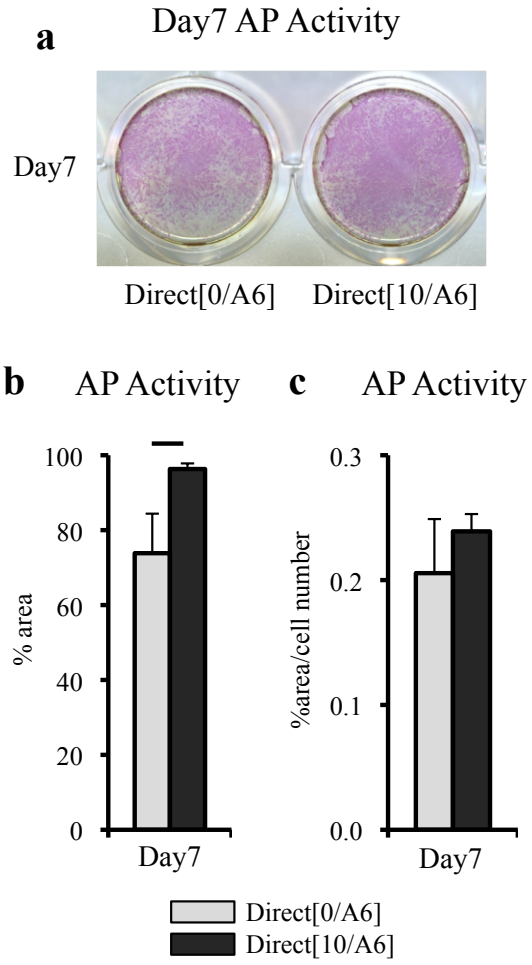

Figure 6.8. Alkaline Phosphatase (AP) enzymatic activity of hMSCs cultured on direct Jagged1/A6 in OGM (n=3). Representative plate scan demonstrating the average amount of AP staining (a). Direct[10/A6] increases % area of AP staining (b), but has no effect when % area is normalized by cell number (c). Solid line indicates significance ($p<0.050$).

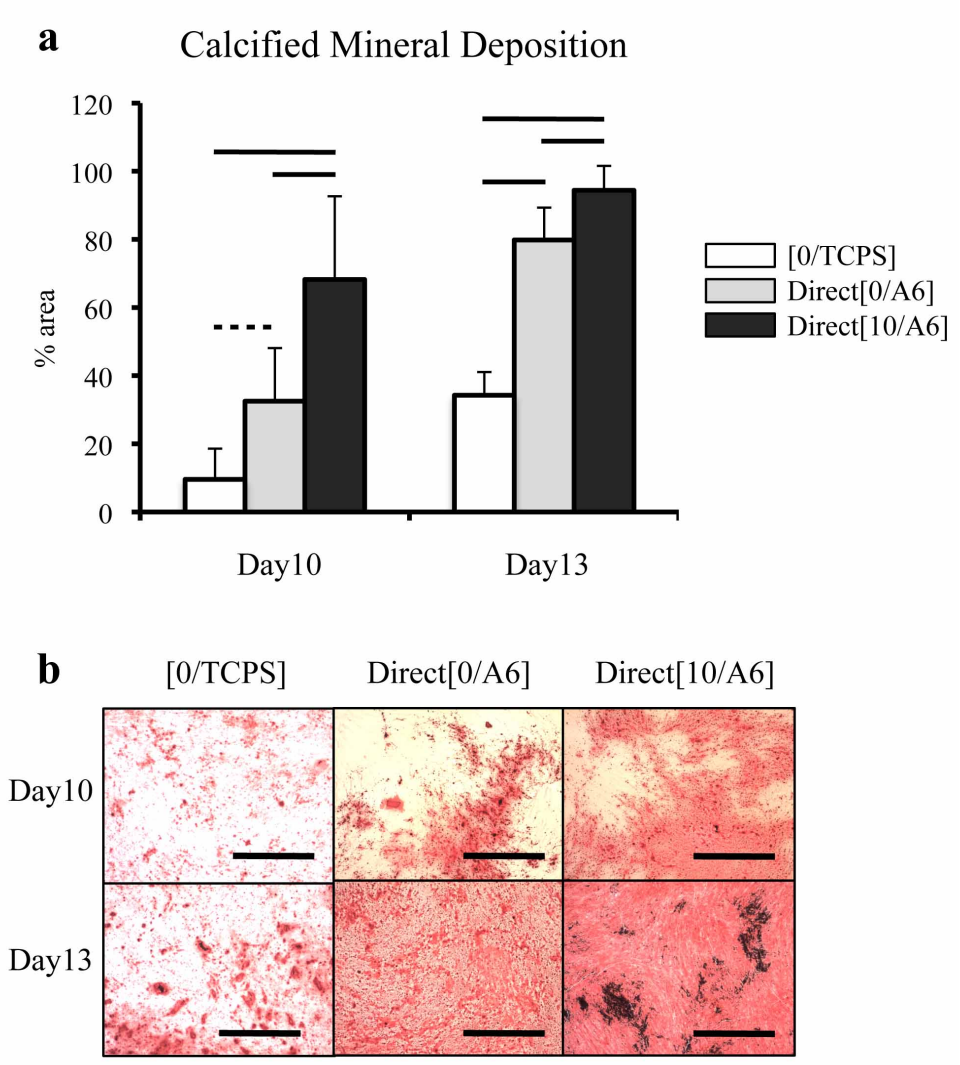

Figure 6.9. Calcified mineral deposition of hMSCs cultured on direct Jagged1/A6 in OGM with [0/TCPS]. Direct[10/A6] increases % area of calcified mineral deposition relative to Direct[0/A6] and [0/TCPS] at days 10 and 13 (a). Direct[0/A6] is also increases relative to [0/TCPS]. Solid lines indicate significance ($p<0.050$) and dashes lines indicate a trend ($p<0.100$). Representative images demonstrating the average amount of mineral produced by cells (b). Mineral stains red. Areas of dense mineral appear black. A6 polymer stains yellow. Scale bars are 1 mm.

6.3.6 In vivo Evaluation of Jagged1/A6

Direct[0/A6] and Direct[10/A6] biomaterial constructs using 1 mm thick porous A6 scaffolds (Figure 6.10a) were implanted in bilateral 3 mm diameter murine calvarial defects. For preliminary experiments, animals were harvested between 5-14 days post injury. 18 total animals were included. However, 12/18 (67%) animals presented with at least one scaffold out of place, demonstrating a suboptimal surgical success rate (33%). Scaffolds were most commonly found to be adhered to the subcutaneous skin surrounding the calvarium (Figure 6.10b) or to have moved medial towards the mid-line suture of the calvarium (Figure 6.10c). Only a single Direct[10/A6] scaffold located within the defect at harvest was successfully processed for histology, sectioned and stained with H&E. This specimen, harvested at 14 days post injury, presented with cellular infiltration and fibrous tissue formation (Figure 6.10d,e).

Direct[10/A6] and Direct[0/A6] fracture wraps using solid A6 biomaterials (0.5 cm x 1.2 cm x 1 mm) were implanted around murine tibial fracture calluses at 3 days post fracture (Figure 6.11a) and harvested at 13 days post fracture. Due to lack of suture pullout strength of A6, fracture wraps were not sutured together. Damage to the surrounding muscle tissue caused by the fracture also prevented muscle from being sutured around the fracture wrap to hold it in place. At the time of harvest, all 15 specimens presented with fracture wraps that had opened up and not adhered to the callus (Figure 6.11b). Specimens were processed for histology and stained with Safranin-O/Fast Green. Images show that solid A6 biomaterials with and without Jagged1 induced a strong a foreign body response in the tibial fracture model with no tissue infiltration (Figure 6.11c). All A6 fracture wraps were entirely encapsulated by macrophages, foreign body giant cells and other inflammatory components involved in the foreign body response (Figure 6.11d,e).

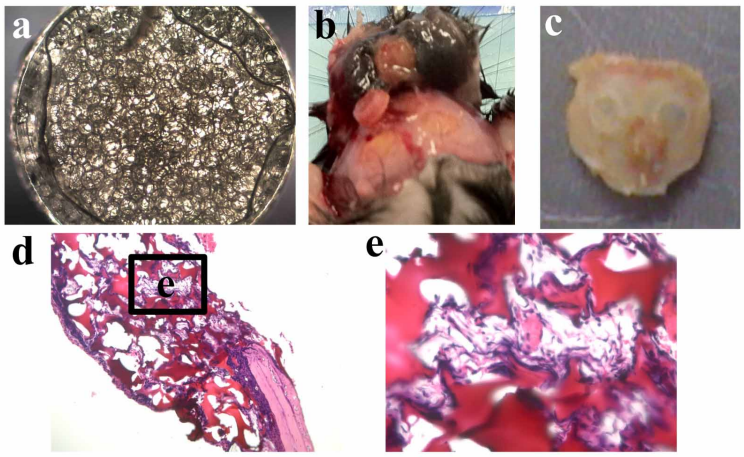

Figure 6.10 (above). Evaluation of Jagged1/A6 porous scaffolds in murine calvarial defects. 1 mm thick porous A6 scaffolds were created (a) and implanted into murine calvarial defects. 67% of implants resulted were unsuccessful, with scaffolds most commonly found adhered to the surround skin (b) or moved towards the mid-line of the calvarium (c). 100x (d) and 400x (e) H&E images of Direct[10/A6] at 14 days post fracture show cell infiltration and fibrous tissue formation.

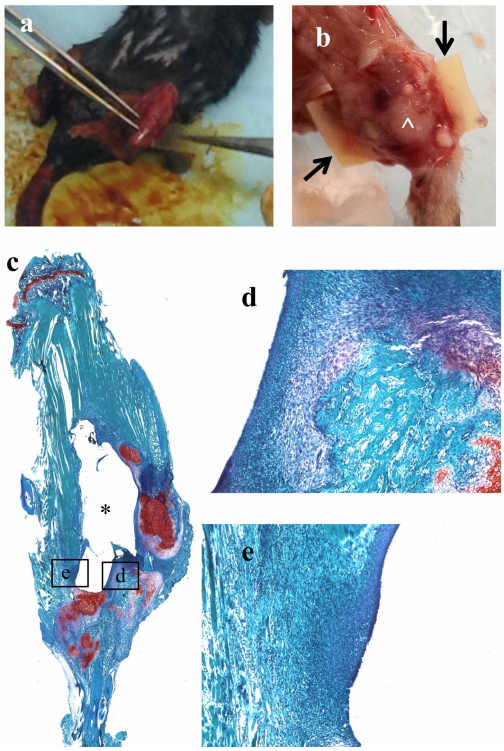

Figure 6.11 (left). Evaluation of Jagged1/A6 fracture wraps in murine tibial fractures. Solid fracture wraps were implanted around tibial fracture calluses at 3 days post fracture (a). At 13 days post fracture, all 15 limbs presented with scaffolds (arrows) that had opened up and were not in direct contact with the callus (^) (b). Safranin-O/Fast green histology images at 20x (c) and 400x (d,e) show that A6 solid scaffolds were completely surrounded by a foreign body response. There was no tissue infiltration of solid wraps causing them to fall out during histological processing. They were located in the empty space between the tibial fracture callus and fibula (*).

6.4 Discussion

Previous studies have demonstrated that the Notch signaling pathway regulates bone tissue formation. Specifically, Jagged1 is the most highly expressed Notch ligand in mesenchymal cells [11, 15] and is the most highly upregulated ligand during fracture healing (Chapter 3) [16]. In Chapter 5, we also demonstrated that endogenous Jagged1 expression during early and late osteoblast differentiation promotes bone tissue formation during embryological bone development and aging. Furthermore, Alagille Syndrome patients with Jagged1 loss-of-function have decreased bone mass and an increased risk of fracture [19, 20]. These results identify Jagged1 as a potential therapeutic target to improve bone tissue formation. Therefore, we developed a translational biomaterial-based cell culture model to evaluate the ability of Jagged1 to activate the Notch signaling pathway and induce osteoblast differentiation.

Our results demonstrate that Jagged1 immobilization to a PBAE scaffold comprised of diethylene glycol diacrylate and isobutylamine (A6) activated the Notch signaling pathway and promoted an osteogenic phenotype in hMSCs. Moreover, direct immobilization was more potent than indirect, suggesting it as a more viable immobilization strategy for clinical use. Results also further demonstrate the osteoconductive properties of A6 that have previously been established [29].

Increased Notch activation via the direct method was most likely due to an increased amount of Jagged1 successfully bound to A6, specifically at the incubation concentration of 10 μg/mL. A previous study showed that at lower Jagged1 incubation concentrations (0.14-1.42 μg/mL), the indirect strategy improved Notch activation, resulting in the hypothesis that optimized Jagged1/Fc protein orientation from indirect anti-Fc antibody binding, leaving the Jagged1 extracellular binding domain exposed, was more effective at activating the Notch pathway than increasing the total amount of protein immobilized [26]. However, for the indirect strategy, Notch activation plateaued for Jagged1 incubation concentrations of 1.42 μg/mL and greater. Our data similarly showed no increase in Notch activation for indirect incubation concentrations between 2.5-10 μg/mL, which corresponded with no change in the amount of Jagged1 successfully

immobilized to A6. The maximum amount of Jagged1 able to bind indirectly is limited by the amount of anti-Fc antibodies that are appropriately oriented. Increasing the anti-Fc incubation concentration could increase the number of available Jagged1/Fc binding locations. However, it could also eventually cause antibody clustering that effectively decreases the number of available locations; and in fact, these two studies found similar plateaus using different anti-Fc antibody incubation concentrations (10 μg/mL [26] and 15 μg/mL), suggesting that the maximum amount of available Jagged1/Fc binding locations may have been achieved or possibly surpassed (clustering). Our study shows that the direct immobilization strategy maximizes the amount of Jagged1 successfully bound to A6, which in turn is primarily responsible for increased Notch activation at higher Jagged1 incubation concentrations. *In vivo* therapeutic applications may require even higher protein concentrations than were evaluated *in vitro*, further indicating direct Jagged1 immobilization as a more viable strategy for clinical use.

We also found that directly immobilized Jagged1/A6 constructs promoted an osteogenic phenotype when cultured in SGM, and induced osteoblast differentiation and calcified mineral deposition when cultured in OGM. This is the first study to demonstrate the osteoinductive potential of Jagged1 using a clinically translatable biomaterial construct. We also identified a positive correlation between Notch target and osteogenic gene expression. Previous studies have also shown that Jagged1 enhances vasculogenesis by promoting endothelial cell proliferation, differentiation and migration [30, 31]. Successful fracture healing is dependent on both callus vascularization and osteoblast activity. These results indicate that the Jagged1/A6 biomaterial construct developed in this experiment may enhance bone tissue regeneration *in vivo*.

Previous studies of embryological bone formation have shown that constitutive or sustained activation of Notch signaling prevents osteoblast differentiation [7, 8]. However, here we demonstrate that Jagged1/A6 transiently activated the Notch signaling pathway, with expression gradually decreasing over time, which in fact enhanced osteoblast differentiation. Transient transfection of immortalized osteogenic cell lines with NICD1, Jagged1, or Dll1 have previously also been shown to promote differentiation [32, 33]. Similar results have been found regarding the temporal regulation of Notch on chondrogenesis as well, where sustained Notch

signaling inhibits differentiation, but a transient Jagged1 signal stimulates it [15]. Collectively, the data suggests that transient Notch activation promotes osteoblast differentiation, whereas constitutive activation may inhibit differentiation. Development of a Jagged1/A6 biomaterial construct with sustained Notch signaling, for example by embedding the Jagged1 protein into the A6 material as well as adsorbing it to the surface such that as the material degrades more Jagged1 is exposed for cells to interact with, would allow for investigation into the temporal regulation of Jagged1-induced Notch activity on osteogenesis in a clinically translatable model.

Alternatively, in Chapter 5, we demonstrated that Jagged1 activity promotes osteoblast differentiation regardless of its temporal expression. These results are in contrast to previous experiments showing that expression of other Notch components in fact inhibits differentiation [7, 8]. However, in the context of the Notch signaling pathway, Jagged1 has also been shown to differentially regulate behavior of other cell lineages. Jagged1 promotes vasculogenesis, whereas Dll4 is inhibitory and Dll1 has no effect [30, 31]. Jagged1 also inhibits osteoclast differentiation whereas Dll4 enhances differentiation [34]. We've previously localized Jagged1 expression to osteogenic cells at varying stages of maturity [16]. However, it is unknown whether the magnitude of expression is consistently high (sustained) or variable (transient). Development of a conditional Jagged1 gain of function mouse model would allow for the investigation of sustained versus endogenous Jagged1 activity on osteoblast differentiation and bone tissue formation.

Sustained and transient Notch activity also appears to differentially regulate cell proliferation. Sustained Notch activity in osteogenic cells strongly promotes proliferation [8], whereas here we show that Jagged1-induced transient Notch activity had only limited effects on proliferation. However, it is unclear if this is due primarily to the effects of Jagged1 or the A6 biomaterial.

In summary, we have developed a biomaterial construct comprised of the osteoinductive Notch ligand Jagged1 and the osteoconductive poly(β-amino ester) polymer A6 that transiently activates the Notch signaling pathway and promotes osteoblast differentiation.

Next, Jagged1/A6 biomaterial constructs were evaluated in two *in vivo* animal models. First, porous scaffolds were implanted into murine calvarial defects. Development and use of this

model is beneficial because it would allow for future investigations into whether Jagged1/A6 can recover function in mice with Notch receptor or Jagged1 loss-of-function, which is applicable to Alagille Syndrome patients. However, porous A6 scaffolds, which had to be at least 1 mm thick for structural stability, did not fit within murine calvaria, which are less than 200 μm thick. The 5x difference in thickness was likely responsible.

Then we created solid biomaterial constructs and implanted them 3 days post fracture during murine tibial fracture healing. Many fractures do not present as segmental defects but still require therapeutic intervention. This biomaterial construct could be used to treat such injuries, as it would be wrapped around the provisional callus, with the hypothesis that Jagged1 would interact with cells on the periosteal surface of the expanding fracture callus. Jagged1/A6 release kinetics show that Jagged1 stays immobilized to the A6 surface, possibly due to the large size of the protein (140kDa). Therefore, the fracture wrap must stay in direct contact with the callus, creating a cell-biomaterial interface in order for Jagged1 to have an effect. However, our inability to suture the biomaterial to the callus resulted in the fracture wrap opening up. Furthermore, alternative to porous A6 scaffolds, which promoted cell and tissue infiltration, solid A6 biomaterials induced a strong foreign body response that completely encapsulated the biomaterial, and prevented Jagged1 from interacting with the mesenchymal callus. Future studies using this implant model should include materials with stronger suture pullout strength and that are less reactive with cells as solid polymers. Furthermore, A6 was originally utilized in these experiments because of its osteoconductive properties. However, in this implant model, it did not serve as a scaffold for cell infiltration and bone tissue formation. A successful therapeutic will likely need to interact with cells inside the callus as well as on the surface. A smaller or lower-affinity binding molecule that will gradually release from the polymer should be used with this implant model.

Future studies investigating Jagged1/A6 should use segmental defect models where A6 could serve as a scaffold for cell infiltration and Jagged1 could promote osteogenesis. A6 has previously been successfully used in rat calvarial defect models (~1 mm thick calvarium) [29]. The scaffold can also be used in long bone segmental defects in rats and larger animal models.

6.5 References

1. Braithwaite, R.S., N.F. Col, and J.B. Wong, *Estimating hip fracture morbidity, mortality and costs.* J Am Geriatr Soc, 2003. **51**(3): p. 364-70.
2. Audige, L., et al., *Path analysis of factors for delayed healing and nonunion in 416 operatively treated tibial shaft fractures.* Clin Orthop Relat Res, 2005. **438**: p. 221-32.
3. Dimitriou, R., et al., *Bone regeneration: current concepts and future directions.* BMC Med, 2011. **9**: p. 66.
4. Friedlaender, G.E., et al., *Osteogenic protein-1 (bone morphogenetic protein-7) in the treatment of tibial nonunions.* J Bone Joint Surg Am, 2001. **83-A Suppl 1**(Pt 2): p. S151-8.
5. Govender, S., et al., *Recombinant human bone morphogenetic protein-2 for treatment of open tibial fractures: a prospective, controlled, randomized study of four hundred and fifty patients.* J Bone Joint Surg Am, 2002. **84-A**(12): p. 2123-34.
6. Carragee, E.J., et al., *Future directions for The spine journal: managing and reporting conflict of interest issues.* Spine J, 2011. **11**(8): p. 695-7.
7. Hilton, M.J., et al., *Notch signaling maintains bone marrow mesenchymal progenitors by suppressing osteoblast differentiation.* Nat Med, 2008. **14**(3): p. 306-14.
8. Engin, F., et al., *Dimorphic effects of Notch signaling in bone homeostasis.* Nat Med, 2008. **14**(3): p. 299-305.
9. Zanotti, S., et al., *Notch inhibits osteoblast differentiation and causes osteopenia.* Endocrinology, 2008. **149**(8): p. 3890-9.
10. Mead, T.J. and K.E. Yutzey, *Notch pathway regulation of chondrocyte differentiation and proliferation during appendicular and axial skeleton development.* Proc Natl Acad Sci U S A, 2009. **106**(34): p. 14420-5.

11. Dong, Y., et al., *RBPjkappa-dependent Notch signaling regulates mesenchymal progenitor cell proliferation and differentiation during skeletal development.* Development, 2010. **137**(9): p. 1461-71.

12. Tao, J., et al., *Osteosclerosis owing to Notch gain of function is solely Rbpj-dependent.* J Bone Miner Res, 2010. **25**(10): p. 2175-83.

13. Kohn, A., et al., *Cartilage-specific RBPjkappa-dependent and -independent Notch signals regulate cartilage and bone development.* Development, 2012. **139**(6): p. 1198-212.

14. Salie, R., et al., *Ubiquitous overexpression of Hey1 transcription factor leads to osteopenia and chondrocyte hypertrophy in bone.* Bone, 2010. **46**(3): p. 680-94.

15. Oldershaw, R.A., et al., *Notch signaling through Jagged-1 is necessary to initiate chondrogenesis in human bone marrow stromal cells but must be switched off to complete chondrogenesis.* Stem Cells, 2008. **26**(3): p. 666-74.

16. Dishowitz, M.I., et al., *Notch signaling components are upregulated during both endochondral and intramembranous bone regeneration.* J Orthop Res, 2012. **30**(2): p. 296-303.

17. Li, L., et al., *Alagille syndrome is caused by mutations in human Jagged1, which encodes a ligand for Notch1.* Nat Genet, 1997. **16**(3): p. 243-51.

18. Oda, T., et al., *Mutations in the human Jagged1 gene are responsible for Alagille syndrome.* Nat Genet, 1997. **16**(3): p. 235-42.

19. Olsen, I.E., et al., *Deficits in size-adjusted bone mass in children with Alagille syndrome.* J Pediatr Gastroenterol Nutr, 2005. **40**(1): p. 76-82.

20. Bales, C.B., et al., *Pathologic lower extremity fractures in children with Alagille syndrome.* J Pediatr Gastroenterol Nutr, 2010. **51**(1): p. 66-70.

21. Vas, V., et al., *Soluble Jagged-1 is able to inhibit the function of its multivalent form to induce hematopoietic stem cell self-renewal in a surrogate in vitro assay.* J Leukoc Biol, 2004. **75**(4): p. 714-20.

22. Beckstead, B.L., D.M. Santosa, and C.M. Giachelli, *Mimicking cell-cell interactions at the biomaterial-cell interface for control of stem cell differentiation.* J Biomed Mater Res A, 2006. **79**(1): p. 94-103.

23. Goncalves, R.M., et al., *Induction of notch signaling by immobilization of jagged-1 on self-assembled monolayers.* Biomaterials, 2009. **30**(36): p. 6879-87.

24. Kramer, H., *RIPping notch apart: a new role for endocytosis in signal transduction?* Sci STKE, 2000. **2000**(29): p. pe1.

25. Varnum-Finney, B., et al., *Immobilization of Notch ligand, Delta-1, is required for induction of notch signaling.* J Cell Sci, 2000. **113 Pt 23**: p. 4313-8.

26. Beckstead, B.L., et al., *Methods to promote Notch signaling at the biomaterial interface and evaluation in a rafted organ culture model.* J Biomed Mater Res A, 2009. **91**(2): p. 436-46.

27. Anderson, T., Hossain, Navarro, Brey, Van Vliet, Langer, Burdick, *A Combinatorial Library of Photocrosslinkable and Degradable Materials.* Advanced Materials, 2006.

28. Brey, D.M., I. Erickson, and J.A. Burdick, *Influence of macromer molecular weight and chemistry on poly(beta-amino ester) network properties and initial cell interactions.* J Biomed Mater Res A, 2008. **85**(3): p. 731-41.

29. Brey, D.M., et al., *Identification of osteoconductive and biodegradable polymers from a combinatorial polymer library.* J Biomed Mater Res A, 2010. **93**(2): p. 807-16.

30. Kwon, S.M., et al., *Specific Jagged-1 signal from bone marrow microenvironment is required for endothelial progenitor cell development for neovascularization.* Circulation, 2008. **118**(2): p. 157-65.

31. Benedito, R., et al., *The notch ligands Dll4 and Jagged1 have opposing effects on angiogenesis.* Cell, 2009. **137**(6): p. 1124-35.

32. Nobta, M., et al., *Critical regulation of bone morphogenetic protein-induced osteoblastic differentiation by Delta1/Jagged1-activated Notch1 signaling.* J Biol Chem, 2005. **280**(16): p. 15842-8.

33. Tezuka, K., et al., *Stimulation of osteoblastic cell differentiation by Notch.* J Bone Miner Res, 2002. **17**(2): p. 231-9.

34. Sekine, C., et al., *Differential regulation of osteoclastogenesis by Notch2/Delta-like 1 and Notch1/Jagged1 axes.* Arthritis Res Ther, 2012. **14**(2): p. R45.

CHAPTER 7

Summary, Limitations and Future Directions, Conclusions

7.1 Summary

Many fractures exhibit delayed healing or develop into non-unions [1, 2]. Current therapeutic interventions to treat these injuries include autologous bone grafts, demineralized bone matrix, and growth factor therapies, such as bone morphogenetic proteins. However, there are several disconcerting issues associated with the use of these therapeutics, including post-surgical pain and limited graft material, limited osteoinductive capability with immunogenic potential, and limited clinical efficiency and safety concerns [3, 4], respectively. Thus, there remains a significant need to develop new methodologies to promote bone regeneration. Our research is based on the premise that the development of new therapeutics must be predicated on a thorough understanding of molecular mechanisms regulating fracture healing. Unfortunately, the molecular mechanisms that regulate the spatiotemporal progression of fracture healing are poorly understood. Therefore, we set out to identify the role of a novel signaling pathway during bone fracture healing, with the down-stream objective of potentially targeting that pathway to improve bone tissue regeneration.

The Notch signaling pathway has been shown to regulate embryological bone development [5-8], and many aspects of embryological development are recapitulated during fracture healing [9-11]. Furthermore, Notch signaling has been shown to be required for tissue repair of other injuries [12, 13], and targeting the pathway can promote regeneration [14]. However, the role of Notch signaling during bone fracture healing and the ability of manipulating the pathway to improve regeneration is unknown. Therefore, the overall objective of this thesis was to determine the role of Notch signaling during bone fracture healing, and to create a clinically translatable therapy to target the pathway and enhance healing.

7.1.1 Specific Aim I (Chapter 3)

In Aim I (Chapter 3), we set out to characterize and compare activation of the Notch signaling pathway during endochondral and intramembranous fracture healing using murine tibial fracture healing as a model of endochondral bone repair and murine calvarial defect healing as a model of intramembranous bone repair. Our results demonstrated that Notch signaling components, including ligands, receptors and target genes were upregulated during both endochondral and intramembranous fracture healing. Notch ligands demonstrated a higher magnitude of change during healing than receptors, suggesting that activation of the pathway may be more regulated by ligand density rather than receptor. Jagged1 was the most highly expressed ligand and was the only ligand to be upregulated during both injury models, suggesting that manipulations of Notch signaling to enhance fracture healing could target Jagged1 for the most potent therapeutic effect. Notch2 was the most highly expressed receptor, and was one of two upregulated during both injury models, the other one being Notch4.

Jagged1 and the activated form of the Notch2 receptor (NICD2) were expressed in the same cell populations during endochondral and intramembranous fracture healing. During chondrogenesis, Jagged1 and NICD2 were widely expressed in undifferentiated mesenchymal cells, but the number of positive cells gradually decreased during differentiation until expression was largely absent in hypertrophic chondrocytes. However, Jagged1 and NICD2 were re-expressed in terminal hypertrophic chondrocytes located in areas of resorbed cartilage that had been infiltrated by vascular endothelial cells, which were also largely Jagged1 and NICD2 positive.

Alternative to chondrogenesis, Jagged1 and NICD2 were expressed in osteogenic cells at all stages of differentiation, from undifferentiated mesenchymal and osteoprogenitor cells located in the early fibrovascular callus, to osteoblasts that aligned the surface of immature and remodeled bone, and to a lesser extent osteocytes embedded within the remodeled matrix. This expression pattern was observed during both endochondral and intramembranous fracture healing.

In summary, these results demonstrate that Notch signaling was active during endochondral and intramembranous bone fracture healing, with expression gradually decreasing during chondrogenesis, but remaining present at multiple stages of osteogenesis. Expression was also widely found in vascular endothelial cells. Furthermore, results identify the Notch ligand Jagged1 as a potential therapeutic target to upregulate the Notch signaling pathway.

7.1.2 Specific Aim II (Chapter 4)

In Aim I (Chapter 3), we found that Notch signaling was active during bone fracture repair. Therefore, in Aim II (Chapter 4), we set out to determine the significance of Notch signaling during bone fracture healing by using a temporally controlled inducible transgenic mouse model to impair canonical Notch signaling in all cells during murine tibial fracture and calvarial defect healing. dnMAML mice were crossed with inducible Mx1-Cre promoter mice such that a series of polyI:C injections just prior to fracture would activate the Mx1 promoter and expression of Cre recombinase in all cell types, which in turn would delete the transcriptional stop sequence upstream of dnMAML allowing for systemic expression [15, 16]. dnMAML is a truncated version of MAML that is able to similarly bind to the NICD-RBPjκ complex, but lacks the binding domain to recruit other co-activators necessary to initiate transcription of Notch target genes, thus inhibiting canonical Notch signaling at the level of transcriptional complex assembly [17]. Wild type mice were negative for Cre recombinase.

Our results demonstrated that Notch signaling is required for the proper spatiotemporal progression of bone fracture healing. However, Notch signaling did not appear to regulate proliferation or apoptosis of cells during repair.

Specifically, inhibition of Notch signaling resulted in a sustained inflammatory phase including increased cytokine gene expression and neutrophil infiltration of the callus.

Notch inhibition also decreased chondrogenic gene expression and overall cartilage formation, though the rate of cartilage maturation was not affected. Notch regulation of cartilage formation was likely due to direct effects on chondrocyte behavior as well as secondary effects from the sustained presence of inflammatory cells and cytokines, which can also inhibit cartilage

formation [18-20]. Expression of vascular endothelial cell markers was also inhibited during bone repair.

Based on previous studies utilizing tissue-specific models of Notch loss- and gain-of-function, we expected Notch inhibition to increase osteoblast and osteoclast activity [5-7, 21, 22]. However, systemic inhibition of Notch signaling in all cells during endochondral fracture healing had no affect on early osteoblast behavior, and in fact osteoblast and osteoclast density was decreased during later stages of remodeling. This resulted in an overall increase in bone volume fraction that was due to a decrease in callus volume with no change in bone volume. Patterning of bone formation was also altered with decreased connectivity density and structural matrix index and increased trabecular thickness. These changes were only observed during later stages of remodeling. Expression of inflammatory cytokines can inhibit osteoblast differentiation [23], and proper callus vascularization is required for osteoblast recruitment to the callus. Secondary effects from sustained inflammation and impaired callus vascularization may be primarily responsible for the observed bone phenotype. We also found that inhibition of Notch signaling altered bone remodeling during intramembranous repair. However, that injury model presented with decreased bone mass.

In conclusion, our results demonstrated that the Notch signaling pathway is required for the proper spatiotemporal progression of bone fracture healing.

7.1.3 Specific Aim III (Chapter 5)

In Aim I (Chapter 3), we found that Notch signaling was active during bone formation. Importantly, Notch ligands demonstrated a higher magnitude of change during healing relative to receptors, suggesting that activation of the pathway may be more regulated by ligand density and type rather than receptor. Jagged1 was the most highly expressed and upregulated Notch ligand during healing, suggesting its potential use as a therapeutic target to upregulate the Notch signaling pathway. In Aim II (Chapter 4), we found that Notch signaling is required for the proper spatiotemporal progression of fracture healing. However, the role of Jagged1 during this process was not studied.

Loss-of-function mutations in Jagged1 result in Alagille Syndrome (ALGS) [24, 25], which is characterized by defects to many organs including the skeleton, where patients present with decreased bone mass and increased risk of fracture [26, 27]. Changes in the skeleton are often assumed to occur secondarily to impaired liver function. However, the direct effects of Jagged1 during bone formation were not known. Therefore, the objective of Aim III (Chapter 5) was to determine the direct role of Jagged1 during bone formation by using two skeletal-specific conditional Jagged1 knockout mouse models.

Floxed Jagged1 mice were first crossed with Prx1-Cre mice. The Prx1 promoter is active in undifferentiated osteochondral progenitor cells such that all mesenchymal lineage cells in the developing mouse limb bud are derived from Prx1-expressing cells [28]. In this model, Jagged1 was conditionally deleted in osteochondral progenitor cells prior to skeletal development. Floxed Jagged1 mice were also crossed with Col2.3-Cre mice. The Col2.3 promoter is active in committed osteoblasts that align trabecular and cortical bone [29, 30]. In this model, Jagged1 was conditionally deleted in an osteoblast-specific cell population later on during differentiation. All wild type mice were negative for Cre recombinase.

Our results demonstrated a similar role for Jagged1 in both models during early and late osteoblast differentiation, where endogenous Jagged1 expression (WT specimens) in whole bone activated Notch target gene expression, promoted osteogenic gene expression, had no effect on osteoclast gene expression, and moderately stimulated proliferation gene expression. This correlated with increased trabecular bone formation at 8 weeks of age that persisted at 9 months. These results demonstrated that endogenous Jagged1 expression during early and late osteoblast differentiation promoted bone formation.

Surprisingly, we found divergent roles for Jagged1 in the trabecular and cortical compartments. When Jagged1 was deleted in cortical bone during early and late osteoblast differentiation, there was no significant change in Notch target gene expression or osteogenic gene expression, but there was an increase in osteoclast gene expression, and moderately enhanced proliferation gene expression. This correlated with decreased periosteal expansion, endosteal resorption and cortical bone mass. We did not uncover the primary mechanism

regulating this phenotype, but we concluded that Jagged1 expression does not appear to regulate Notch target gene activity in the cortical compartment, suggesting that alterations to cortical bone are due to non-canonical Notch activity or secondary effects independent of Notch signaling.

We also found that expression of Jagged1 and Notch target genes Hey1 and Hes1 were positively correlated with expression of osteogenic markers regardless of whether it was of trabecular or cortical origin.

In conclusion, this study demonstrated that Jagged1 expression in the skeleton directly and positively regulated bone formation. This suggests liver transplantations for ALGS patients as an incomplete therapeutic strategy. The pro-osteogenic role for Jagged1 also indicated that delivery of Jagged1 could potentially enhance bone formation during fracture healing.

7.1.4 Specific Aim IV (Chapter 6)

In Aim I (Chapter 3), we found that Notch signaling was active during bone formation. In Aim II (Chapter 4), we found that Notch signaling was required for the proper spatiotemporal progression of fracture healing, where Notch inhibition did not result in improved healing. In Aim III (Chapter 5), we found that Jagged1 expression in the osteoblast lineage enhanced osteogenic gene expression and bone formation. Collectively, the studies identified Jagged1 as a potential therapeutic target to promote bone regeneration. Therefore, the objective of Aim IV (Chapter 6) was to develop a clinically translatable biomaterial construct comprised of Jagged1 and an osteoconductive scaffold, and evaluate its ability to induce bone tissue formation. The poly(β-amino ester) polymer comprised of diethylene glycol diacrylate and isobutylamine, known shorthand as A6, was chosen as the osteoconductive scaffold because it was previously shown to promote bone formation when used as a carrier polymer for BMP2 [31].

We first set out to compare direct and indirect Jagged1/A6 immobilization strategies on human MSC behavior in standard growth media. Overall, Jagged1/A6 biomaterial constructs transiently activated the Notch signaling pathway and induced an osteogenic phenotype. However, direct Jagged1/A6 was more effective than indirect at upregulating Notch target Hey1 gene expression. This correlated with increased surface density of Jagged1 successfully bound

to A6 via the direct method versus the indirect method at the same Jagged1 incubation concentrations. Furthermore, direct Jagged1/A6 was more effective at stimulating bone sialoprotein gene expression as well as alkaline phosphatase gene expression and enzymatic activity. These results identified direct Jagged1/A6 as a more viable immobilization strategy for potential clinical use. Additionally, Hey1 gene expression was positively correlated with bone sialoprotein gene expression independent of Jagged1 concentration, immobilization strategy or time post plating, further identifying Jagged1 and the Notch signaling pathway as potential therapeutic targets to enhance bone tissue formation.

Therefore, we next set out to evaluate the ability of directly immobilized Jagged1/A6 biomaterial constructs to induce human MSC osteoblast differentiation in osteogenic media. We found that direct Jagged1/A6 enhanced osteoblast differentiation, indicated by increased alkaline phosphatase enzymatic activity and importantly increased calcified mineral deposition of cells, which is indicative of terminal osteoblast differentiation. The A6 polymer alone also increased calcified mineral deposition relative to tissue culture polystyrene control wells with no A6 or Jagged1, further demonstrating the osteoconductive properties that were previously established [31].

In conclusion, we developed a biomaterial construct using Jagged1 and the osteoconductive scaffold A6, and demonstrated its ability to activate the Notch signaling pathway and induce osteoblast differentiation and calcified mineral deposition.

7.2 Limitations and Future Directions

7.2.1 Specific Aim I (Chapter 3)

Aim I utilized tibial fracture healing as a model of endochondral bone repair and calvarial defect healing as a model of intramembranous bone repair. Previous studies have shown that bones derived from different embryological germ layers have distinct tissue matrix compositions [32]. The calvarium and tibia originate from the ectoderm and mesoderm [33], respectively, which could explain the difference in basal expression levels of Notch genes in those tissues. Utilizing a

tibial fracture segmental defect model with rigid fixation, for example through an external fixator, would have allowed us to study intramembranous repair in the tibia, controlling for factors intrinsic to the tissue, and this could have been compared to the calvaria to determine whether differences that exist between tibia and calvaria are related to germ layer of origin or location. It is possible that Notch signaling may not be equivalent during intramembranous ossification in all types of bone. However, in this study we demonstrated that expression of Notch components are equivalently localized in osteogenic cells regardless of germ layer origin, embryological development, or method of healing. This suggests that similar results would be expected in all models of endochondral and intramembranous bone repair. Furthermore, we chose to use the long bone fracture and calvarial defect models in order to develop a broader understanding of Notch signaling with applications to both craniofacial and appendicular skeletal regeneration.

Future studies can use specimens collected from this study to screen for other cell signaling pathways known to regulate repair of other injuries but have yet to be studied during bone repair. Furthermore, ongoing studies are characterizing activation of Notch signaling during bone repair in geriatric mice. Future studies could also look into characterizing Notch activation during fracture healing in mice in various diseased states. Correlation of Notch activity with impaired fracture outcome would identify the Notch signaling pathway as a potential therapeutic target to improve healing in that diseased state.

7.2.2 Specific Aim II (Chapter 4)

The dnMAML transgene used in Aim II inhibits canonical Notch signaling at the level of transcriptional complex assembly [17]. However, there are other known functions of the Notch pathway that dnMAML does not affect. NICD binds to the required transcription factor Runx2 to inhibit osteoblast differentiation [5]. While dnMAML binds to the NICD-RBPjκ complex, it is unlikely that this impacts the ability of NICD to have other, non-canonical effects. A recent study also demonstrated non-canonical and cell non-autonomous functions of Notch signaling during embryological bone formation [34]. dnMAML would not affect these behaviors. Finally, there is

evidence of potential reverse ligand intracellular domain signaling in the ligand-expressing signaling cell [35, 36]. dnMAML would also not affect this pathway.

Heterozygous dnMAML mice were used in this study. The use of homozygous mice could have resulted in stronger phenotypes with clearer interpretations into the role(s) of certain cell populations during repair. However, in general, use of heterozygous mice can be more clinically relevant since potential therapeutic applications are likely to achieve partial but not complete ablation of function. Since dnMAML is not an endogenous gene, we were not as concerned with compensatory effects from a redundant protein that are more likely to occur in heterozygous mouse models. There are also other models of inhibition of canonical Notch signaling that could have been used, such as Notch receptor knockout mice [5, 7], or mice with conditional deletion of RBPjκ [8, 22, 34, 37], but again, or goal was to modulate Notch signaling, not completely ablate it.

Both males and females were included in this study, but were appropriately separated into different groups and not compared to each other since they present with different amounts of bone during development [38]. However, many previous studies have demonstrated similar responsivity of male and female mice to manipulations of Notch signaling [6, 7, 21, 22] and male and female mice follow the same spatiotemporal pattern of healing. Therefore, it is scientifically justifiable to conclude that the phenotype of females during cartilage formation is equivalent to what would be observed in males, and vice versa during bone formation.

As with all studies, including later time points closer to or after expected complete healing would allow for better understanding of the final outcome due to Notch inhibition. However, only three time points were chosen due to resource and time constraints, and the time points chosen were based on critical stages of fracture healing (5dpf – mesenchymal callus formation; 10dpf – cartilage formation and early bone formation; 20dpf – bone formation and remodeling) that also allow for comparison across many studies.

Importantly, our results demonstrated the importance of Notch signaling to resolve the inflammatory phase. However, our experimental design did include time points during peak

inflammation, which occurs immediately after injury. Future studies should additionally investigate the role of Notch activity during peak inflammation.

Because of the complexity of the spatiotemporally changing population of cells and tissues during healing, we were unable to assess the role of Notch signaling in distinct cell populations, including osteoblasts and osteoclasts. To address this limitation, future studies could utilize tissue-specific models of Cre recombinase expression to activate dnMAML in specific lineages. Utilizing Prx1, Col3.6 or Col2.3 promoters would inhibit Notch signaling in undifferentiated mesenchymal progenitors, osteoprogenitors, or committed osteoblasts, respectively. Similarly, TRAP promoters would inhibit Notch signaling in osteoclast lineage cells, and expressing Cre in lineage-restricted inflammatory cells would be useful for exploring the contribution of inflammatory cells.

Alternatively, the use of gamma secretase inhibitors (GSI) would allow temporal control of Notch signaling to isolate or exclude the role of Notch signaling in specific phases of healing. For example, GSI injections following the conclusion of the acute inflammatory phase could exclude any secondary effects of altered inflammation on the rest of healing, providing a model to better understand the direct role of Notch signaling in cartilage formation, callus vascularization, and bone formation and remodeling. Similarly, GSI injections starting at the cartilage-to-bone transition would isolate the role of Notch signaling during bone formation and remodeling.

Calvarial defect experiments included in this thesis are at this stage preliminary work demonstrating the broader application of Notch relevance. More research is needed to fully understand the role of Notch signaling during calvarial defect healing. However, results from the tibial fracture model demonstrate that Notch signaling is needed for successful repair. Future calvarial defect studies should focus on creating a smaller defect since 1.8 mm diameter injuries result in non-union [39]. Using an intramembranous repair model that normally regenerates would allow for better understanding into the requirement of Notch signaling for successful intramembranous fracture healing.

Finally, in Aim I, we identified Jagged1 as the most highly upregulated ligand, suggesting it as a potential therapeutic target to manipulate Notch signaling. Future studies should look into

evaluating the role of Jagged1 during fracture healing using a similar experimental design to Aim II. However, we have had difficulty in generating Mx1-Cre+;Jagged1$^{f/f}$ mice because of small litter size and poor animal health.

7.2.3 Specific Aim III (Chapter 5)

In Aim III, Jagged1 was inhibited during early and late osteoblast differentiation using the Prx1-Cre and Col2.3-cre promoter mouse models, respectively. Prx1 trabecular bone phenotypes were present in both males and females. However, trabecular phenotypes in Col2.3 mice were more pronounced in males. A previous study showed that using the Col2.3 promoter model, 50% of females showed recombination in the absence of germ line transmission of the Cre recombinase gene [40], presumably due to spurious Cre expression in maternal gametes. This mouse would be considered to be wild type, but would have the transgenic protein deleted. Intriguingly, only 15% of males showed this unexpected recombination. Thus, aberrant activity of the Col2.3 promoter in female gametes may account for the lack of trabecular phenotypic differences. Furthermore, in general, the use of tissue-specific promoters can result in unintended expression. As one example, lineage tracing of the Col2.3 promoter has identified positive cells in the growth plate, though results were variable [29].

Results from these experiments demonstrated that early and late endogenous Jagged1 expression promotes osteoblast differentiation and bone formation. In Aim I, we showed that Jagged1 is expressed in osteogenic cells at various stages of differentiation. However, the magnitude and frequency (sustained vs. cyclical) of Jagged1 expression during differentiation is unknown. Use of in situ hybridization or immunoflourescence would allow us to quantify the relative amounts of Jagged1 RNA or protein expressed per cell, respectively. Because it can be difficult to identify various osteogenic lineage cells and specific stages of differentiation based on morphology alone, co-localization of Jagged1 with markers of differentiation such as Prx1, Col3.6, Col2.3, or Ocn via immunoflourescence would help compartmentalize the magnitude of Jagged1 expression in undifferentiated mesenchymal cells, osteoprogenitors, committed osteoblasts, and mature osteoblasts, respectively. Furthermore, development of a conditional Jagged1 gain-of-

function mouse model would allow for the investigation of sustained versus endogenous Jagged1 activity on osteoblast differentiation and bone formation.

Further characterization of Col2.3-Cre;Jagged1$^{f/f}$ and Prx1-Cre;Jagged1$^{f/f}$ mice is required to better understand the role of Jagged1 on cellular behavior. Ongoing studies are harvesting bone marrow-derived mesenchymal progenitor cells to quantify the effect of Jagged1 deletion during early and late differentiation on mesenchymal progenitor number (CFU-F assay), cell proliferation (Alamar Blue assay), and osteoblast differentiation (Alizarin Red S staining). Furthermore, histological analysis of bones will help localize the observed gene expression changes from QPCR, as well as allow for analysis of the cartilaginous growth plate.

Future studies can also focus on the clinical relevance of these findings with regards to ALGS patients. For example, liver transplants are currently used to treat patients with impaired bone mass. This study suggests that increasing Jagged1 activity in the skeleton is what is actually required to promote bone tissue formation. Creation of mice with conditionally deleted Jagged1 in the skeleton as well as the liver would allow for investigation into whether localized delivery of Jagged1 is sufficient to restore a successful fracture healing outcome, or if Jagged1 delivery in combination with liver transplantation is needed.

This study also identified a novel role for Jagged1 that was not observed in Notch receptor loss-of-function mouse models. Creating combined receptor and Jagged1 loss-of-function mice would allow for investigation into whether bone development or fracture healing is regulated primarily by ligand or receptor activity.

7.2.4 Specific Aim IV (Chapter 6)

In Aim IV, we developed a biomaterial construct by immobilizing Jagged1 to a poly(β-amino ester) polymer. We decided to use two well-described immobilization strategies, direct adsorption and indirect binding through an anti-Fc antibody (that binds to the Fc portion of the Jagged1/Fc recombinant protein) that is first adsorbed [41]. Although there are other immobilization strategies, for example covalent binding [42], we decided to take the simplest approach for maximal translatability to the clinic. Developing an easy to use ‘off-the-shelf’

therapeutic should involve minimal processing prior to implantation. Direct adsorption of a protein to a material, which was shown to be most effective, is a simple technique that can be used in any operating room.

Our data demonstrated that transient Notch activation via Jagged1 delivery enhances osteoblast differentiation. However, gain-of-function mouse models have shown that sustained Notch activation in fact inhibits differentiation [5, 7]. Development of a Jagged1/A6 biomaterial construct with sustained Notch signaling, for example by embedding the Jagged1 protein into the A6 material as well as adsorbing it to the surface such that as the material degrades more Jagged1 is exposed for cells to interact with, would allow for investigation into the temporal regulation of Jagged1-induced Notch activity on osteogenesis in a clinically translatable model.

Jagged1/A6 biomaterial constructs were evaluated in two *in vivo* animal models. First, porous Jagged1/A6 scaffolds were implanted into murine calvarial defects. However, scaffolds had to be at least 1 mm thick for structural stability, whereas murine calvaria are less than 200 μm thick. We believe that this 5-fold difference in thickness ultimately prevented scaffolds from consistently staying within the defect.

Solid biomaterial constructs were also implanted 3 days post fracture during murine tibial fracture healing. They were wrapped around the provisional callus so that the Jagged1 would interact with cells on the periosteal surface of the expanding fracture callus. However, our inability to suture the biomaterial in place resulted in the fracture wraps not maintaining contact with the callus. Furthermore, relative to porous scaffolds that promoted cell and tissue infiltration, solid biomaterials induced a strong foreign body response, which completely encapsulated the biomaterial, therefore preventing Jagged1 from interacting with the mesenchymal callus. Future studies using this implant model should include materials with stronger suture pullout strength, and that cause a minimal foreign body response. Similarly, a lower-affinity binding molecule that is likely to be released should be used. Our results demonstrated that Jagged1 does not release from the biomaterial during 40 days of culture. This would limit Jagged1 to interacting with only the periosteal surface of the callus. Successful therapeutics would likely need to interact with cells

inside the callus as well. Furthermore, A6 was included in this study based on its osteoconductive properties but in this model was alternatively used as a biocompatible delivery vehicle instead.

Future studies investigating Jagged1/A6 should use segmental defect models where A6 would serve as a scaffold for cell infiltration and Jagged1 would promote osteogenesis. A6 has previously been successfully used in rat calvarial defect models (~1 mm thick calvarium). This biomaterial construct can also be evaluated in long bone segmental defects in rats and larger animal models.

7.3 Conclusion

This thesis was the first to discover the Notch signaling pathway as an important regulator of bone fracture healing, and identify the pathway as a therapeutic target to improve repair. Specifically, Notch signaling was shown to be active during bone fracture healing. Inhibition of the pathway altered the temporal progression of events required for healing. The Notch ligand Jagged1 was shown to promote embryological bone formation. Finally, development of a biomaterial construct comprised of Jagged1 and a poly(β-amino ester) polymer containing diethylene glycol diacrylate and isobutylamine was shown to activate the Notch signaling pathway and induce osteoblast differentiation. Future studies should evaluate the ability of this tissue engineering therapy to improve bone regeneration *in vivo*.

Importantly, the study design outlined in this thesis can serve as a model for future experiments looking to uncover novel signaling pathways that regulate, and therefore could potentially enhance, bone fracture healing or any other injury: 1) identify whether the target is active during healing, 2) identify the role of the target, 3) attempt to improve healing by upregulating, inhibiting, or modulating the target depending on its observed role.

7.4 References

1. Braithwaite, R.S., N.F. Col, and J.B. Wong, *Estimating hip fracture morbidity, mortality and costs.* J Am Geriatr Soc, 2003. **51**(3): p. 364-70.

2. Audige, L., et al., *Path analysis of factors for delayed healing and nonunion in 416 operatively treated tibial shaft fractures.* Clin Orthop Relat Res, 2005. **438**: p. 221-32.

3. Carragee, E.J., et al., *Future directions for The spine journal: managing and reporting conflict of interest issues.* Spine J, 2011. **11**(8): p. 695-7.

4. Einhorn, T.A., *Clinical applications of recombinant human BMPs: early experience and future development.* J Bone Joint Surg Am, 2003. **85-A Suppl 3**: p. 82-8.

5. Engin, F., et al., *Dimorphic effects of Notch signaling in bone homeostasis.* Nat Med, 2008. **14**(3): p. 299-305.

6. Zanotti, S., et al., *Notch inhibits osteoblast differentiation and causes osteopenia.* Endocrinology, 2008. **149**(8): p. 3890-9.

7. Hilton, M.J., et al., *Notch signaling maintains bone marrow mesenchymal progenitors by suppressing osteoblast differentiation.* Nat Med, 2008. **14**(3): p. 306-14.

8. Mead, T.J. and K.E. Yutzey, *Notch pathway regulation of chondrocyte differentiation and proliferation during appendicular and axial skeleton development.* Proc Natl Acad Sci U S A, 2009. **106**(34): p. 14420-5.

9. Vortkamp, A., et al., *Recapitulation of signals regulating embryonic bone formation during postnatal growth and in fracture repair.* Mech Dev, 1998. **71**(1-2): p. 65-76.

10. Ferguson, C., et al., *Does adult fracture repair recapitulate embryonic skeletal formation?* Mech Dev, 1999. **87**(1-2): p. 57-66.

11. Gerstenfeld, L.C., et al., *Fracture healing as a post-natal developmental process: molecular, spatial, and temporal aspects of its regulation.* J Cell Biochem, 2003. **88**(5): p. 873-84.

12. Chigurupati, S., et al., *Involvement of notch signaling in wound healing.* PLoS One, 2007. **2**(11): p. e1167.

13. Conboy, I.M., et al., *Notch-mediated restoration of regenerative potential to aged muscle.* Science, 2003. **302**(5650): p. 1575-7.

14. Gude, N.A., et al., *Activation of Notch-mediated protective signaling in the myocardium.* Circ Res, 2008. **102**(9): p. 1025-35.

15. Kuhn, R., et al., *Inducible gene targeting in mice.* Science, 1995. **269**(5229): p. 1427-9.

16. Tu, L., et al., *Notch signaling is an important regulator of type 2 immunity.* J Exp Med, 2005. **202**(8): p. 1037-42.

17. Weng, A.P., et al., *Growth suppression of pre-T acute lymphoblastic leukemia cells by inhibition of notch signaling.* Mol Cell Biol, 2003. **23**(2): p. 655-64.

18. Keffer, J., et al., *Transgenic mice expressing human tumour necrosis factor: a predictive genetic model of arthritis.* EMBO J, 1991. **10**(13): p. 4025-31.

19. Niki, Y., et al., *Macrophage- and neutrophil-dominant arthritis in human IL-1 alpha transgenic mice.* J Clin Invest, 2001. **107**(9): p. 1127-35.

20. Lubberts, E., et al., *IL-1-independent role of IL-17 in synovial inflammation and joint destruction during collagen-induced arthritis.* J Immunol, 2001. **167**(2): p. 1004-13.

21. Salie, R., et al., *Ubiquitous overexpression of Hey1 transcription factor leads to osteopenia and chondrocyte hypertrophy in bone.* Bone, 2010. **46**(3): p. 680-94.

22. Tao, J., et al., *Osteosclerosis owing to Notch gain of function is solely Rbpj-dependent.* J Bone Miner Res, 2010. **25**(10): p. 2175-83.

23. Caparbo, V.F., et al., *Serum from children with polyarticular juvenile idiopathic arthritis (pJIA) inhibits differentiation, mineralization and may increase apoptosis of human osteoblasts "in vitro".* Clin Rheumatol, 2009. **28**(1): p. 71-7.

24. Li, L., et al., *Alagille syndrome is caused by mutations in human Jagged1, which encodes a ligand for Notch1.* Nat Genet, 1997. **16**(3): p. 243-51.

25. Oda, T., et al., *Mutations in the human Jagged1 gene are responsible for Alagille syndrome.* Nat Genet, 1997. **16**(3): p. 235-42.

26. Bales, C.B., et al., *Pathologic lower extremity fractures in children with Alagille syndrome.* J Pediatr Gastroenterol Nutr, 2010. **51**(1): p. 66-70.

27. Olsen, I.E., et al., *Deficits in size-adjusted bone mass in children with Alagille syndrome.* J Pediatr Gastroenterol Nutr, 2005. **40**(1): p. 76-82.

28. Logan, M., et al., *Expression of Cre Recombinase in the developing mouse limb bud driven by a Prxl enhancer.* Genesis, 2002. **33**(2): p. 77-80.

29. Liu, F., et al., *Expression and activity of osteoblast-targeted Cre recombinase transgenes in murine skeletal tissues.* Int J Dev Biol, 2004. **48**(7): p. 645-53.

30. Kalajzic, I., et al., *Use of type I collagen green fluorescent protein transgenes to identify subpopulations of cells at different stages of the osteoblast lineage.* J Bone Miner Res, 2002. **17**(1): p. 15-25.

31. Brey, D.M., et al., *Identification of osteoconductive and biodegradable polymers from a combinatorial polymer library.* J Biomed Mater Res A, 2010. **93**(2): p. 807-16.

32. van den Bos, T., et al., *Differences in matrix composition between calvaria and long bone in mice suggest differences in biomechanical properties and resorption: Special emphasis on collagen.* Bone, 2008. **43**(3): p. 459-68.

33. Chung, U.I., et al., *Distinct osteogenic mechanisms of bones of distinct origins.* J Orthop Sci, 2004. **9**(4): p. 410-4.

34. Kohn, A., et al., *Cartilage-specific RBPjkappa-dependent and -independent Notch signals regulate cartilage and bone development.* Development, 2012. **139**(6): p. 1198-212.

35. D'Souza, B., A. Miyamoto, and G. Weinmaster, *The many facets of Notch ligands.* Oncogene, 2008. **27**(38): p. 5148-67.

36. Bray, S.J., *Notch signalling: a simple pathway becomes complex.* Nat Rev Mol Cell Biol, 2006. **7**(9): p. 678-89.

37. Dong, Y., et al., *RBPjkappa-dependent Notch signaling regulates mesenchymal progenitor cell proliferation and differentiation during skeletal development.* Development, 2010. **137**(9): p. 1461-71.

38. Glatt, V., et al., *Age-related changes in trabecular architecture differ in female and male C57BL/6J mice.* J Bone Miner Res, 2007. **22**(8): p. 1197-207.

39. Cooper, G.M., et al., *Testing the critical size in calvarial bone defects: revisiting the concept of a critical-size defect.* Plast Reconstr Surg, 2010. **125**(6): p. 1685-92.

40. Cochrane, R.L., et al., *Rearrangement of a conditional allele regardless of inheritance of a Cre recombinase transgene.* Genesis, 2007. **45**(1): p. 17-20.

41. Beckstead, B.L., et al., *Methods to promote Notch signaling at the biomaterial interface and evaluation in a rafted organ culture model.* J Biomed Mater Res A, 2009. **91**(2): p. 436-46.

42. Goncalves, R.M., et al., *Induction of notch signaling by immobilization of jagged-1 on self-assembled monolayers.* Biomaterials, 2009. **30**(36): p. 6879-87.